Val d'Agri, 15-17 October 2007

FIELDTRIP GUIDE
TO
ACTIVE TECTONICS STUDIES IN THE HIGH AGRY VALLEY

(In the 150th anniversary of the 16 December 1857, Mw 7.0 Earthquake)

Edited by
Luigi Ferranti (UniNa), Laura Maschio (UniNa) and Pierfrancesco Burrato (INGV)

Contributors:
Francesco Bucci (UniSi), Riccardo Civico (UniRomaTre), Giuliana D'Addezio (INGV), Paolo Marco De Martini (INGV), Alessandro Giocoli (CNR-IMAA), Luigi Improta (INGV), Marina Iorio (CNR-IAMC), Daniela Pantosti (INGV), Sabatino Piscitelli (CNR-IMAA), Luisa Valoroso (UniNa), Irene Zembo (UniMi)

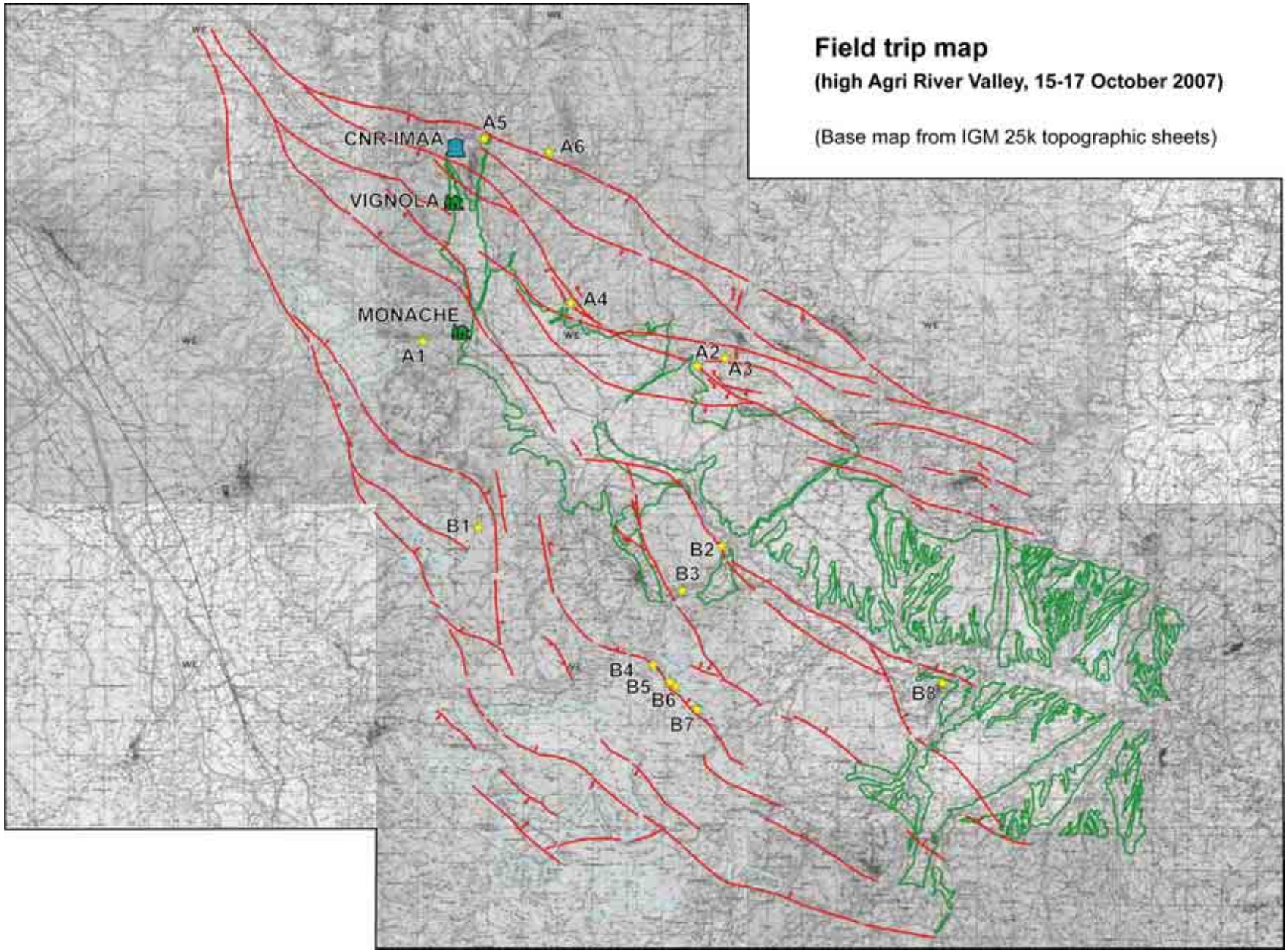

Field trip map

(high Agri River Valley, 15-17 October 2007)

(Base map from IGM 25k topographic sheets)

List of stops

Day 1 (16 October 2007)
Mainly devoted to the eastern valley shoulder

A1- View point along the SP273 Paterno-Mandrano on the high Agri Valley
structural and geomorphic overview of the valley

A2- Barricelle quarry
structural observation on a W-dipping fault zone

A3- road to Marsicovetere
overview of the W-dipping fault zone and observation of the Agri R. asymmetry

A4- Galaino quarry
deformation of slope deposits

A5- Marsico Nuovo dam
flat iron of the back limb of the Monte Lama-Calvelluzzo anticline

A6- Camporeale
discussion on converging morphologies: flat iron vs. fault scarp

Day 2 (17 October 2007)
Mainly devoted to the western valley shoulder

B1- View point from Camporotondo on the high Agri Valley and the Monti della Maddalena range
panoramic view on the "hat-like" topography of the Maddalena Mts. crest
eastern branch of the MMFS and the Monte Aquila fault

B2- Monticello quarry
E-dipping border fault and Agri R. behaviour
description of the eastern part of the ESIT700 seismic section

B3- Tramutola cemetery
discussion on the Tramutola mountain front: thrust vs. normal fault
description of the western part of the ESIT700 seismic section

B4- Cozzi Crocevie quarry
Overview of the Monte Aquila fault: geometry and bedrock expression

B5- Trench 1 site
Monte Aquila fault: morphotectonic, paleoseismology and geophysics

B6- Covoni site (trench 2)
Monte Aquila fault: morphotectonic, paleoseismology, speleoseismology and geophysics

B7- F.ce di Calce site
Monte Aquila fault: morphotectonic, paleoseismology and geophysics

B8- Grumento Nova
panoramic on the Agri River gorge
coffee and farewell party

Foreword

The year 2007 is the 150 anniversary of the Great Neapolitan Earthquake which on 16 December 1857 struck a vast region of Southern Italy and was centered in the Val d'Agri (Agri River valley), one of the largest basins of the Southern Apennines mountain chain. The earthquake effects were promptly studied by Robert Mallett, an Irish engineer who published an extensive report considered a landmark in the modern Seismology [Mallet, R., 1862. The great Neapolitan earthquake of 1857. The first principles of observational seismology. Chapman and Hill (Publ.), London].
Although this earthquake is one of the largest (M~7) in the national seismic catalogue, the location and geometry of the causative fault are object of a warm debate which has blazed in the last years within the scientific community. The *querelle* is not limited to the identification of seismogenic sources in the Val d'Agri area but, obviously, imbues models of the Quaternary tectonic evolution of the Apennines.
Taking the occasion of this recurrence, the *Università degli Studi di Napoli Federico II*, the *Istituto Nazionale di Geofisica e Vulcanologia* (INGV) and the *Istituto di Metodologie per l'Analisi Ambientale* del CNR (CNR-IMAA) in Tito (Potenza), with the contribution of the Università della Basilicata at Potenza, have promoted a three-day meeting in the Val d'Agri with the aim of discussing field evidences and models for active tectonics in the area.
We will spend the first day in introducing and discussing the next two days field-trip, devoted to the eastern and the western shoulders of the high reach of the basin, respectively.
The purpose is to bring scientists with a broad range of expertise all together for discussing results on multidisciplinary researches carried out in the area, in order to approach the active tectonics of the Val d'Agri from as different and wide angles as possible.
We hope an integrated approach involving extensive geological, geomorphological and geophysical studies of active faulting will help shed light on the particularly difficult case of the Val d'Agri and, more in general, to active deformation in the Southern Apennines.

This Workshop has been prepared in the framework of the celebration for the 150th anniversary of the 1857 earthquake held in the Basilicata and Campania regions. We thank G. Ferrari for support and coordination with local administrations.

We also thank the local Civil Protection (Gruppo Lucano) in the person of Antonio Priore for helping organizing and for logistic support.

Introduction

Regional tectonic outline

The Apennine orogen is characterized by Neogene belts of contraction and extension which migrated easterly during roll-back and crustal delamination of the Adriatic slab (Malinverno & Ryan, 1986; Patacca et al. 1990). Since the Miocene, growth of the fold-and-thrust belt to the E accompanied to hinterland extension to the W, where the deep Tyrrhenian basin developed.

Shortening in the Southern Apennines lasted until the Early Pleistocene (Patacca et al. 1990), when impingement of the thick Apulian sector of the Adriatic lithosphere at the subduction zone slowed the foreland propagation of contraction (inset in Fig. 1; Doglioni et al. 1994; Ferranti & Oldow, 2005).

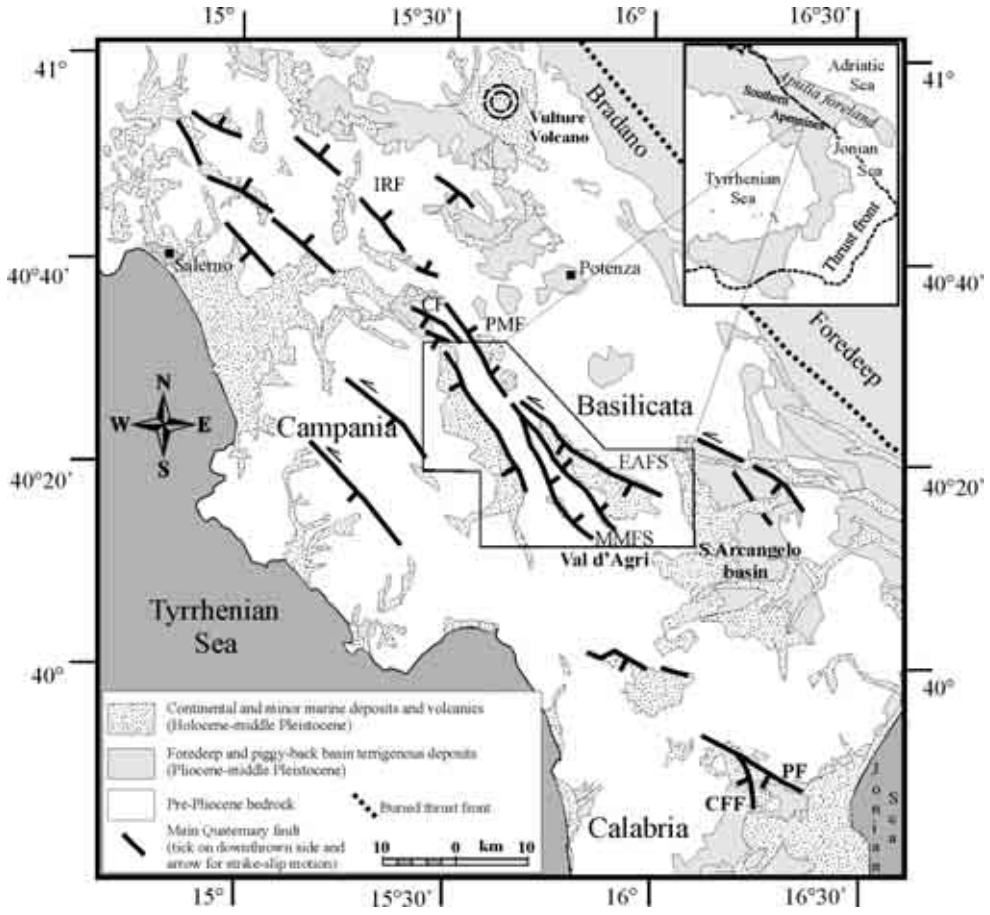

Figure 1. Map of the Campania–Lucania Apennines showing the distribution of Quaternary intermontane basins and major Middle Pleistocene - Holocene normal and strike-slip faults. Faults with inferred or ascertained present activity are labeled as follow: Irpinia sud Fault (IRF); Caggiano Fault (CF); Pergola-Melandro Fault (PMF); Castrovillari-Frascineto Fault (CFF); Pollino Fault (PF). The central frame indicates the Val d'Agri and the Vallo di Diano areas and some of the mapped fault arrays (Eastern Agri fault system, EAFS; Monti della Maddalena fault system, MMFS). Inset shows a schematic map of the Southern Apennines (slightly modified from Maschio et al., 2005)

In the western portion of the orogen, migration of the extensional front behind the thrust belt marked the progressive fragmentation of the upper crust, which was accommodated by Pliocene low-angle normal faults (Ferranti et al. 1996) and Early Pleistocene normal to left-oblique transtensional faults (Hippolyte et al. 1994;

Monaco et al. 1998; Schiattarella, 1998; Catalano et al. 2004). Since the Middle Pleistocene, deformation was characterized by NE-SW extension on NW-SE striking high-angle normal faults (Fig. 1).
The Middle Pleistocene kinematic pattern is ongoing as documented by seismicity and borehole breakouts (Gasparini et al. 1985; Amato et al. 1995; Amato & Montone, 1997; Frepoli & Amato, 2000; Montone et al., 2004; Harvard CMT and INGV QRCMT Catalogues, and INGV Seismic Bulletin), field studies on active and seismogenic faults (Hippolyte et al. 1994; Pantosti & Valensise, 1990; Maschio et al., 2005) and geodetic velocity fields (Hunstad et al., 2003; Ferranti et al., 2007).
Extensional focal mechanisms, historical seismicity and active faults are localized along the narrow topographic culmination of the chain (Fig. 2). In spite of this, several destructive historical and instrumental earthquakes hit also the foredeep and foreland areas of the southern Apennines chain, with left lateral focal mechanisms on E-W trending planes, shading light to the presence and activity of deep trascurrent shear zones (e.g. Fracassi & Valensise, 2007 for the 1456 earthquake; Ekström, 1994 for the 1990 Potenza earthquake; and Chiarabba et al., 2005 for the 2002 Molise earthquakes).

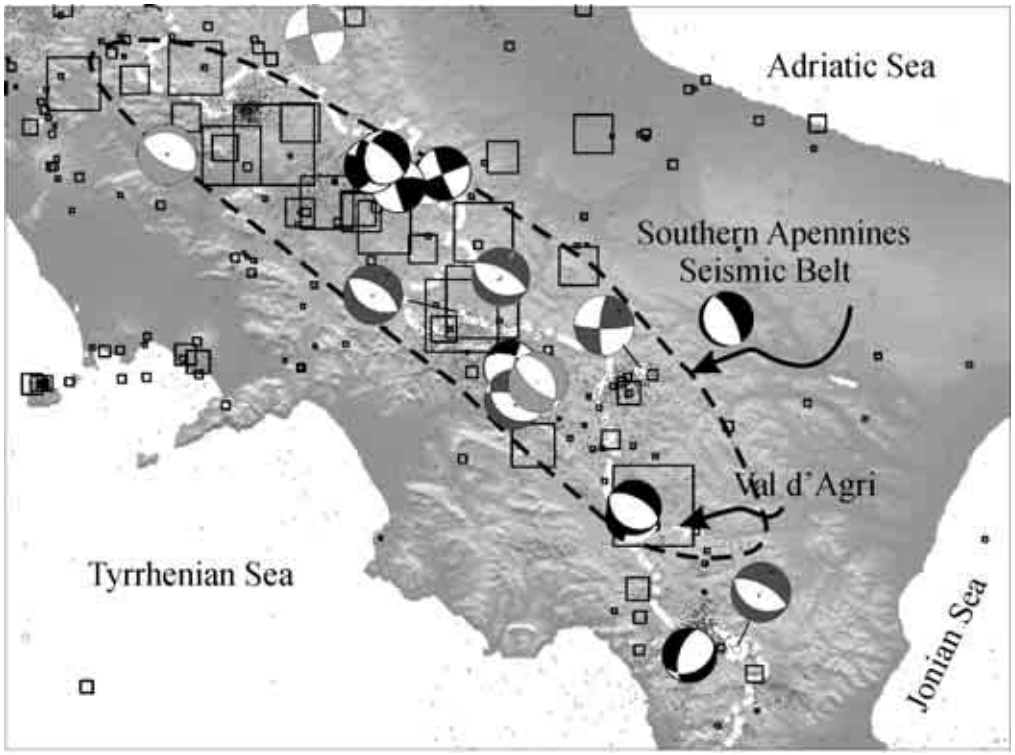

Figure 2. Map of the Southern Apennines seismic belt (after Maschio et al., 2005; thick and white dotted-dashed line indicates the regional divide). Instrumental events (black dots) and historical seismicity (squares, scaled for Me, equivalent magnitude) are from CPTI04 Catalogue (CPTI Working Group, 2004) and INGV Seismic Bulletin (available at http://legacy.ingv.it/~roma/reti/rms/bollettino/index.php. Focal mechanisms (4.2≤M≤6.9) are derived from 1976-2004 Harvard CMT Catalogue (grey; http://www.seismology.harvard.edu/CMTsearch.html), 1997-2004 INGV QRCMT Catalogue (lighter grey; http://earthquake.rm.ingv.it/qrcmt.php)

Pliocene to Quaternary extension accompanied to surface uplift before ultimate tectonic subsidence beneath the Tyrrhenian Sea to the west (Cinque et al. 1993; Ferranti & Oldow, 2005). Since the Middle Pleistocene, uplift concentrated within the axial portion of the chain where extension prevailed (Bordoni & Valensise, 1998;

Schiattarella et al., 2003). Thus, the present-day landscape of the western and axial sectors of the chain results from the interplay between regional uplift and fault displacement, and is expressed by mountain ranges separated from basins filled by continental deposits (Fig. 1).
Whereas many of the range-bounding Pleistocene faults are suspected to be seismically active (Galadini et al. 2000) and have a prevailing south-westerly polarity of extension, with hanging-wall blocks displaced toward the Tyrrhenian basin (Fig. 1; Cinque et al. 1993; Hippolyte et al. 1994; Monaco et al. 1998), in the Southern Apennines seismogenic faulting mostly nucleates on faults which cross-cut the Pleistocene topography and have a north-easterly polarity of block displacement away from the back-arc basin and toward the foreland (DISS Working Group, 2007). This occurrence was dramatically documented by the 1980 coseismic slip on the Irpinia sud Fault (Pantosti & Valensise, 1990; IRF in Fig. 1). Besides a few cases, however, location of active faults and of the detailed geometry of the seismogenic belt are not adequately defined and most of the Pleistocene range-bounding faults are thought to be potentially active (e.g. Galadini et al. 2000; Papanikolau & Roberts, 2007).

Geology of the Val d'Agri basin area

The Val d'Agri basin, located in the axial part of the Campania-Lucania sector of the Southern Apennines, is a NW-elongated basin filled by Quaternary continental deposits which cover down-thrown pre-Quaternary rocks of the Apennine chain (Fig. 3).
Pre-Quaternary rock assemblages which floor the Val d'Agri basin and surrounding regions (Fig. 3) are constituted by Mesozoic-Cenozoic platform and by slope carbonates (Alburno-Cervati and Monti della Maddalena Units, D'Argenio et al. 1975, which form two different thrust imbricates) and are thrust over coeval pelagic rocks (Lagonegro Units, Scandone, 1967) and their Miocene synorogenic cover (Fig. 4). The thrust contact is usually marked by a pervasive cataclastic texture mostly developed at the expenses of brittle carbonate rocks of the upper plate.

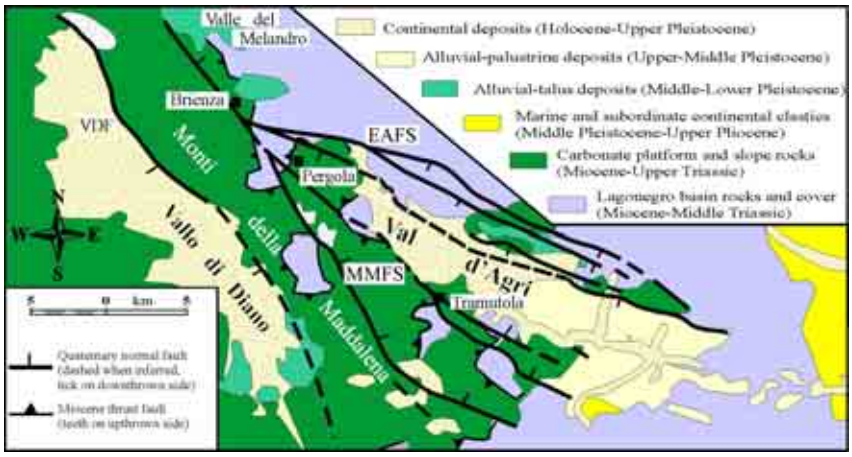

Figure 3. Schematic geologic map of the High Agri Valley-Vallo di Diano region (location in Fig. 1), showing distribution of lithotectonic assemblages and main thrust and extensional faults (slightly modified from Maschio et al., 2005): Vallo di Diano fault (VDF); Eastern Agri fault system (EAFS); Monti della Maddalena fault system (MMFS).

At the footwall, the Lagonegro units consist of Triassic-Miocene carbonate, siliceous, marl and siliciclastic rocks and are grouped into two (Scandone, 1972; Carbone et

al., 1991) or more (Mazzoli et al., 2001) imbricates. The Lagonegro rocks are thrust over buried 6÷7 km-thick Mesozoic-Tertiary shallow-water carbonates and overlying Pliocene foreland rocks, which are the westerly extension of the Apulia foreland platform and are, themselves, involved in the Pliocene-Pleistocene shortening and uplift (Fig. 4; Noguera and Rea, 2000; Shiner et al., 2004; Corrado et al., 2005).

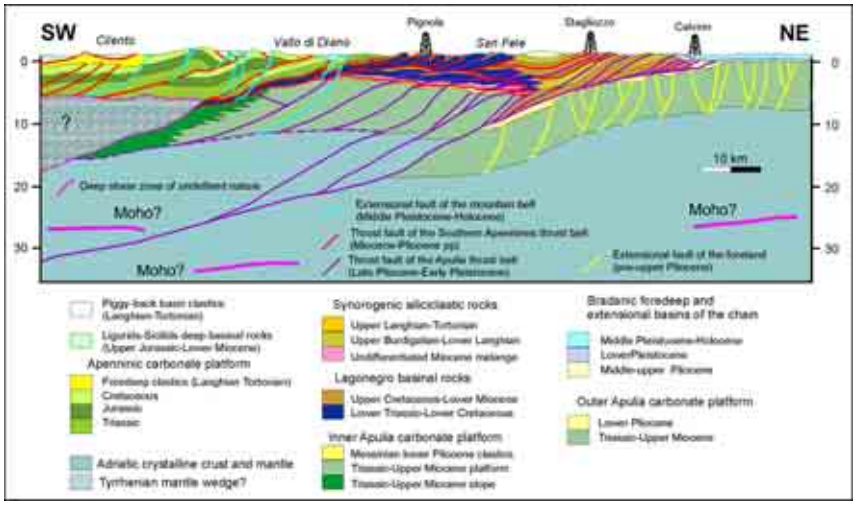

Figure 4. Crustal profile across the Campania-Lucania Apennines located just north of the Val d'Agri basin (re-drawn and modified from Menardi Noguera & Rea, 2000).

The present morphologic-structural frame of the area is mostly the result of thrust tectonism and only subordinately of Quaternary transtension and extension. Rocks of the Lagonegro basin mainly outcrop on the eastern side of the basin and in sparse tectonic windows beneath the Monti della Maddalena thrust sheet in the western side (Fig. 5). Conversely, limited outcrops of the carbonates are found E of the basin where the leading edge of the thrust sheet is located.

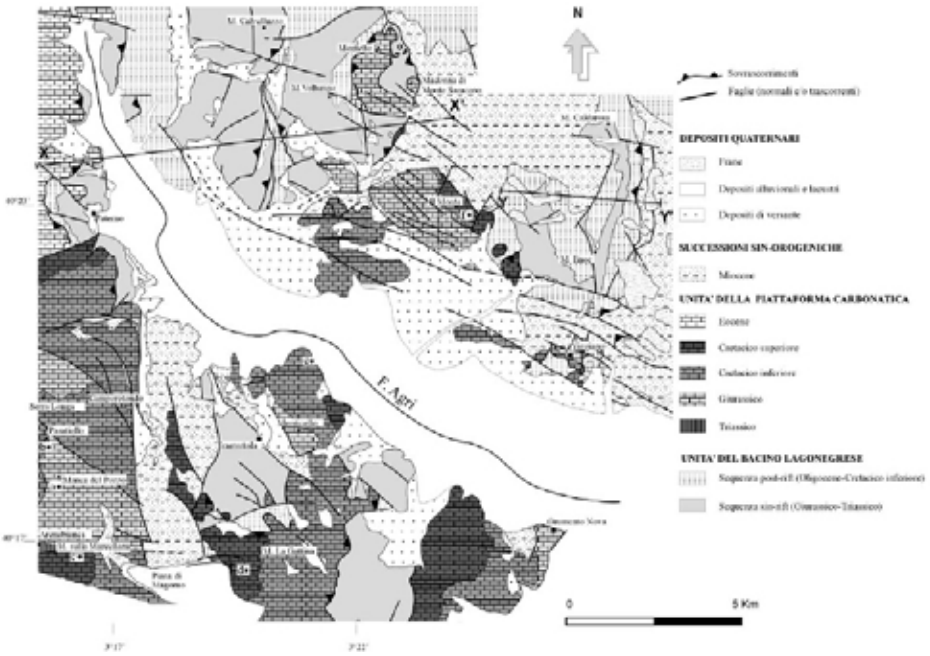

Figure 5. Geological sketch map of the high Agri River valley area (after Cello et al., 2004).

The complex Neogene structural history can be summarized as follows (Scandone, 1972; Lazzari & Lentini, 1991; Mazzoli et al. 2001; Cello et al., 2002; Ferranti et al., 2005):

1- early (pre-Tortonian) deformation is responsible for development of (present-day) ~N-S to NW-SE trending major buckle folds and subsequent out-of-limb thrusts which formed major pop-ups in the Lagonegro rocks. Buckling was favored by a pre-existing articulated passive margin architecture characterized by lateral juxtaposition of fault-bounded blocks;

2- early folding was followed by regional overthrusting of more proximal over more distal rocks of the Lagonegro basin (which is observed in the Val d'Agri along the Marsico Nuovo thrust, Fig. 6) and accompanied to detachment and eastward displacement of the Upper Cretaceous-Paleogene section of the Lagonegro basin (Fig. 4);

3- by Middle Tortonian, emplacement of the Monti della Maddalena imbricate had occurred on top of the already deformed Lagonegro assemblage (see truncation of Lagonegro folds and thrust sheets in Fig. 6); the platform to slope thrust sheet shows dramatic age and thickness lateral changes reflecting an earlier extensional deformation;

4- during the Pliocene, the accretionary wedge was thrust over the Apulia platform rocks and their cover (Fig. 4); regional overthrusting developed break-through thrusts onto the already imbricated wedge (e.g. thrust on right side in Fig. 6) and a thick mélange zone between the wedge and the underlying flexed foreland;

5- during the Late Pliocene-Pleistocene, the Apulian rocks were involved in shortening (Fig. 4); the ~N-S trending Miocene structures were superposed by (present-day) ~E-W structures related to ~N-S Pliocene-Pleistocene shortening, developing the interference pattern observed in all the assemblages of the upper wedge;

6- low-angle extensional contacts, mostly in the carbonate platform rocks, possibly developed during this last imbrication, although they may partly reflect an older (pre-orogenic?) or a younger deformation;

7- left-slip transtensive faults were active during Early-Middle Pleistocene and formed the modern Agri valley on the back-limb of a major anticlinorium in the Lagonegro nappe (Fig. 6);

8- NE-SW extension replaced left-lateral slip during Middle Pleistocene.

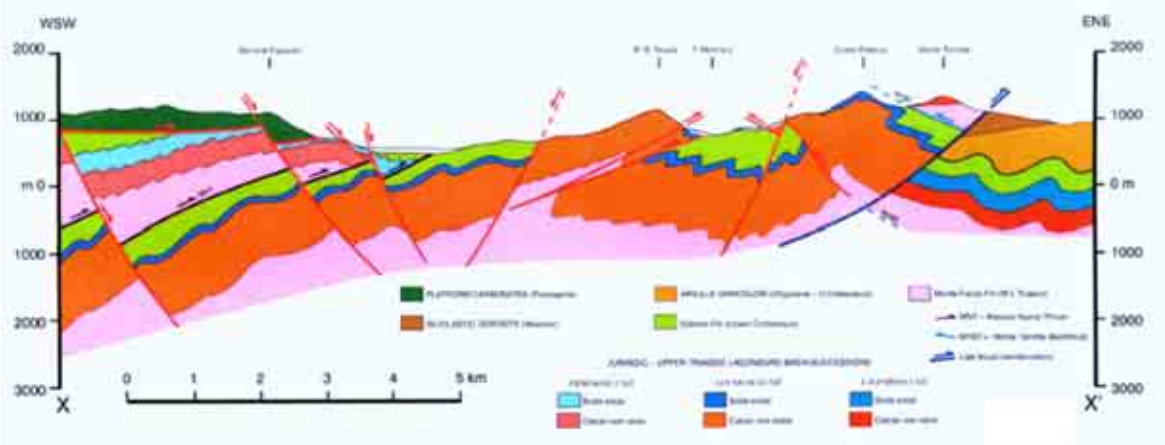

Fig. 6. Geological section across the High Agri Valley (after Cello et al., 2004). Location in Fig. 4.

Quaternary evolution

Quaternary deposits of the High Agri Valley are represented by Lower-Middle Pleistocene talus breccia (Brecce di Marsico, Di Niro and Giano, 1995), Middle-Upper Pleistocene alluvial-lacustrine sediments (Complesso Val d'Agri, Di Niro et al. 1992) and Upper Pleistocene-Holocene alluvial deposits (Figs 3, 7).

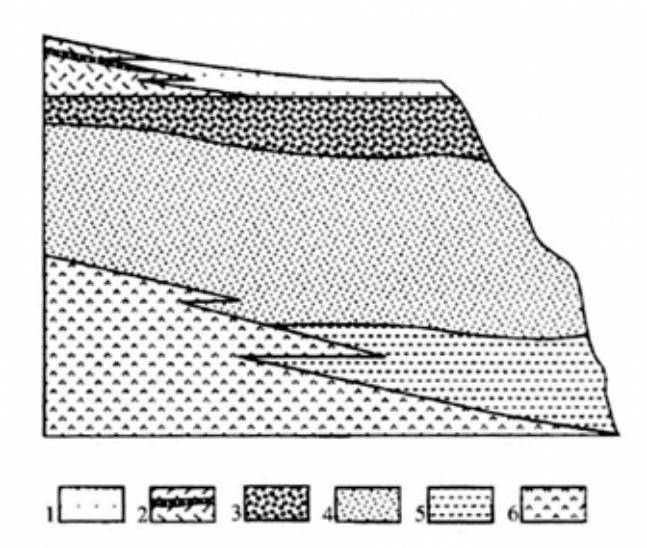

Figure 7. Stratigraphic relationships among Quaternary deposits (after Giano et al., 2000). Legend: (1) Recent colluvial and alluvial deposits; (2) coarse-grained slope deposits with interbedded palaeosoils (Holocene-Upper Pleistocene); (3) Complesso Val d'Agri: upper interval (Upper-Middle Pleistocene); (4) Complesso Val d'Agri: intermediate interval (Middle Pleistocene); (5) Complesso Val d'Agri: lower interval (Middle-?Lower Pleistocene); (6) coarse-grained slope deposits (Middle-Lower Pleistocene).

The Lower-Middle Pleistocene talus breccia are cut by transtensional faults and uplifted at various elevations along the north-eastern flank of the Val d'Agri. On the contrary, the Middle-Upper Pleistocene alluvial-lacustrine deposits, which outcrop in the southern portion of the valley, are only mildly faulted and are incised and terraced by the modern Agri River and its lateral streams (Fig. 3). Finally, recent alluvial

sediments of the Agri River mostly outcrop in the central and northern side of the basin, the latter displaying a flat morphology typical of an alluvial bottom valley.
Transtensional displacement on high-angle faults controlled the formation and evolution of the Val d'Agri basin during the Pleistocene. Turco and Malito (1988) first proposed a strike-slip origin of the basin, considering the valley as a pull-apart basin. More recent studies have singled out two main steps in basin development (Giano et al. 2000; Maschio et al., 2005). During Early-Middle Pleistocene, the ancestral Agri basin formed by left transtension on N120° trending master faults, which controlled the bulk of sedimentation at releasing bends. At this stage, master faults were mostly located at the eastern border of the basin. The left-oblique transtension was responsible for accumulation, tilting and uplift of the talus deposits and for deposition of alluvial to lacustrine sediments mainly in the southern portion of the High Agri Valley (Fig. 3). Starting from Middle Pleistocene, NE-SW extension on the same or newly formed master faults contributed to basin widening and subsidence.
During Quaternary, subsidence in the basin accompanied to generalized uplift of the area at ~0.6 mm/a (Schiattarella et al., 2003; Boenzi et al., 2004). A cumulative 1.2÷1.3 km of surface uplift led to formation of a flight of land-surfaces located at different elevations both around the mountain tops and along the valley flanks. Three generations of landsurfaces, hanging above the depositional surface on top of Middle Pleistocene alluvial conglomerate (580÷650 m a.s.l.) are recognized in the Maddalena mountain range, W of the Val d'Agri (Fig. 8).

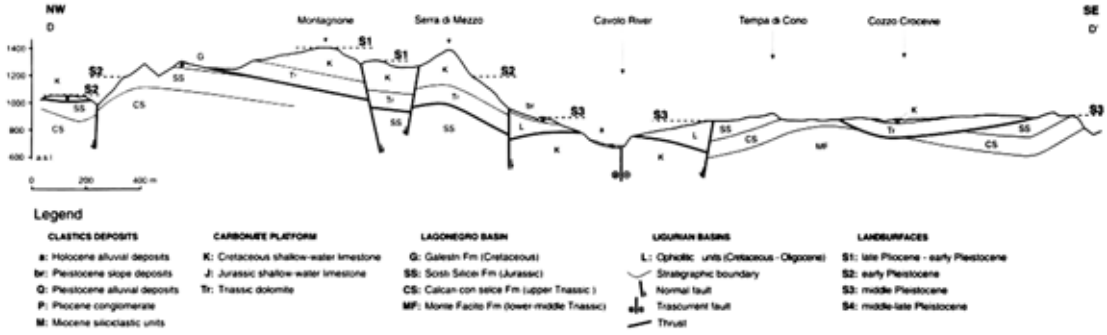

Figure 8. Morphostratigraphic section (vertical exaggeration ¼ 2x) from the Maddalena Mts. (after Schiattarella et al., 2003).

Based on the fact surfaces belonging to the same generation are found at different elevations across NE-dipping faults of the Maddalena range, slip rates of 0.5÷0.8 mm/a during the Sicilian (1.2÷7.8 Ma) are estimated for NE-dipping faults in this mountain range (Fig. 9; Schiattarella et al., 2003; Boenzi et al., 2004).

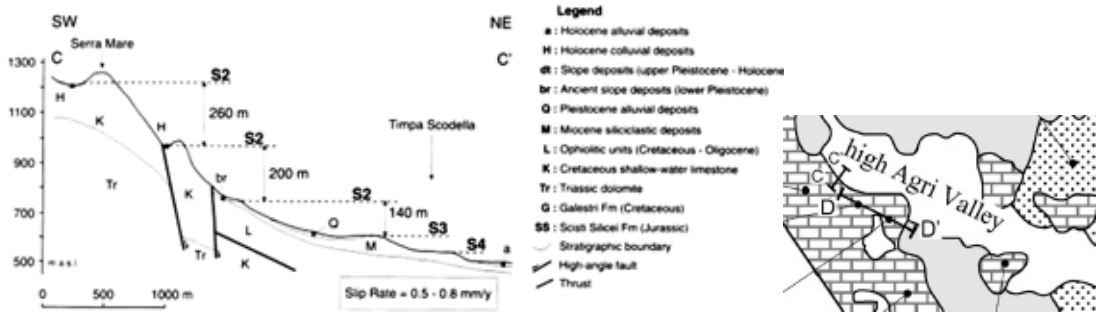

Figure 9. Detailed morphostratigraphic cross-section (vertical exaggeration ¼ 2x) from the Agri valley, adopted for slip rate calculation (after Schiattarella et al., 2003).

Basin architecture

The deep architecture of the basin related to Quaternary faulting and deposition is poorly imaged by conventional seismic profiles which are targeted to the oil-bearing top of the Apulia platform at depth >2-3 km. Schematic interpretation (Fig. 4; Menardi and Rea, 2000; Mazzoli et al., 2001; Shiner et al., 2004) as well published snapshots of seismic profiles (Fig. 10; Barchi et al., 2007) indicates throws of some hundred meters on faults located on the eastern side of the basin, and commonly do not show faults on the western side. In the seismic sections of Barchi et al. (2007), the basin fill is thickest on the eastern side and is found down few msec TWT (Fig. 10), roughly corresponding to a 3-400 m thickness.

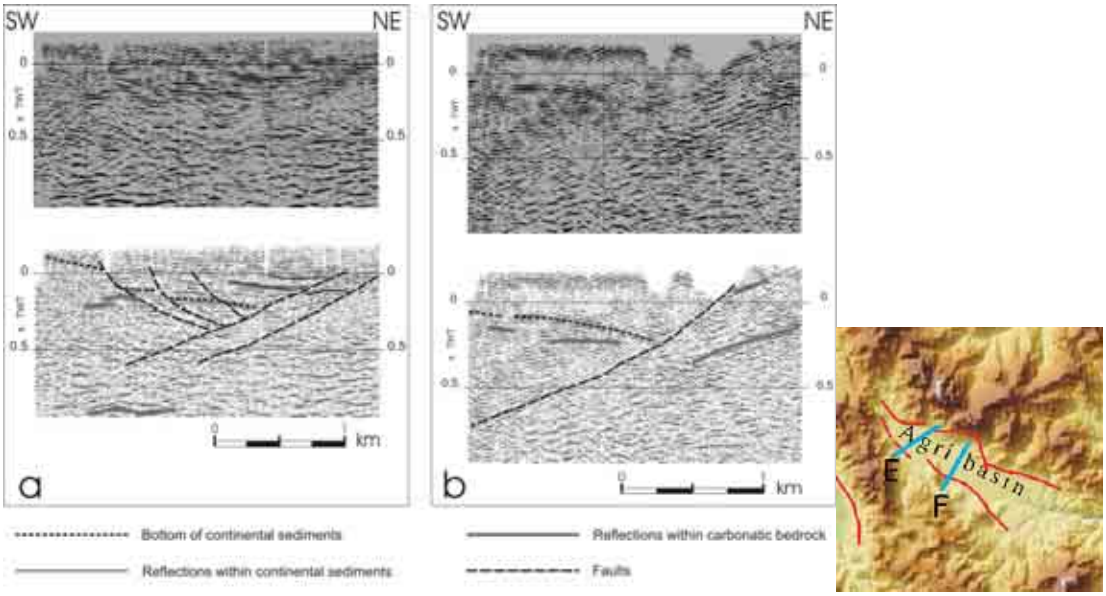

Figure 10. Seismic reflection profiles through the Agri basin, a=E and b=F in location map) (from Barchi et al., 2007).

Borraccinni et al. (2002) propose a 3D structural model of the basin based on extensive oil-exploration data. The model involves decoupling between most of the surface faults, which appear rooted within the melange zone above the Apulian platform, and deeper faults in the Apulian unit (Fig. 11). The main faults controlling the basin are two NW-striking and SW-dipping faults buried in the Apulian rocks in the center of the basin.

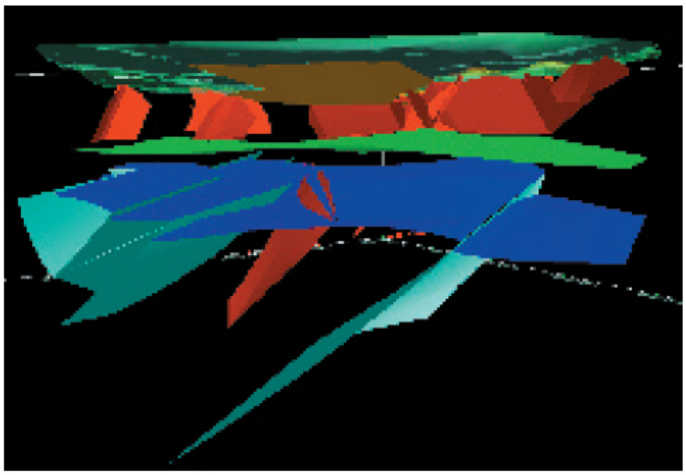

Figure 11. Three-dimensional structural model of the High Agri Valley, view from SE, showing lack of continuity between normal faults in the shallow layer (i.e. the allochthon, red) and those in the deep brittle domain (blue) (from Borraccinni et al., 2002)

High-resolution images of the shallow basin architecture have been provided by electrical resistivity tomography (ERT), which highlights the irregular shape of the basin (Colella et al. 2004). In longitudinal cross-section, the basin appears as a mosaic of fault-bounded blocks forming three different depocenters separated by intrabasinal highs (Fig. 12). In transverse cross-section, the basin is an irregular graben, locally asymmetric to the northeast, and with secondary grabens due to antithetic faults (Fig. 13).

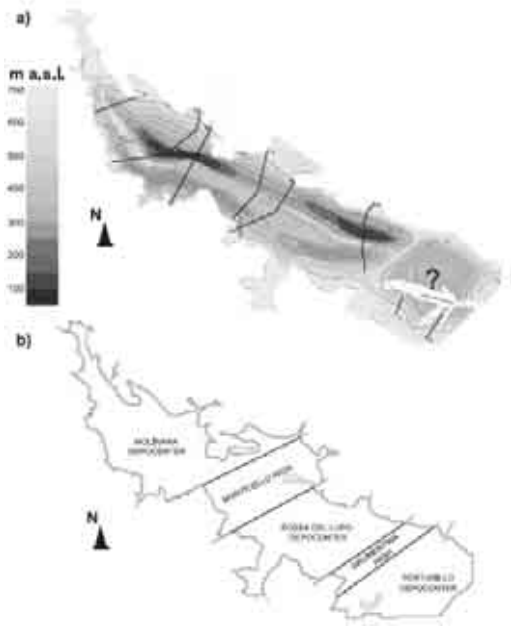

Figure 12. Sketch of the High Agri valley basin architecture inferred from interpretation of deep and shallow ERT and the analysis of stratigraphic data: (a) altitude (m a.s.l) of the top of the pre-Quaternary bedrock. (the transversal black lines are the ERT profiles). (b) The basin consists of three main depocenters separated by two structural highs. The maximum thickness of the basin fill occurs in the Molinara depocenter, the minimum in the Pertusillo depocenter (from Colella et al., 2004).

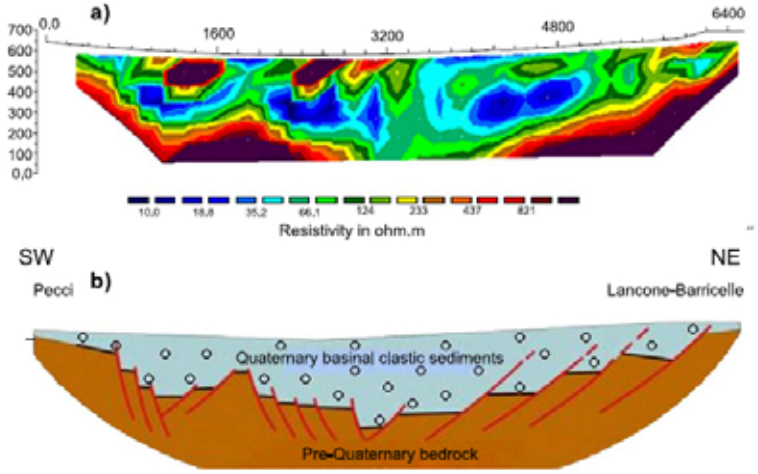

Figure 13. Electrical resistivity tomographic and interpretated geological sections transversely to the northern part of the High Agri Valley, showing the contact between the upper clastic basin fill and the lower pre-Quaternary bedrock, and inferred normal faults. The basin, up to 500 m deep, appear as an irregular graben with a minor graben due to antithetic faults (from Colella et al., 2004).

The study of Morandi and Ceragioli (2002) integrates high-resolution seismic and resistivity images and show changes in location and geometry of three low-resistivity bodies interpreted as the Quaternary filling of the valley (Fig.14). The two older bodies, which comprise the bulk of basin sediments (about 200 m), can be fairly correlated with the Early-Middle Pleistocene Brecce di Marsico and Complesso Val d'Agri sequences.

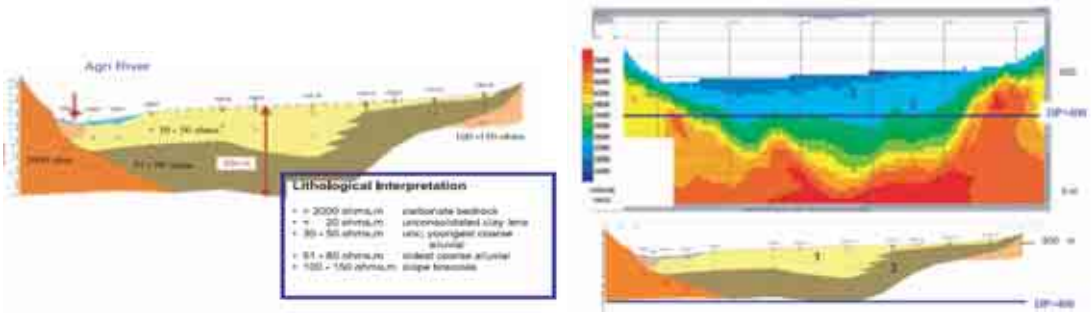

Figure 14. HR resistivity and tomography versus lithology (from Morandi & Ceragioli (2002).

These bodies are thicker along the eastern margin of the basin and may be interpreted as reflecting coeval SW-dipping faulting activity. Conversely, the overlying low-resistivity body represents an alluvial depocenter which thickens toward the west, and this is interpreted by Morandi & Ceragioli (2002) as reflecting recent fault control at the western side of the valley (Fig. 15).

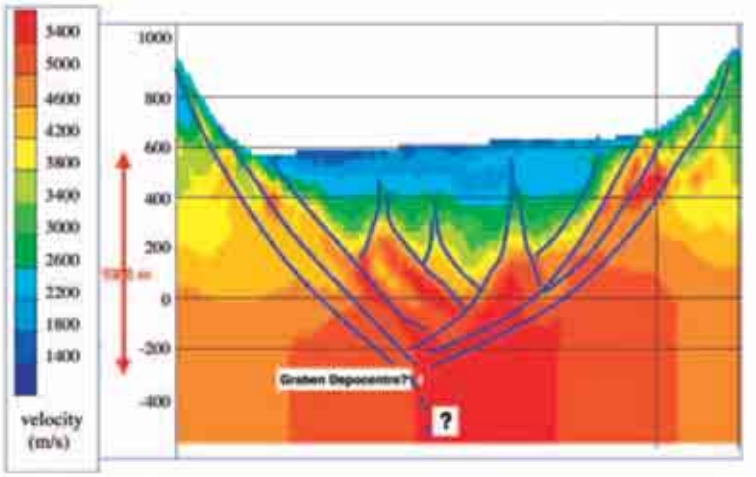

Figure 15. Near tomography velocity – depth section – structural interpretation of the Val d'Agri half-graben (from Morandi & Ceragioli (2002).

Quaternary fault systems and seismogenic structures

In the last decade, several Authors provided scientific contributions on activity and/or on seismogenic potential knowledge of fault systems in the Val d'Agri area and are here briefly summarized.

Early geological investigations of the 1857 earthquake immediately focused on the 20-km stretch of the High Agri Valley extending from Marsico Nuovo to Grumento Nova as the locus of its causative fault (Pantosti and Valensise, 1988; Burrato, 1995; Burrato, 2001, in DISS database v 2.0: Valensise and Pantosti, 2001b), proposing on the basis of geomorphic observations of drainage anomalies of the axial Agri River and analysis of the damage pattern, the existence of a major NW-SE trending, NE-dipping normal fault outcropping along the Monti della Maddalena range.

Benedetti et al. (1998) pointed out geomorphic evidence at different scales for active faulting along the Val d'Agri Fault System. From Marsico Nuovo to Montemurro villages they report a continuous scarp trace, about 30 km-long, arranged in 2.5 km-long segments, which strike NNE to WNW. The Authors stress that east of Marsico Nuovo, at Serra Calvelluzzo, 30°÷40°-dipping triangular facets apear to cut the steeper beds (60°W dip) of previously folded Mesozoic limestones and radiolarite, at the base of which a 15 m high cumulative scarp with smaller wine glass rill channels would indicate ongoing motion. Whilst at Il Monte, two further steep cumulative scarps can be traced, 10÷30 m high, which cut the base and the top of the Pleistocene slope suggesting a post-glacial motion.

Giano et al. (2000) documented recent and possibly ongoing tectonic activity of the whole perimeter of the Val d'Agri basin and for adjacent structural depressions by radiocarbon dating of samples from loose slope deposits and palaeosoils involved in faulting. Chronological constraints based on radiometric ages (39 and 18 ka) were firstly placed on extensional motion for this sector of the Southern Apennines.

Cello et al. (2000; 2003) mapped, along the eastern flank of the basin, a Quaternary kinematically coherent system (namely Val d'Agri fault system -VAFS) constituted of (1) N120-trending left-lateral strike-slip faults, for a total length of about 15 km (Cello et al., 2001), (2) N020°÷N030° trending, right-lateral faults, (3) N080°÷N100° trending, normal to left-lateral transtensional faults and N130°÷N150° trending, left-lateral transpressional faults. The SW-dipping active fault zone exposed along the northern flank of the basin is «tentatively considered as the surface expression of a local seismogenic source» and a few fault segments of both the VAFS and the Vallo di Diano fault system (DIFS) are considered active during the upper Pleistocene.

Based on seismic reflection profiles and other oil-exploration data, Borraccinni et al. (2002) suggested that two NW-striking and SW-dipping faults buried in the Apulian rocks in the center of the basin are the “big players” and as such are inferred to have the real seismogenic potential. Conversely, Hi-Re seismic and resistivity images allowed Morandi and Ceragioli (2002) to state that the active fault system rests on the western side of the valley and dips to the NE in order to account for the vertical and lateral distribution of different velocity and resistivity bodies.
Maschio et al. (2005) studied the relative contribution to basin evolution of the eastern border (EEFS or Eastern Agri Fault System) and western border (MMFS or Monti della Maddalena Fault System) faults, the latter firstly mapped in this work, and pointed out the main role of the MMFS in controlling the recent tectonic activity in the area as reflected in structural and geomorphologic data.
Barchi et al. (2007) showed the interpretation of a set of seismic reflection profiles across the Auletta, Diano and Agri basins, in the axial zone of the Southern Apennines. For the Diano and Val d’Agri basins, a similar half graben geometry is controlled by SW-dipping, normal faults.
Most recently, on the basis of a re-reading of the Mallet’s (1862) report and of the study made by Branno et al. (1983), Burrato & Valensise (2007) suggested that the 1857 earthquake ruptured in a cascade fashion two adjacent and relatively well known faults: first the smaller NE-dipping Melandro-Pergola fault, commonly believed to represent a seismic gap between the causative faults of the 1857 and of the 1980 Irpinia (Mw 6.9) earthquakes; then the larger NE-dipping Agri Valley fault proper.

Based on these works we outline in the following the Quaternary structural frame of the basin, which at surface is characterized by two fault system (Fig. 16). The main fault system controlling the basin formation is located on its eastern border and is known as Val d’Agri Fault System (VAFS; Cello et al., 2003) or Eastern Agri Fault System (EAFS; Maschio et al., 2005). Conversely, to the west in the Monti della Maddalena range, tectonic activity is documented on two NE-dipping fault branches forming the Monti della Maddalena Fault System (MMFS; Maschio et al., 2005).

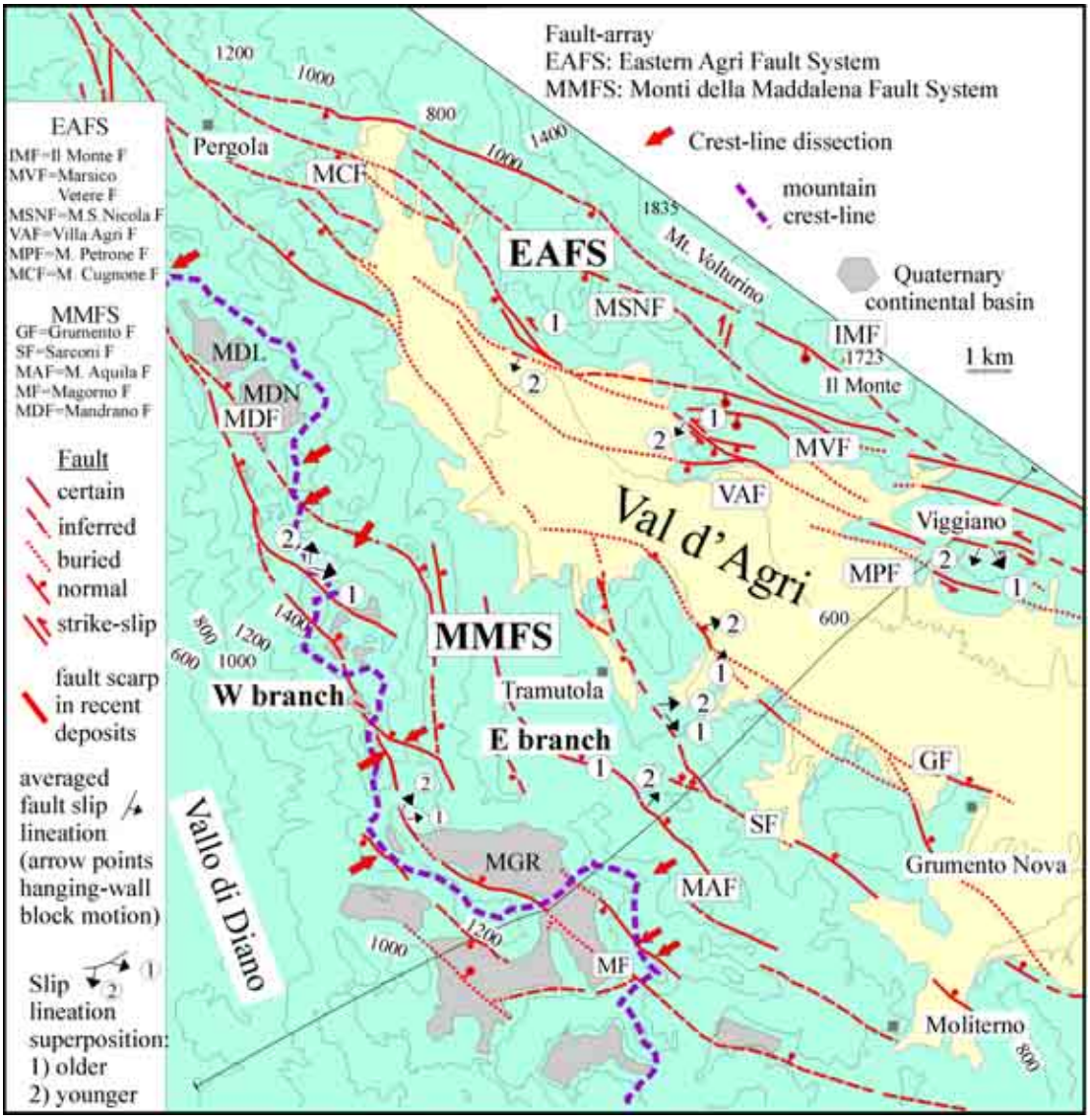

Figure 16. Morphostructural map of the High Agri Valley area showing the main Quaternary fault systems (modified after Maschio et al., 2005). Trace shows location of Fig. 17

The **EAFS** is composed of five main fault strands (MPF, VAF, MVF, MSNF and IMF, Fig. 16) which tend to anastomose and have several branches splaying off the main traces (Fig. 16). To the north, near the village of Pergola, the strands tend to merge. The fault strands show a fairly constant map spacing of about 1 km, are rectilinear and continuous in trace, are associated with mature fault-line scarps, and form a regular stair-case profile on the western mountain flank of the Mt. Volturino-Il Monte ridge. Branching points are characterized by marked bends in fault traces, which locally develop transtensional or transpressional features (Giano et al., 1997).

No detailed definition exists on the length of the fault system (see Gambini, 20XX), which based on mapped faults between Pergola and Viggiano villages is more than 25 km.
Fault kinematics analysis and mapping indicate a main left oblique-slip episode with NW-SE trending tensile axis (Cello et al., 2003; Maschio et al., 2005), lateral displacement in excess of 1 km (Gambini,, 2200xx) and integrated vertical (e. g. Barchi et al., 2007) displacement of about 500 m. Superposition of a second set of

~NE-SW slip lineations is observed on the lowermost fault strands, which are thus reactivated as normal (Maschio et al., 2005). Truncation of a ~32 ka paleosoil at Viggiano (Giano et al., 2000) occurred in response to this second slip episode.

The **MMFS** runs for about 25 km between Pergola and Moliterno villages. South of Pergola, the MMFS broadens and splits into two main branches (Fig. 13). Typically, faults are aligned with small basins perched at high elevation within the range or split the mountain crest (Fig. 16, red arrows). The western branch keeps a NNW-SSE strike and may be traced along the Mandranello and Mandrano basins (MDL and MDN in Fig. 16). Further to the south, it bounds the western side of the Magorno basin, but it becomes less defined south of Magorno.

The eastern branch can not be clearly identified in its northern part and might coincide with a swarm of small faults north-east of the MDL-MDN basins, which step down to the edge of Val d'Agri basin. Be as it may, the branch is well defined between Tramutola and Grumento Nova, where it splits in at least three strands (MAF, SF and GF in Fig. 16). Around the village of Moliterno, the two branches appear to splay into several subsidiary faults which progressively vanish in outcrop, and change their orientation toward a more easterly strike.
North of Pergola village, the MMFS apparently merges with the SW-dipping EAFS (Fig. 16). The northern boundary might not be located at Pergola, however, and, the MMFS might run further northward up to Brienza village for a total length of ~35 km. Thus, the estimated length of the MMFS ranges between 22 and 35 km.

Fault kinematic data reveal a prominent normal component of slip on the MMFS with computed average extensional slip vector between N30°÷N40°E (Fig. 16). A moderate throw (~300 m) is suggested by the offset of Miocene-Pliocene contractional structures. Additionally, relics of at least two generations of nearly horizontal erosional surfaces are found at about 1000÷1250 m and 950÷750 m a.s.l. across the mountain range. These surfaces are attributed to the Early (~1.2 Ma) and Middle (~0.75 Ma) Pleistocene, respectively (Schiattarella et al. 2003; Boenzi et al., 2004), and on the assumption that their elevation range is due to faulting, a post-Middle Pleistocene throw of ~200-400 m on the MMFS is plausible. Since the displacement on the MMFS is nearly normal, a slip rate of ~0.25÷0.55 mm/a is estimated for the whole fault system.
Near Pergola faulting with normal-oblique offset affects a debris deposit which includes a 21 ka old paleosoil (Giano et al. 2000) and even more recent deposits are faulted in this area (Moro et al., 2007). South of Tramutola, Late Pleistocene and Holocene deposits are faulted along the eastern branch (D'Addezio et al., 2007).

The morphologic and structural evidence of recent faulting accommodated along the MMFS is consistent with the observed behavior of the Agri River. Whereas foundering of the Agri basin and accumulation and faulting of lower-middle Pleistocene sediments occurred to the E and were controlled by motion on the EAFS, the locus of middle-late Pleistocene to Holocene subsidence and sedimentation appears shifted to the west (e. g. Morandi and Ceragioli, 2002). This is documented by the aggrading behavior of the recent alluvial plain in the upper part of the valley, which is coincident with the westerly asymmetric position that the Agri River keeps along the early part of its course. These anomalies point to active shift of the river course and evidence for a subsiding area toward the western border of the Agri basin, suggesting progressive displacement on the NE-dipping MMFS (Maschio et al., 2005).

The localized subsidence along the western side of the Agri basin is competing with a background regional uplift (Bordoni & Valensise, 1998; Ferranti & Oldow, 2006;

Schiattarella et al. 2003) which is documented in the area by the deep dissection of the Middle Pleistocene depositional surface and formation of strath terraces (Di Niro et al. 1992; Di Niro & Giano, 1995). Quaternary uplift rates established for the axial zone of the Lucania Apennines range from 0.2 to 1.2 mm/a and have maximum values in the Val d'Agri area (Schiattarella et al. 2003). Thus, the longitudinal behavior of the Agri River and of its recent alluvial valley, with differential base-level variations between the north-western aggrading section of the valley and the south-eastern part which is undergoing erosion, results from the superposition of tectonic subsidence produced by the MMFS upon a ~1 mm/a of regional uplift.

Deep geometric relationships between the EAFS and MMFS

Although geomorphologic and structural observations suggest active deformation is concentrated within the Monti della Maddalena range, a kinematic co-ordination during recent slip between the EAFS and MMFS is viable. This is suggested by the presence of the second-generation slip lineations on segments pertaining to both fault systems, and by the occurrence of faulted Late Pleistocene-Holocene palaeosoils on both sides of the valley (Giano et al. 2000; D'Addezio et al., 2007).

Figure 17, based on the work of Mazzoli et al., 2000, illustrate the main characteristics of the two fault systems at depth in the seismotectonic context of the area: (1) they cut at different depths the thrust surface which emplaces the Apenninic thrust system over the Apulia foreland plate the throw is limited and thus cannot be resolved in conventional seismic profiles; (2) displacement does not solely occur at the contact between the mountain front and the Val d'Agri basin, but fault strands of the MMFS with comparable throw are distributed within the Monti della Maddalena range; (3) the integrated throw for the MMFS provided by offsets of buried thrusts (Mazzoli et al. 2000) is about 300 m and is superposed to a larger scale bulge of the thrust system with tens of km wavelength; (4) whereas faults of the eastern branch of the MMFS clearly dip towards NE, dip direction for faults of the western branch is less obvious since they lay in close proximity with a SW-dipping fault system (Vallo di Diano Fault, VDF). The VDF accrued almost 1 km of throw (Catalano et al. 2004) and controlled the evolution of the Vallo di Diano basin (Ascione et al. 1992), largely coeval to Early-Middle Pleistocene slip on the EAFS. Geometric truncation of the EAFS against the eastern branch of the MMFS is consistent with the field-based contention concerning the MMFS' activity is more recent than that for large part of the motion on the EAFS.

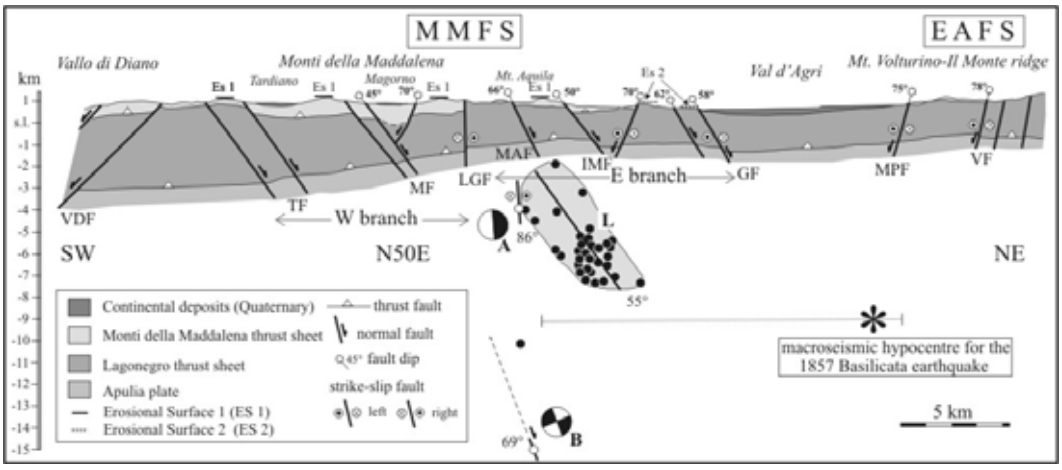

Figure 17. Profile showing the deep geometry of the Monti della Maddalena fault system (MMFS) and Eastern Agri fault system (EAFS) derived from integration of geological and seismicity data. Geometry of the thrust stack after the interpreted

seismic profile of Mazzoli et al. (2000). Surface fault dips are derived from field data; crustal dips are inferred from nodal planes of focal mechanisms (here shown in vertical projection) and 1996 sequence cluster elongation (redrawn from Cucci et al. 2004). Hypocentral depth for the 1857 Basilicata earthquake as calculated in Branno et al. (1985) is also plotted, as well as the uncertainty bar of maximal isoseimal line of its related macroseismic field (from Maschio et al., 2005).

Figure 17 also displays the present deformation pattern derived from instrumental and historical seismicity down to a depth of ~15 km (Branno et al. 1985; Gasparini et al. 1985; Cucci et al. 2004). Although the instrumental seismicity is low in the Val d'Agri, it spatially coincides with the MMFS. The seismic activity on faults of the MMFS is documented by the well elongated 50° NE-dipping cluster of the 1996 $2.1 \leq M \leq 3.0$ seismic sequence (Cucci et al. 2004). Furthermore, the 1980 Md 4.2 event (B in Fig. 17) might be nucleated on the NE-dipping plane, which has a high-angle dip as commonly observed for upper crustal earthquake ruptures and recent normal faults in the Campania-Basilicata region (Westaway and Jackson, 1987; Hippolyte et al. 1994).

The M. Aquila Fault

The most thoroughly investigated recent structure in Val d'Agri is the M. Aquila Fault (MAF), one strand of the eastern branch of the MMFS (Fig. 16) where multidisciplinary geological and geophysical studies have been conducted in the last few years following early documentation of active motion (Maschio et al., 2005; D'Addezio et al., 2007).

The NE-dipping MAF consists of a main northern segment which is ~10 km long and two smaller segments with cumulative length of ~10 km, thus bringing the total length to ~20 km; the three segments are arranged in a right-stepping en-echelon pattern (Fig. 18). Detailed work has been focused along the southern ~5 km stretch of the northern segment (inset in Fig. 18).

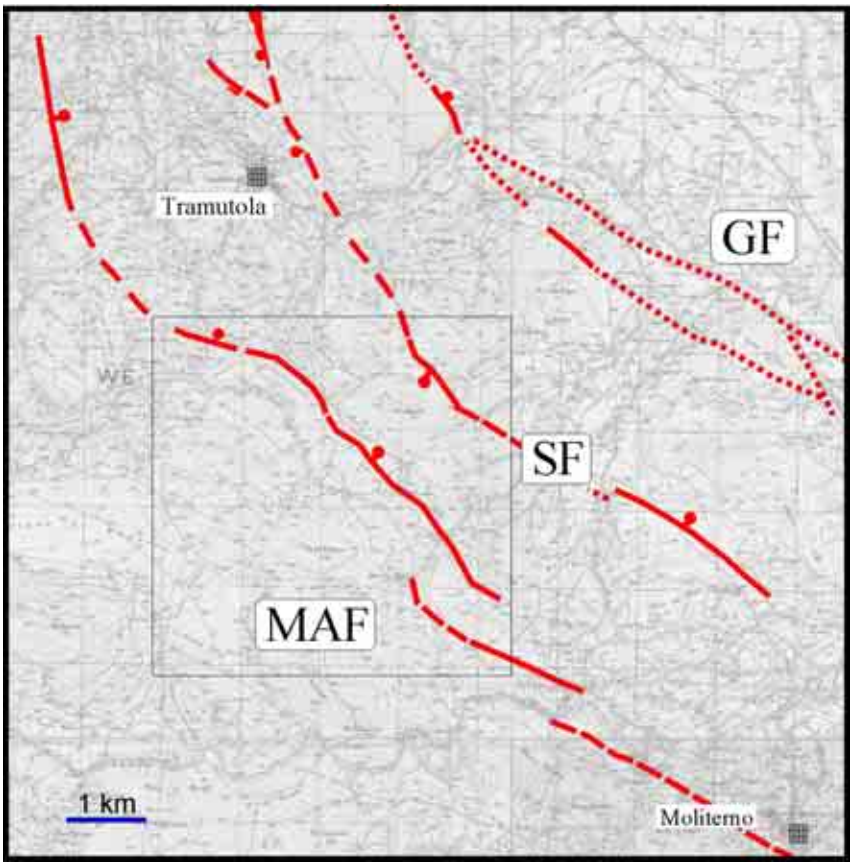

Figure 18. Map of the M. Aquila fault (MAF) and Eastern branch of the MMFS (SF=Sarconi Fault and GF=Grumento fault). Inset locates Fig. 19.

This part of the northern segments is itself composed of individual scarps (Fig. 19) The fault has been traced combining on-strike outcrops of bedrock slip surfaces (e. g. Cava site), scarps in colluvium and soil (Giano Pepe, Scarpata and Covoni site) and geomorphic anomalies (e.g. Fiumicello site), supplemented by extensive paleoseismological trenching and electrical resistivity and seismic tomographic imaging (Giano Pepe, Scarpata, Trincea, Covoni, Fornace and Petenella sites).

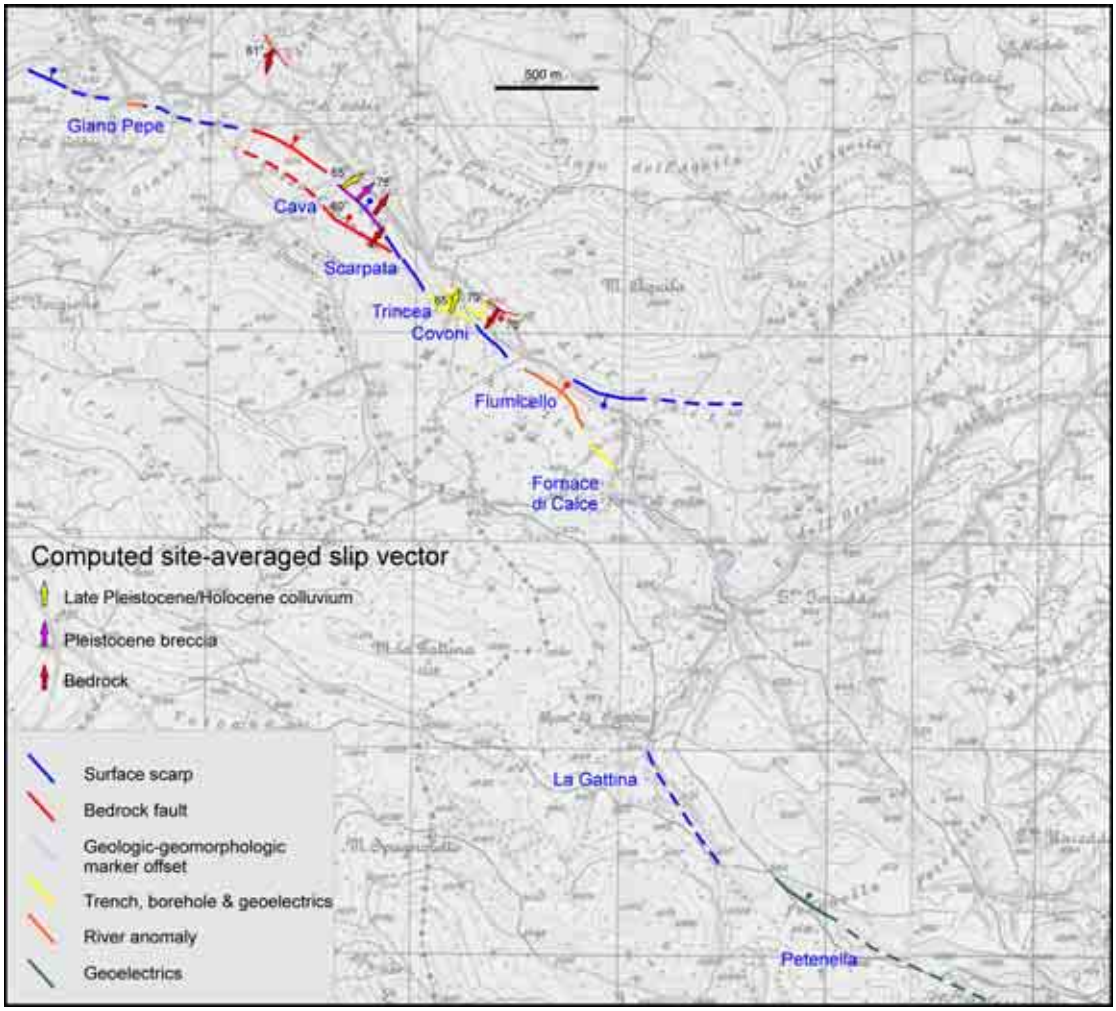

Figure 19. Map of the central part of the M. Aquila fault.

This sector of the MAF has an average NW-SE strike and turns to WNW in the north (Giano Pepe segment, Fig. 19), possibly to accommodate left-stepping linkage with a NNW-SSE striking segment west of Tramutola (Fig. 18). Single scarps between Giano Pepe and Fornace sites are arranged in right-stepping en-echelon fashion (similar to the arrangement between segments, e.g. from Fornace to La Gattina-Petenella) mainly in the southern part of the fault (from Scarpata to Fornace sites, Fig. 19).
Locally, two or more sub-parallel scarps or fault zones (m-scale shear zones made of closely-spaced faults) have been observed both in bedrock and in colluvium exposed in trenches (e. g. Trincea and Covoni sites). Minor-length antithetic faults, both bedrock and scarp in soils, splay locally from the main fault trace (Fig. 19).
The dip of the fault planes (both on the MAF and on synthetic faults), where observed in surface exposures or in seismological trenches, is quite high, ranging from 65° to 80° (Fig. 19).
Although evidence of older left-lateral slip has been observed on bedrock fault surfaces, the main slip recorded on the fault is related to NE-SW extension (Fig. 19). This extension direction has been computed by fault slip inversion from exposures of fault planes in Mesozoic rocks, in Pleistocene breccia cemented to a various degree, and from faults juxtaposing bedrock and alluvium dated to the last 40 ka. Thus, main motion on the M. Aquila fault is chiefly extensional as displayed by computed pseudo-focal mechanisms for the northern (Cava site) and central (Trincea) parts of this sector (Fig. 20).

The right panel in Figure 20 shows the slip lineations collected on the main fault exposed in the paleoseismological trench at Trincea site. The derived focal mechanism is transtensional and has a T-axis trending N19°E, in good agreement with the T-axes derived from inversion of bedrock fault slip lineations along the MAF (Fig. 19), and with the seismologically recorded T-axis in the region.

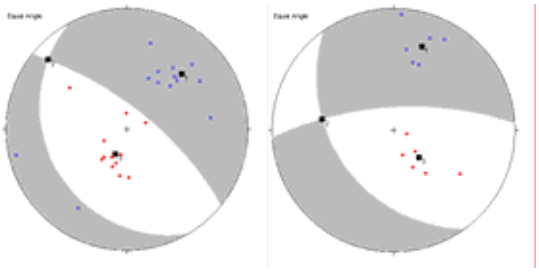

Figure 20. Pseudo-focal mechanisms for the northern (left) and central (right) sectors of Fig. 19.

Recent displacement on the MAF has led to the growth of small intermontane basins aligned along the fault (e. g. Macchitelle and Macchia Lombardi basins, Fig. 21).
Estimate of the total throw on the MAF is provided by displacement of geological markers. At Fornace site, a low-angle thrust, emplacing the Monti della Maddalena carbonates above the Lagonegro argillite shows ~50 m vertical offset across the MAF (right lower corner of Fig. 21).

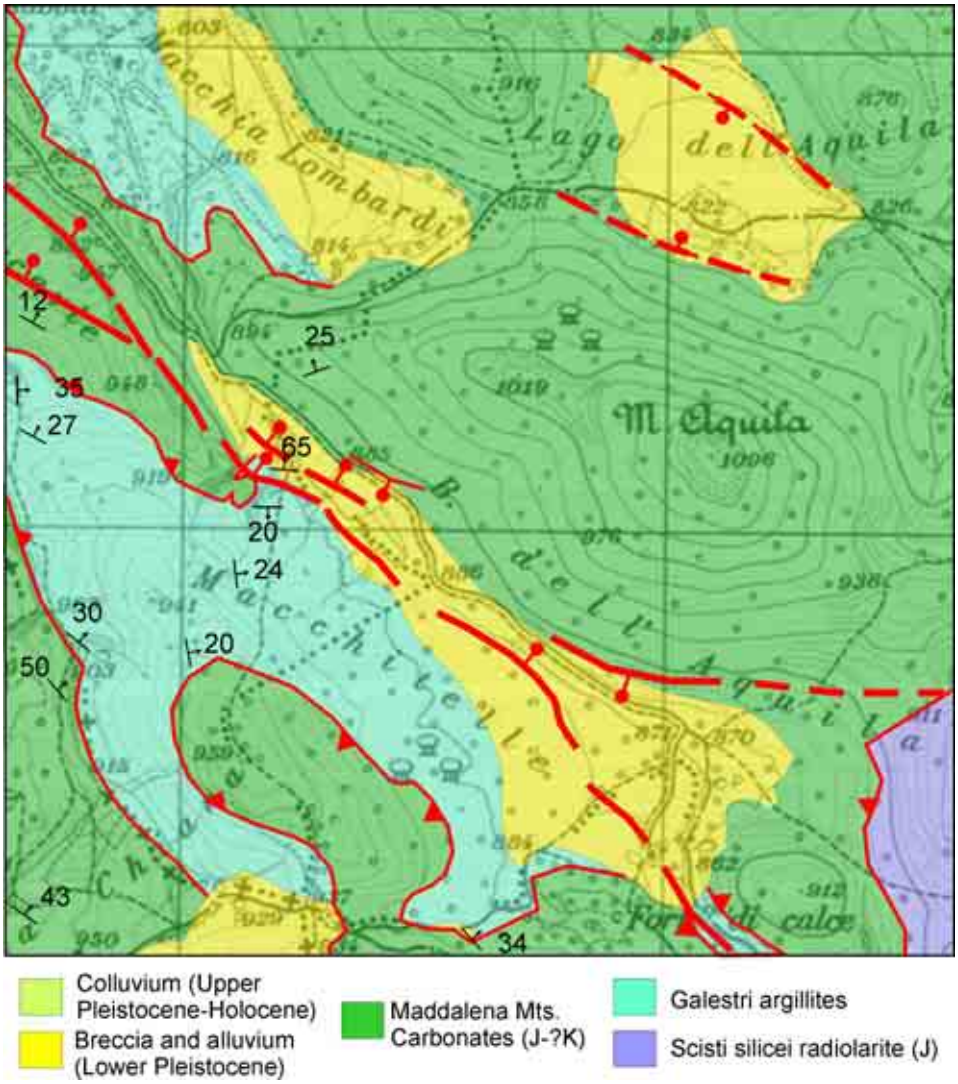

Figure 21. Geological map of the central part of the M. Aquila fault northern segment

Comparable values are estimated by the offset of two ancient erosional surfaces of probable fluvial origin, whose relics are locally preserved in the area (Fig. 22). Specifically, relics of a surface assigned to the Middle Pleistocene (cfr. Boenzi et al., 2004) rests at ~950 m in the footwall and is dropped down to ~900 m in the hanging-wall of the MAF to the NE (Fig. 22). Given a 0.73 Ma age of the youngest surface, a minimum slip rate of 0.07 mm/a is estimated, but it is probably a very conservative value. Comparison with the longer term (~0.73 Ma) estimate for the whole MMFS (~0.25÷0.35 mm/yr.), suggests that the MAF in the eastern branch has accommodated about one fourth of the cumulative displacement rate.
Limited vertical offsets of few tens of meters are also jointly recorded by the resistivity and seismic tomographic images (see Stop section). This offset nearly matches the vertical throw estimated from displacement of geological and geomorphological markers (Fig. 21 and 22).

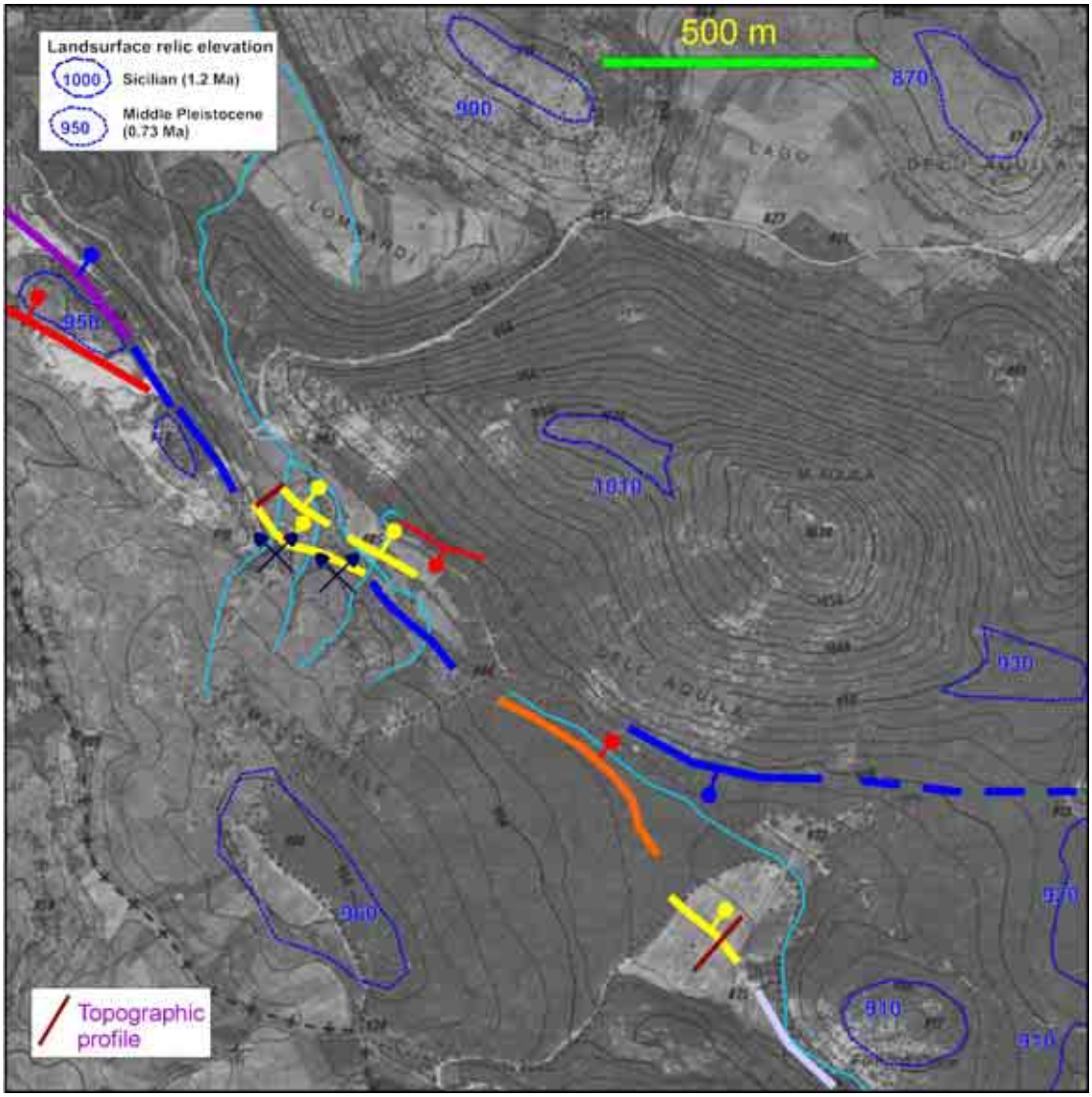

Figure 22. Geomorphological map of the central part of the M. Aquila fault northern segment. Mine symbols indicate paleosismological trenches.

The scarp associated to the MAF is relatively well exposed in the ~1 km long Macchitelle basin (Fig. 21). Here, the MAF is composed of six scarplets locally arranged en échelon. Whereas a left-en échelon arrangement of scarplets is found in the northern part of the basin, a right-en échelon pattern is found at morphologic saddles in bedrock (e.g. Cozzi Crocevie to the north, and east of Fornace di Calce to the south, Fig. 21).
Detailed micro-topographic profiles across the main scarp (Fig. 23) show a cumulative morphologic throw of ~3.5 m. This estimate is consistent in different locales even in presence of variable dips of the scarp, which can be related to difference in erosion retreat processes for different lithologies. Where the MAF cuts across carbonate rocks (Cozzi Crocevie ridge, NW part of Fig. 21), the scarp is best preserved in the overlying soil, has a nearly 60° dip (Fig. 23) and reaches several ten of meters in length, locally exposing fault surfaces in carbonate rocks.
On the other hand, where the fault affects the argillite of the Lagonegro assemblage (e.g. Fornace di Calce site), the scarp shows a lower dip of 30°÷40° (Fig. 23). At Fornace di Calce site, the scarp displays two distinct slope surfaces characterized by dip angles of α=13° and β=19°, respectively (Fig. 23). The steeper slope (β=19°) is embodied in the gentler one and is presumably younger. Values of morphologic

throws on the two slope surfaces are 1.8 m and 3.5 m, respectively, suggesting the more gently dipping surface has cumulated two distinct slip episodes with a comparable throw of ~1.8 m. Similar value are estimated by recent detailed bore-hole analysis (see Stop section).

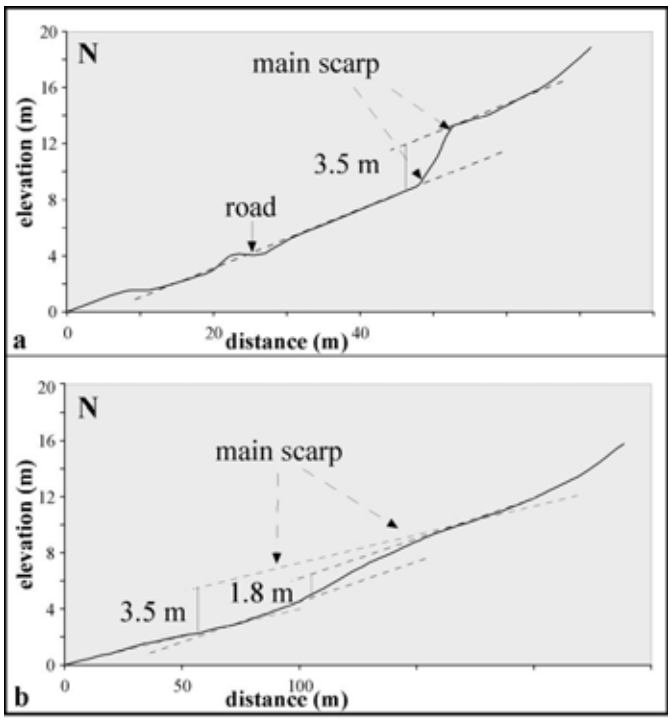

Figure 23. Detailed microtopographic profiles across the Mt Aquila fault scarp (location in Fig. 22). Profile (a) at the Cozzi Crocevie site, the main scarp is a well preserved prominent feature with a 3.5-m vertical displacement of the topographic surface; profile (b) at the Fornace di Calce site, the scarp is diffused for over 80 m and shows two distinct morphologies of the topography (from Maschio et al., 2005).

Several arguments allow discarding a gravitational origin for the scarp and for the fault itself. Firstly, the fault may be traced, although with variable geomorphic expression, across different lithologies, and attains a nearly equal cumulative throw at different locales (Figs. 21 and 22). Second, the fault runs both along small basins and across saddles between adjacent ridges. Finally, the scarp dips to the NE towards both lower and higher elevations, the highest local elevation (Mt. Aquila, 1098 m a.s.l.) being located in the hanging-wall of the MAF.
Throws estimated on the surface scarp are grossly consistent with slip per event retrieved in paleoseismological trenches at Trincea and Covoni sites (see Stop section).
The E-W strike of the trench main fault results in a dextral strike-slip component (Fig. 20, right) which is consistent with the observed flower structure in the clastic sequence (see Stop section).
On the other hand, faults with strike north from ~290° are predicted to have an increasing component of sinistral displacement. Thus, the left-lateral stream and ridge offset coinciding with the fault trace (Fig. 22) might indicate that the fault has a ~NW-SE strike aligned with the main trace of the MAF. All the observation suggests that the E-W striking fault in the trench represents a small releasing bend of the MAF and thus accommodate basin deposition at this site.

Historical and instrumental seismicity

The axial zone of the Southern Apennines is the locus of major historical and instrumental seismicity (Fig. 24). The Mw 7.0 1857 earthquake is classified as one of the strongest events by the Italian seismic catalogues, and hit the region southwest of the epicentral area of the Ms 6.9 1980 Irpinia earthquake. Southwest of the Val d'Agri area no major historical earthquakes are reported. However, the Ml 5.5 1998 Castelluccio earthquake and a medioeval event discovered by means of palaeoseismological trenches on the Castrovillari fault (Cinti et al., 2002) highlight the activity of some seismogenic sources in this area, otherwise considered as a seismic gap.

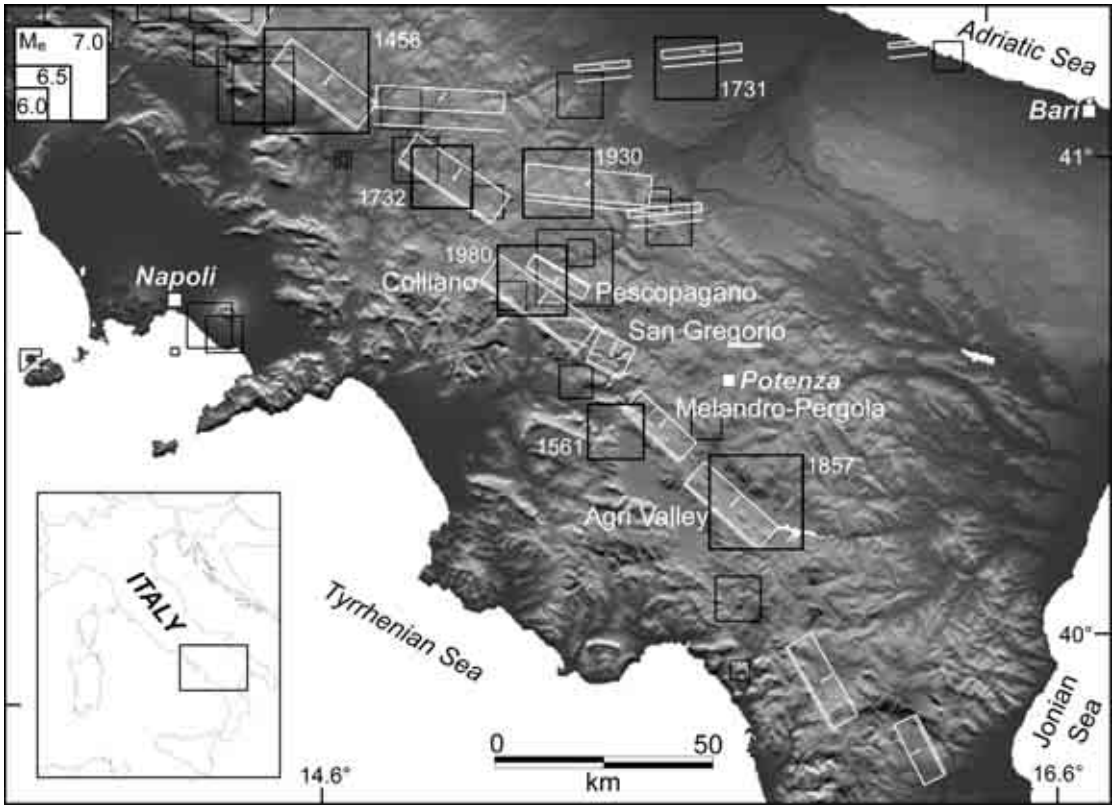

Figure 24. Distribution of Southern Apennines seismicity from the Catalogo dei Forti Terremoti in Italia (Boschi et al., 2000), and surface projection of individual seismogenic sources from DISS database, shown as rectangles (DISS Working Group, 2007; Basili et al., 2007; http://www.ingv.it/DISS/). The line next to the rectangle is the fault cut-off. The stick inside each rectangle indicates the sense of slip (from Burrato & Valensise, 2007).

Some important earthquakes fall outside of the main extensional seismogenic trend that follows the Apennines axes. These historical and instrumental events located east of the chain have been interpreted as due to the activity of regional E-W trending shear zones (Fracassi & Valensise, 2007; DISS Working Group, 2007). The Irpinia region is bounded to the south by one of these trascurrent shear zones, that is the source of the Mw 5.8 1990 Potenza earthquake (Di Luccio et al., 2005).

Present-day seismic activity of the Val d'Agri broad region is represented by low-magnitude back-ground seismicity. The only two seismic sequence registered, with M_{wmax} 4.4, were localized close to the northwestern margin of the Melandro-Pergola basin (2002 earthquakes), and near the southeastern termination of the eastern branch of the MMFS (Fig. 25, Cucci et al., 2004).

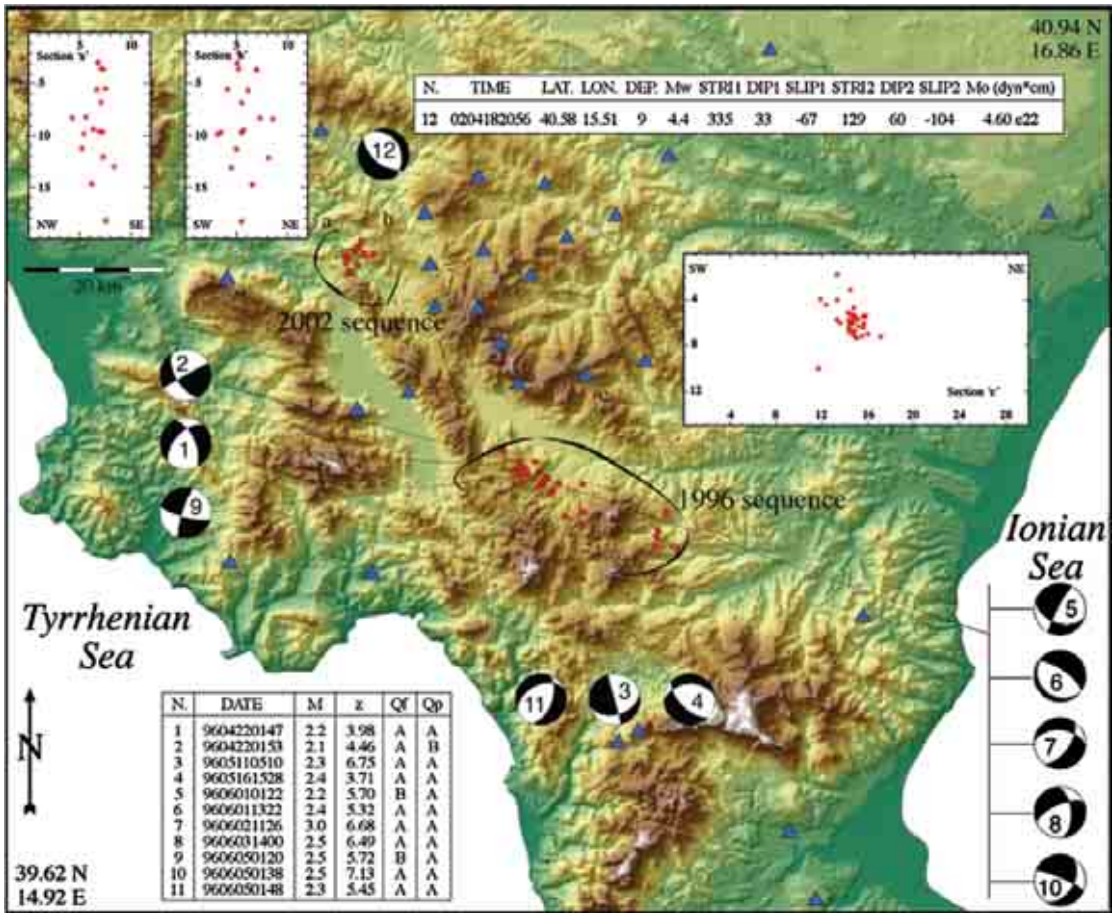

Figure 25. Map showing the localization of the 1996 and 2002 seismic sequences, and the corresponding focal mechanisms (1-11, 1996 sequence; 12, main shock of the 2002 sequence) (from Cucci et al., 2004).

The 1857 earthquake

The catastrophic earthquake that struck southern Italy on 16 December 1857, killing over 11,000 people (19,000 according to unofficial sources) and causing widespread destruction in the High Agri Valley (HAV), Melandro-Pergola Valley (MPV) and Vallo di Diano (VD) (Fig. 26). The earthquake generated considerable interest among contemporary European scholars, some of whom traveled a long way to survey the earthquake effects. Among them was Robert Mallet, the founder of Seismology as the science that investigates the shaking of the Earth and that he regarded as "*...the youngest branch of cosmical science...*" (Mallet, 1848). Soon after the earthquake Mallet sought a grant from the Royal Society of London that would allow him to make a reconnaissance journey through the region struck by the earthquake. He was prepared to devote "*...a month or five weeks to the enquiry...*", and considered that "*... for this a sum of about One Hundred and Fifty Pounds would.... be required...*" (from Mallet, 1862; page IX of Preface). Eventually Mallet's proposal was accepted, although the expedition turned out substantially more expensive and nearly twice as long as originally envisioned. Upon his return to England in April 1858 Mallet started collecting his experience in a volume (Mallet, 1862) that represents one of the most important contributions to the early development of Seismology and that has been recently been rediscovered and republished (Melville and Muir Wood, 1987; Ferrari, 2004).

Mallet reached the HAV from the VD (Fig. 26) crossing the southern termination of the Monti della Maddalena range and passing by the Magorno Plain, which at that

time was a lake (*Lake Maorno*). He spent a considerable amount of time in the VD inspecting heavy damage suffered by Polla, one of the largest settlements of the area, and a number of smaller villages. Unbeknown to him, he was only at the outskirts of the true meizoseismal area, the large concentration of damage having been caused by extensive and sustained site amplifications at Polla and its nearby villages (Mucciarelli et al., 1999). He later inspected all villages settled on both sides of the HAV, reporting the damage sustained by buildings as well as natural phenomena that accompanied the earthquake (Fig. 26). In spite of the earthquake magnitude, similar or even greater than that of the surface breaking, 23 November 1980, Irpinia event (Mw 6.9) that occurred a few tens of km further to the northwest (Fig. 24), during his visit Mallet did not describe any evidence that could be positively ascribed to surface faulting.

The earthquake was generated along the well-known Apennines-top seismogenic trend (Pantosti and Valensise, 1988; Galadini et al., 2001; Valensise and Pantosti, 2001a). Although no instrumental evidence exists for such an old earthquake, its location, the characteristics of the modern seismic release in the region (e.g. Cucci et al., 2004; Vannucci and Gasperini, 2004), the nature of the modern stress field (Montone et al., 2004), residual GPS velocities (Ferranti et al., 2007) and the abundant active tectonics evidence (Maschio et al., 2005; Galli et al., 2006; Moro et al., 2007), all suggest that the 1857 event was caused by normal faulting along a NW-trending plane.

Overall, the tectonic style of the 1857 earthquake appears to be very similar to that of the well-investigated 1980 earthquake, yet there has been considerable debate over the exact geometry and kinematics of its causative source (e.g. Benedetti et al., 1998; Borraccinni et al., 2002; Cello et al., 2003; Galli et al., 2006; Maschio et al., 2005).

Modern automatic analyses of intensity data yield an equivalent moment magnitude 7.0 (Gasperini et al., 1999; CPTI Working Group, 2004), making 1857 one of the largest Italian earthquakes of all times and implying a rupture length of roughly 50 km (Wells and Coppersmith, 1994) (see black rectangle in Fig. 26).

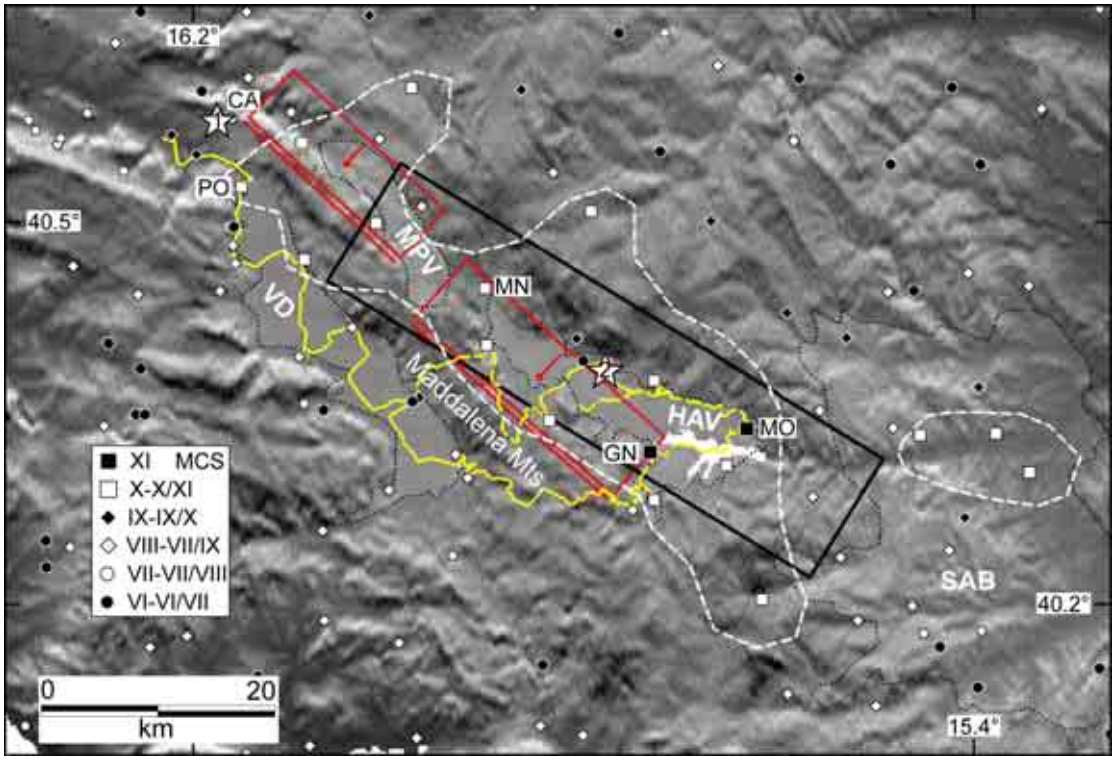

Figure 26. Intensities available for the 16 December 1857 earthquake (MCS scale) from a study reported in the Catalogo dei Forti Terremoti in Italia (Catalogue of Strong Italian Earthquakes: Boschi et al., 2000), plotted over the Melandro-Pergola (to the northwest) and Agri Valley (to the southeast) seismogenic sources from the DISS database. A white dashed line contours all intensities X and above. The black rectangle is the macroseismic source derived by automatic analysis of intensity data (Gasperini et al., 1999). The stars numbered 1, 2 are the epicenters proposed by Mallet and obtained by automatic analysis (Gasperini et al., 1999; Boschi et al., 2000), respectively. The yellow line with arrows highlights the route followed by Mallet in the Vallo di Diano and High Agri Valley (see text). Basins: HAV, High Agri Valley; MPV, Melandro-Pergola Valley; SAB, Sant'Arcangelo Basin; VD, Vallo di Diano. Localities: CA, Caggiano; GN, Grumento Nova; MN, Marsico Nuovo; MO, Montemurro; PO, Polla.

The earthquake caused extensive damage over an exceptionally large area. Intensity X and larger (MCS scale) were reported over a 900 km^2 region (Fig. 26). Most of the damage was suffered by the HAV, although intensity IX and X reports are spread over a region extending from the northern end of the VD to the Sant'Arcangelo Basin. The HAV is also the geographic area where Robert Mallet spent most of his time. As a result of these circumstances the 1857 is commonly referred to as the "Val d'Agri earthquake", in spite of it having generated considerable damage outside the HAV proper.

A careful examination of 1857 earthquake reports suggests that a significant foreshock occurred about two minutes before the mainshock. According to Branno et al. (1983), this foreshock was a significant (M 6.0 or larger) event that produced damage in an area located to the north of Val d'Agri and roughly corresponding with the Melandro-Pergola basin (Fig. 27). This area falls within the largest intensity isoseismal as mapped by Mallet in 1858, and almost entirely within the intensity X area of Boschi et al. (2000) (Fig. 26).

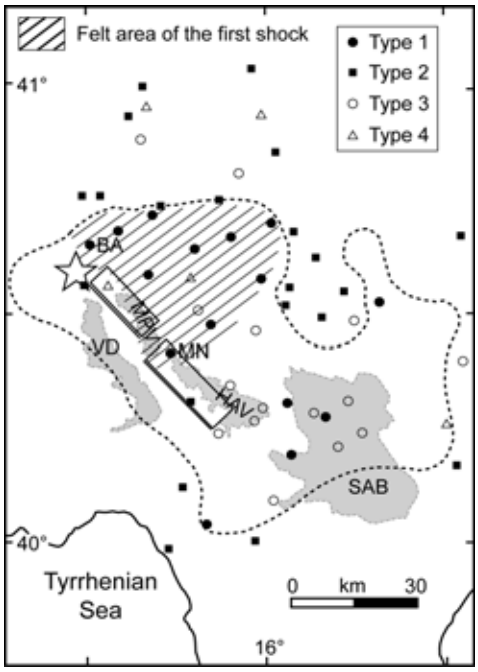

Figure 27. Intensity VIII contour for the 1857 earthquake and the area (highlighted with diagonal bands) where the first shock was distinctly felt (from Branno et al., 1983, redrawn). Type 1 and 2 localities are those where people were able to distinguish the two shocks (solid circles and solid squares, respectively); Type 3 are

those localities where only one large shock was felt; Type 4 are localities not evaluated. Notice that the intensity pattern obtained by Branno et al. is different from that later published by Boschi et al. (2000), shown in Figure 26. Also shown are Quaternary basins (outlined by a hachured pattern), relevant DISS seismogenic sources and Mallet's proposed epicenter (shown by a star: same as in Figure 26). Basins: MPV, Melandro-PergolaValley; SAB, Sant'Arcangelo basin; HAV, High Agri Valley; VD, Vallo di Diano Basin. Localities: BA, Balvano; MN, Marsico Nuovo (from Burrato & Valensise, 2007).

Burrato & Valensise (2007) in their recent reappraisal of the 1857 earthquake rupture sequence propose that this was a complex event caused by the rupture of two adjacent, kinematically compatible faults, the Melandro-Pergola and the Val d'Agri faults (Fig. 28). Their conclusion is based on three independent lines of evidence that can be summarized as follows:

1- Earthquake magnitude and rupture length. The MPV and HAV faults on the basis of their dimension are assigned a potential for generating earthquakes of Mw 6.7 and 6.6, respectively. These geology-based magnitudes must be compared with the estimates obtained for 1857 from intensity data that is Mw 7.0. Hence, even rupturing both faults in a single large earthquake results in a magnitude that is at least 0.1 M units smaller. The mismatch suggests not only that the participation of both the HAV and MPV faults to the 1857 earthquake is a viable scenario, but also that the length, width or coseismic slip of the fault may still be underestimated.
Besides, the relationships derived by Wells and Coppersmith (1994) for normal faulting suggest that a M 6.8-7.0 earthquake requires rupturing of a 44 to 68 km-long fault. There is therefore ample room for an 1857 rupture involving both adjacent segments, even if the magnitude estimated by Branno et al. (1983) is assumed (M 6.84).

2- Evidence for earthquake complexity. The information brought forward by Baratta (1901) and Branno et al. (1983) on the exact timing of the mainshock and the reconstruction of the damage associated with the first shock presented by Branno et al. (1983) (Fig. 28) supply compelling evidence for faulting complexity. Earthquake source complexity is a common occurrence in Italian earthquakes, although the time lapse between subsequent shocks may vary substantially. The nearby 1980 Irpinia earthquake may be taken as an example of complex earthquake involving multiple rupture on different fault segments.

3- Earthquake epicentral location. Mallet's epicenter falls within 5 km of the northern end of Melandro-Pergola seismogenic source listed by the DISS database (Figure 26). Even allowing for a substantially greater epicentral uncertainty than that admitted by Mallet, it is remarkable that (a) the presumed rupture nucleation falls near one end of the meizoseismal area, and (b) the location of Mallet's epicenter falls about 30 km from the CPTI catalogue location. This evidence suggests that the 1857 may have ruptured in a cascade fashion the MPV fault first, then the larger HAV fault (Figure 28). The rupture would have initiated from the northwestern edge of the MPV fault and propagated unilaterally towards the southeast.

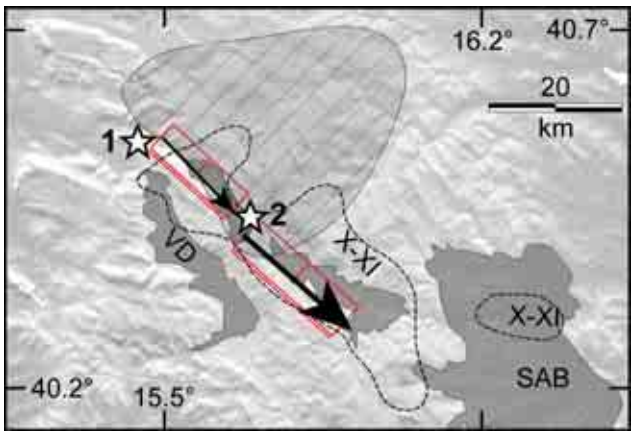

Figure 28. Scheme of the proposed cascade-style rupture for the 1857 earthquake. The arrows show the hypothesized rupture directivity that could explain comparatively larger damage in the southeastern portion of the felt area. The stars marked with 1 and 2 are Mallet's epicenter of the first shock and the proposed nucleation for the second shock, respectively. In red the seismogenic sources of the DISS database (from Burrato & Valensise, 2007).

A1 Stop: View point along the SP273 Paterno-Mandrano

Location and aim

This stop is devoted to an introductory overview of the geology, geomorphology and tectonics of the high Agri Valley (HAV). It is located along the road SP273 Paterno-Mandrano that joins the HAV with the Vallo di Diano basin passing through the Mandrano plain on top of the Maddalena mountain range. This road offers scenic views of the HAV, of both valley shoulders and of the alluvial plain. With clean weather, it is possible to see on the far east distance the valley outlet through the gorge cut into the middle-upper Miocene Gorgoglione Flysch.

The road probably follows the same route taken by Robert Mallet during its expedition, when he left the HAV to go back to the Vallo di Diano.

Outcrop description

The road SP273 intercepts the tectonic contact between the Mesozoic–Cenozoic platform and slope carbonates (Monti della Maddalena unit), which overthrusts coeval pelagic rocks of the Lagonegro units (Marsico Nuovo thrust). The thrust contact is marked by a pervasive cataclastic texture mostly developed at the expenses of brittle carbonate rocks of the upper plate. On the opposite side of the valley the rocks of the Lagonegro units display ~N-S to NW-SE trending major folds (e.g. Monte Lama and M. Volturino folds).

The NW–SE trending Val d'Agri basin is bounded to the northeast by the rough peaks of the Mt. Volturino - Il Monte range that reaches elevation of up to 1800 m a.s.l. (Fig. 5). To the southwest, Maddalena Mts. range separates the HAV from the Quaternary Vallo di Diano basin to the west (Fig. A1_1). The regional water divide runs along the Monti della Maddalena range (Fig. A1_1), the Val d'Agri basin is axially drained by the Agri River, which flows 100 km eastwards into the Jonian Sea.

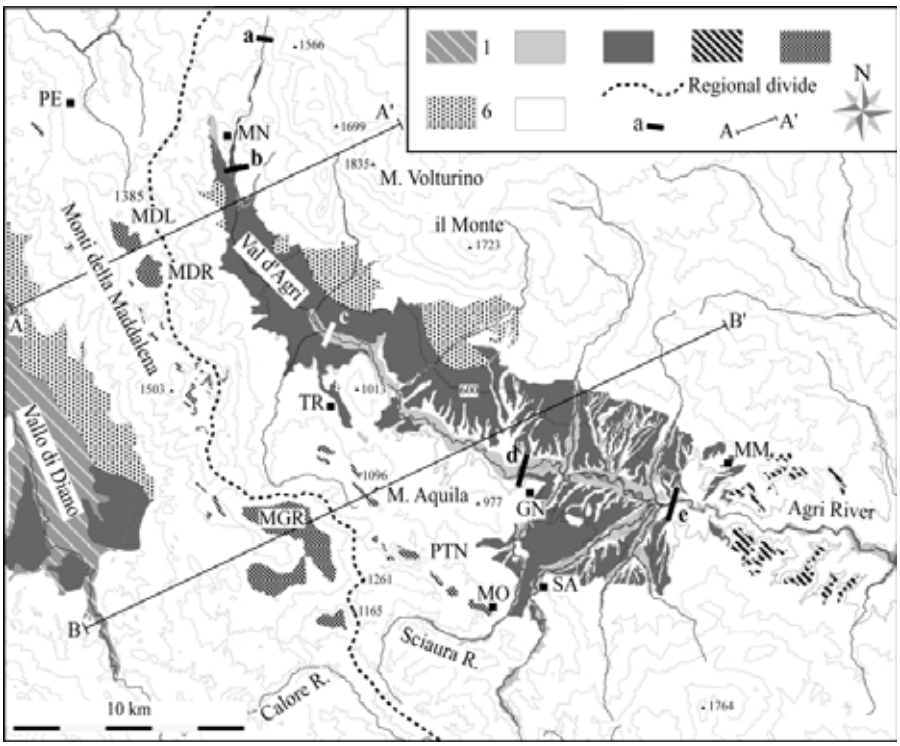

Fig. A1_1. Generalized geomorphologic map of the Val d'Agri and Maddalena Mts. range. Simplified topography is shown with 200-m contour lines. Towns: GN, Grumento Nova; MM, Montemurro; MN, Marsico Nuovo; MO; Moliterno; PE, Pergola; SA, Sarconi; TR, Tramutola. Basins: MDL, Mandranello; MDN, Mandrano; MGR,

Magorno; PTN, Petenella. Keys: 1, Holocene alluvial deposits; 2, Upper Pleistocene alluvial deposits; 3, Middle–Upper Pleistocene alluvial and lacustrine deposits; 4, Middle Pleistocene erosional surfaces; 5, Upper Pleistocene—Holocene colluvial and lacustrine deposits; 6, Middle Pleistocene fan and talus breccia deposits; 7, pre-Quaternary bedrock assemblage; a to e) way-points in longitudinal profiles along the Agri river; A-A' and B-B' traces of topographic profiles (Fig. A1_2). From Maschio et al., 2005.

Topographic profiles across the Val d'Agri show different morphologies for the eastern and western shoulders of the valley (Fig. A1_2). To the west, the Maddalena Mts. range is characterized by a "hat-like" topography produced by small depressions perched along its crest (Fig. A1_2). These basins are filled by recent colluvial and marsh deposits, and are aligned NW–SE for over 15 km from Mandranello–Mandrano (MDL–MDN; Fig. A1_1) southwards to Magorno (MGR in Fig. A1_1). A second subparallel, and topographically lower, alignment of smaller basins is found to the east for about 10-km stretch, between the villages of Tramutola and Moliterno (Fig. A1_1). No obvious range-bounding fault outcrops along this side of the valley. On the contrary, the eastern flank of the Val d'Agri displays a rectilinear trend of the mountain front and is characterized by a mature staircase profile sloping towards the valley, generated by (Fig. A1_2). This mountain front is punctuated by two prominent alluvial fans, generated by the Molinara and Alli creeks. These fans are now abandoned and incised by their formerly feeding streams (Fig. A1_1).

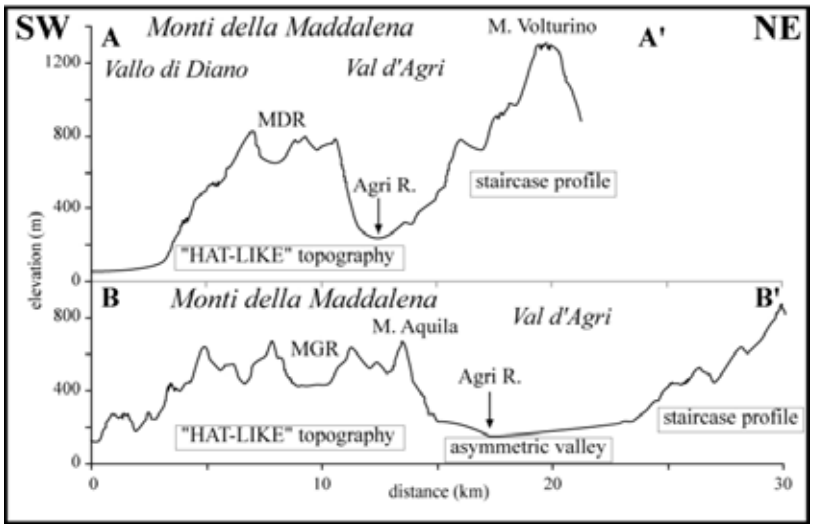

Fig. A1_2. Topographic profiles across the Val d'Agri area, showing different morphologies characterizing the two valley shoulders: staircase profile for the eastern side, and hat-like topography for the western side. Intramontane basins of the Maddalena Mts. range: Mandrano, MDN; Magorno, MGR. From Maschio et al., 2005, modified.

This stop offers a nice view of the central section of the High Agri Valley that is characterized by a flat bottom and the asymmetric position of the axial Agri River. This section corresponds with the northernmost and deeper of the three depocenters that form the High Agri basin (see Fig. 12). Here, the sedimentary sequence attains a thickness of about 400 m (basin floor at about 600 m asl). The active alluvial plain begins to be incised near the Monticello ridge that is the outcropping portion of a buried threshold limiting to the east the first depocenter.

A2 Stop: Barricelle quarry

Location and aim

This stop is located on the second of the five fault strands that form the Eastern Agri fault system (see Field trip map), and is designed to give insight into the kinematic relations between two different fault episodes on this fault array.

Outcrop description

Exposures are provided by a quarry exploiting the pervasive cataclastic fabrics affecting the bedrock, which is formed by well bedded and locally laminated grey limestone (ooid and lithoclasts grainstone to floatstone), of probable Jurassic age.
This cataclastic fabric is not the product of Quaternary faulting, but derives from older low-angle faulting. As a matter of fact, cataclasite and gouge textures are structured along low-angle shear bands and surfaces, and an equilibrium slope profile is carved upon these structures (Fig. A2_1). At the base of the slope, a basinward-dipping high-angle fault surface cut across the low-angle cataclastic bands, and is marked at the surface by a ~1 m tall step in the slope profile (Fig. A2_1). Along this linear step, matrix-rich breccia talus deposits (Lower Pleistocene Marsico Breccia) are faulted against the Mesozoic bedrock (Fig. A2_2).

Fig. A2_1

Fig. A2_2

These observations indicate that: a) cataclasite produced by the low-angle (Pliocene?) faulting was regularized during modeling of the slope; 2) this slope was controlled by slip along high-angle faults during and after deposition of the lower Pleistocene Marsico Breccia; 3) the m-scale slope-break is the product of probably very recent slip.

The high-angle faults are marked by small width (10-20 cm) cataclastic shear bands and by a polished and planar slip surface. Two sets of slip lineations are observed on these surfaces (Fig. A2_3).

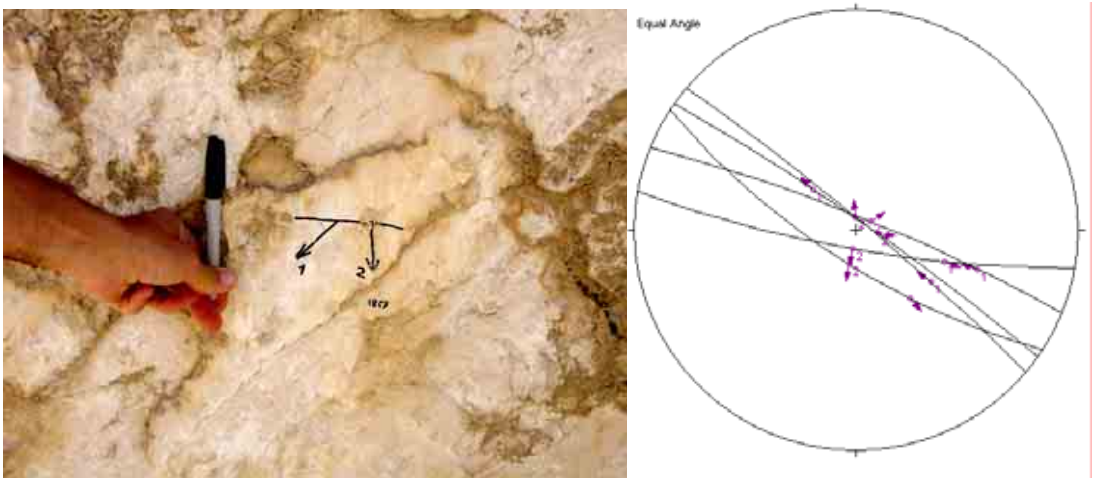

Fig. A2_3a and A2_3b

The first set indicates left-oblique slip on northwest-striking surfaces (Fig. A2_3; A2_4a) and characterizes the main fault morphology, and presumably the larger slip accrued on the fault (Fig. A2_5). The pseudo-fault plane solution derived from the inverted slip lineations shows strike-slip nodal planes and an extensional axis striking N167E (Fig. A2_4b).

Fig. A2_4a and A2_4b

Fig. A2_5

The second set of slip lineations indicates dip-slip motion, with a computed extensional pseudo-focal solution and tensile axis trending N33E (Fig. A2_3; A2_6).

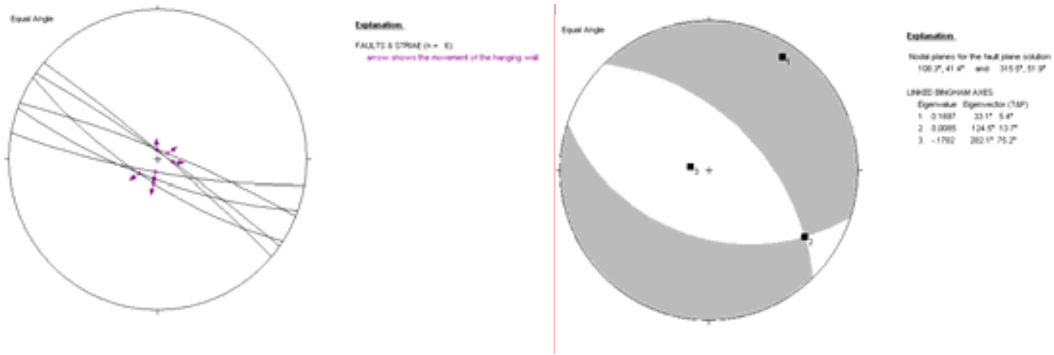

Fig. A2_6a and Fig. A2_6b

The second slip event is marked by short (dm-scale) and variably developed lineations, which are ostensibly superposed on the first set and on the main fault morphology without erasing the imprint of the older motion (Fig. A2_7). It is likely that these slips occurred in the near surface in recent times.

Fig. A2_7

Outside the quarry, a systematic pattern of fracture is observed in the faulted Marsico Breccia, with dominant ENE-WSW strike (Fig. A2_8). The fracture orientation is consistent with the ~SSE trending extensional axis of the first slip episode (Fig. A2_4b), setting an age of strike-slip faulting not older than early Pleistocene.

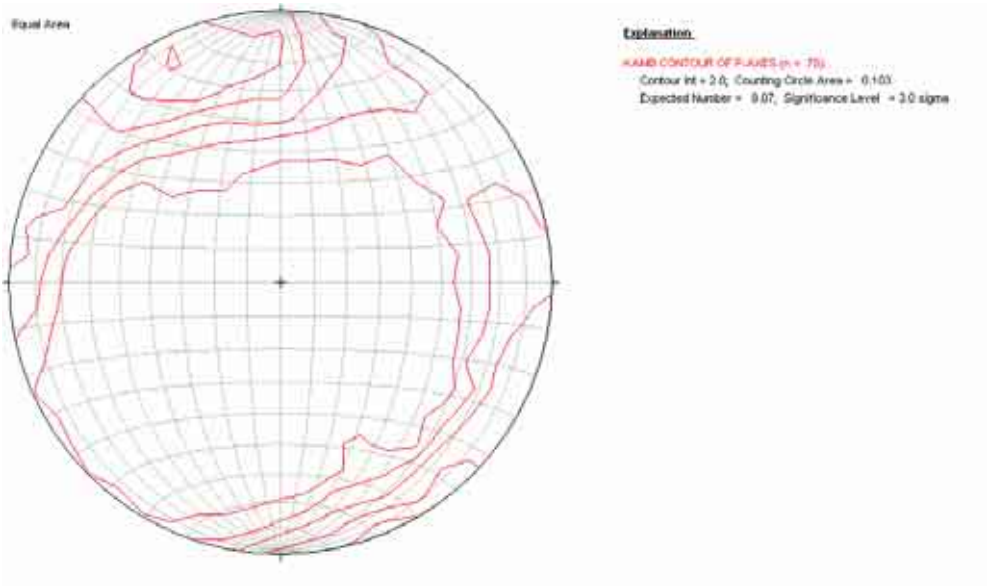

Fig. A2_8

(fault and fracture data collected with S. I. Giano and M. Schiattarella)

A3 Stop: road to Marsicovetere

Location and aim

This stop is along the windy road that climbs the eastern valley shoulder to reach Marsicovetere, displaying nice scenaries of the basin. The goal of this stop is to give a closer look to the Eastern Agri Fault System (EAFS), and observe the morphology of the central section of the valley where the Agri River attains its maximum asymmetry towards the western valley side.

Outcrop description

Limestones of Jurassic age and Lower-Middle Pleistocene talus breccia (Brecce di Marsico, Di Niro and Giano, 1995) are exposed along the road. The bedrock outcropping in this area is the same found in the Monticello ridge, to the south and just on the other side of the valley (see description of the Stop 8 – Monticello quarry, Day 2). The outcrops of Jurassic limestones on both side of the valley define the position of a second order buried threshold that separates the northernmost depocenter from the central one (see Fig. 12).

From this stop we can observe the transition from the depositional section of the alluvial plain, upstream of the Monticello ridge (b-c in Figs. A1_1 and A3_1), to the erosional section, where the Agri River is down cutting its own sediments, with increasing efficiency (Figs. A3_1 and A3_2).

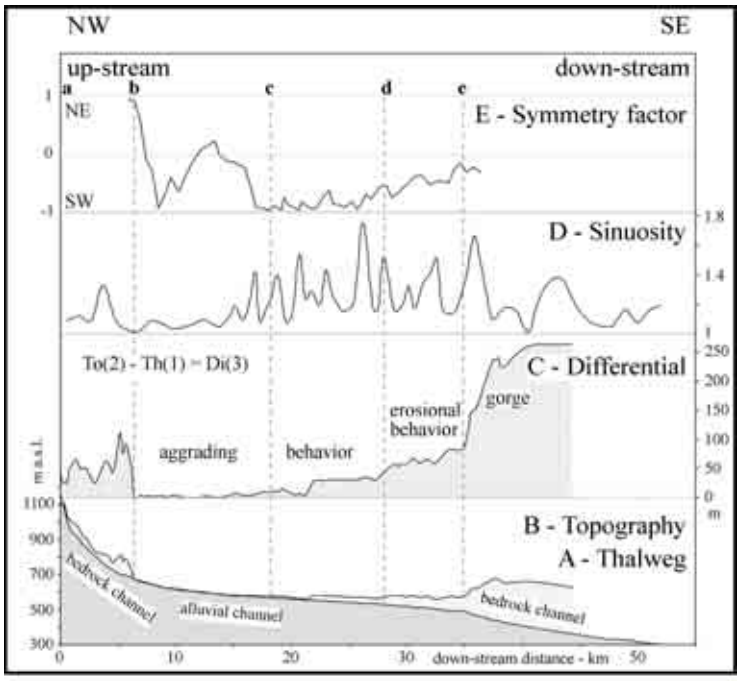

Fig. A3_1. Longitudinal profiles along the Agri river: (A) elevation profile of the thalweg; (B) elevation profile of the adjacent topography; (C) differential profile; (D) sinuosity profile; (E) symmetry factor profile (after Maschio et al., 2005).

Profile C of Fig. A3_1 was obtained subtracting the elevation of the thalweg of the Agri River (profile A) from the elevation of the active alluvial plain or of the lowermost abandoned fill terrace (profile B). Increasing difference between the two highlights increasing erosional behavior of the river, triggered by base-level fall. The aggrading section is possibly related to the active tectonic subsidence of the plain. Thanks to the increasing erosion by the Agri River and its tributaries getting closer to the basin

threshold, the Middle-Upper Pleistocene alluvial-lacustrine sediments (Complesso Val d'Agri, Di Niro et al. 1992) are exposed in the lower d-e section of the valley (see Stop B8; Zembo, 2007).

Fig. A3_2. Panoramic view of the central section of the High Agri Valley from the eastern valley shoulder.

A4 Stop: Galaino quarry

Location and aim

This stop is located on the same fault strand observed at Barricelle (stop A_2), ~3.5 km to the NW of that outcrop (see Field trip map). The stop is devoted to the inspection of a contractional structure developed in Quaternary deposits in a restraining bend of the EAFS.

Outcrop description

A quarry exposes ?Lower Pleistocene fanglomerate resting above highly shattered Triassic Calcari con Selce of the Lagonegro unit (Fig. A4_1). The fanglomerate probably represents the transition between the Marsico slope breccia and the lower part of the Complesso Val d'Agri filling the Early-Middle Pleistocene Val d'Agri basin.

The fanglomerates are moderately sorted and crudely stratified, and reach a thickness of more than 30 m. The deposits are involved in a monocline which dips steeply toward the Agri basin to the ESE (Fig. A4_1). Bedding dips are slightly lesser moving to the west documenting a gentle fold. Detailed inspection shows growth of the fanglomerate body during tilting and folding, including extensional growth-fault.

Fig. A4_1

Moving laterally and toward the mountain front, it can be observed that the Calcari con Selce bedrock forms a push-up ridge underlying the fanglomerate (Fig. A4_2).

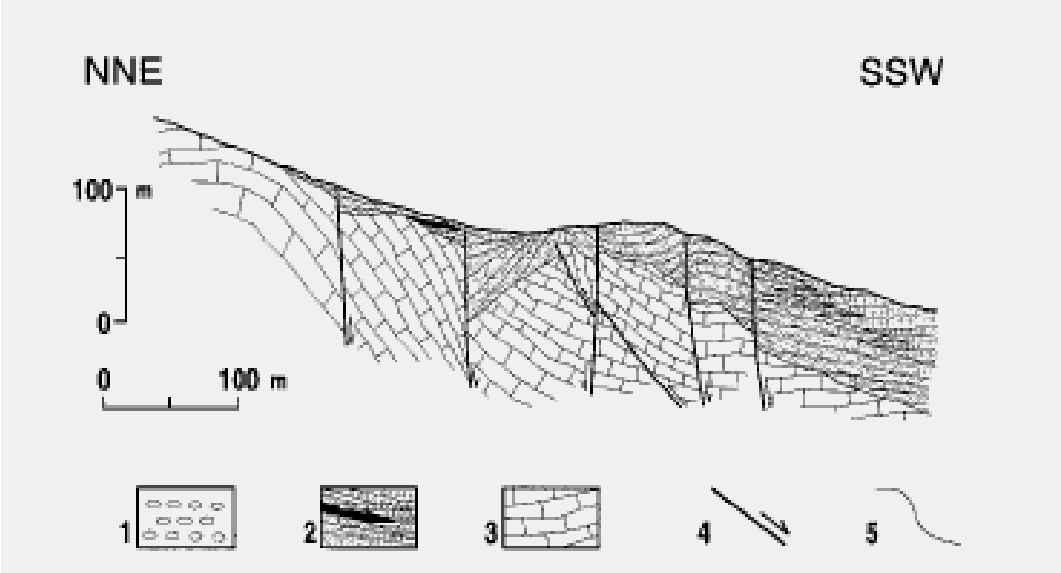

Fig. A4_2. Geological cross-section of the Galaino area. Legend: (1) Holocene colluvium; (2) Pleistocene coarse-grained slope deposits with interbedded palaeosoil; (3) upper Triassic Calcari con Selce Fm; (4) fault; (5) stratigraphic contact (from Giano et al., 1997).

The structure involving both bedrock and Pleistocene cover has been interpreted as a push-up ridge formed at a restraining bend of the left-oblique EAFS (Giano et al., 1997). Local transpression at this bend would have been responsible for tilting and gentle folding of the fanglomerate.

The fanglomerate is covered by a palaeosoil and both are cut by a depositional glacis underlying a younger, more crudely bedded fanglomerate, which is locally tilted mountainward (Fig. A4_3).

Fig. A4_3. L.Pl.=Lower Pleistocene fanglomerate; U.Pl.=Upper Pleistocene fanglomerate. The dashed line marks the contact approximately.

The upper fanglomerate is also laterally inserted into the older deposit (see Fig. A4_3), and small terraces lying only few m over the present course of the Galaino stream probably represent still younger fan sediments which are still in depositional contact with the source area upslope.
The palaeosoil separating the upper and lower fanglomerate is formed by 1 m thick, compacted red clay, which can be followed for ~20 m without appreciable lateral variation in thickness and facies. The paleosoil is slightly tilted and affected by NW-SE striking faults (Fig. A4_4a). Structural analysis of the faults shearing through the palaeosoil (Giano et al., 2000) shows both dextral transtension and pure normal faulting (Fig. A4_4b). These data are consistent with ENE-WSW extension producing partitioning between extensional and dextral transtensional faults.

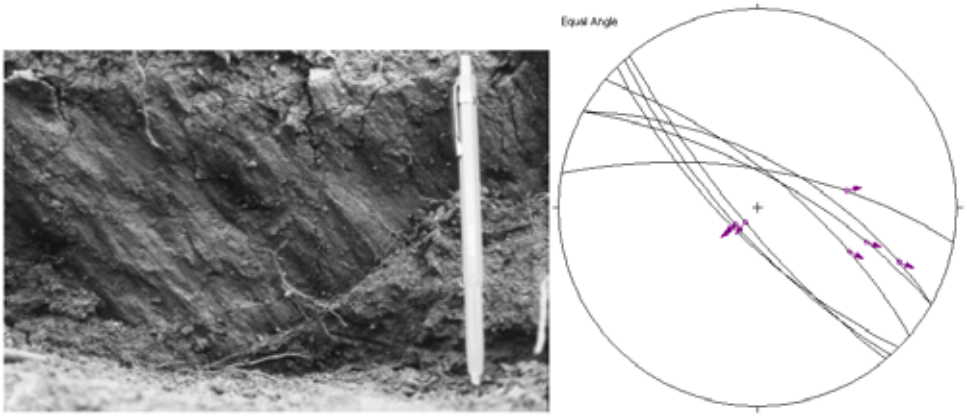

Fig. A4_4a and b (adapted from Giano et al., 2000).

Age of the paleosoil
The paleosoil was aged by Dipartimento di Fisica of University of Rome la Sapienza (Laboratory code R-3124). All the results for sample R-3124 were very close to the range of radiocarbon dating
(about 40 ka) and the best obtained measurement was >39,600 yr BP (Giano et al., 2000). However, it was noted that every measurement of the sample R-3124 was distinguished from the background, and Giano et al. (2000) attributed the still unresolved result simply to a slow laboratory separation process. Consequently, the obtained age was considered grossly reliable.

Summary
The main structure is considered a product of left-lateral transpression during the early-middle Pleistocene. Fault-kinematics data from the paleosoil document faulting with possible structure reactivation incompatible with the strain responsible for deformation of the older fanglomerate, but consistent with a broad NW-SE extension acting after ~40 ka.

A5 Stop: Marsico Nuovo dam

Location and aim
Aim of this stop is to discuss, from a panoramic vantage point, the geometry of a prominent anticline in Lagonegro rocks and the resulting nature of the western flank of Serra di Calvelluzzo, and alternative hypothesis about the location of the EAFS.

Outcrop description
At this top we enjoy a frontal view of one of the most impressive morphology of the High Agri Valley, namely the pentagonal facets of Serra Calvelluzzo (Fig. A5_1).

Fig. A5_1. Pentagonal facets of Serra Calvelluzzo.

These morphologies have long been known and shown to researchers and students to represent a remarkable example of flat-irons, developed upon inclined beds of Calcari con Selce.
The tilted beds form the western limb of the Monte Lama-Monte Calvelluzzo (MLMC) anticline, a prominent N-trending structure in the Lagonegro thrust system (Mazzoli et alii, 2001). The MLMC anticline consists of the Mesozoic succession of the Unità Lagonegrese I (Scandone, 1972) or San Nicola unit (Mazzoli et al., 2001), and exposes Upper Triassic Calcari con Selce in the core and Jurassic Scisti Silicei on the limbs. The morphologic low ringing the structure is floored by Cretaceous Galestri cropping out in the Torrente Molinara (Fig. A5_2).

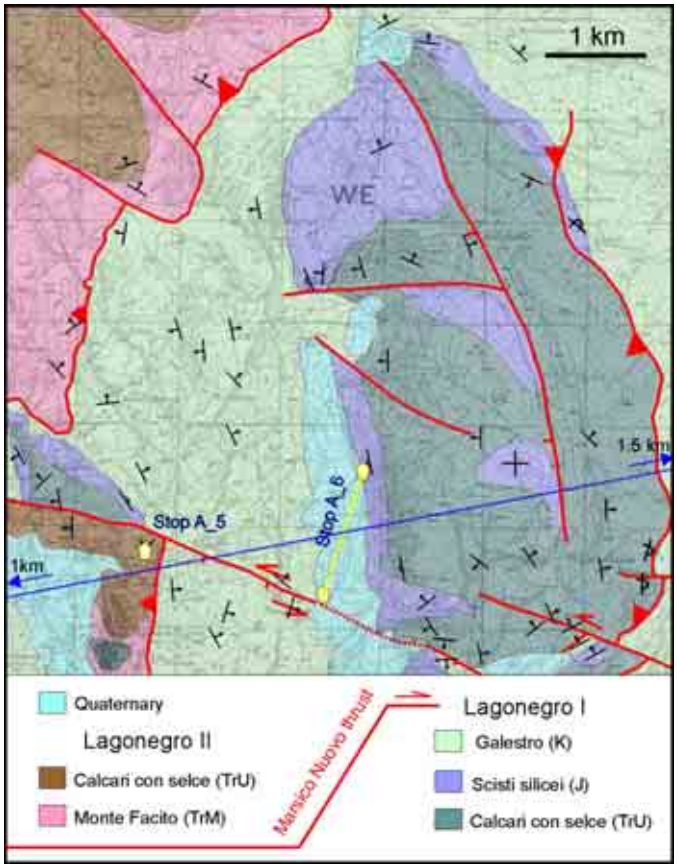

Fig. A5_2. Geologic map of the M. Lama-Calvelluzzo anticline (redrawn and slightly modified from Cello et al., 2003).

The fold geometry consists of a more than 8 km long box fold with a marked northern plunge. The anticline shows a vertical western limb and a steep to overturned eastern limb, both offset by minor out-of-limb thrusts, and a double vergence of associated fold structures (Fig. A5_3).

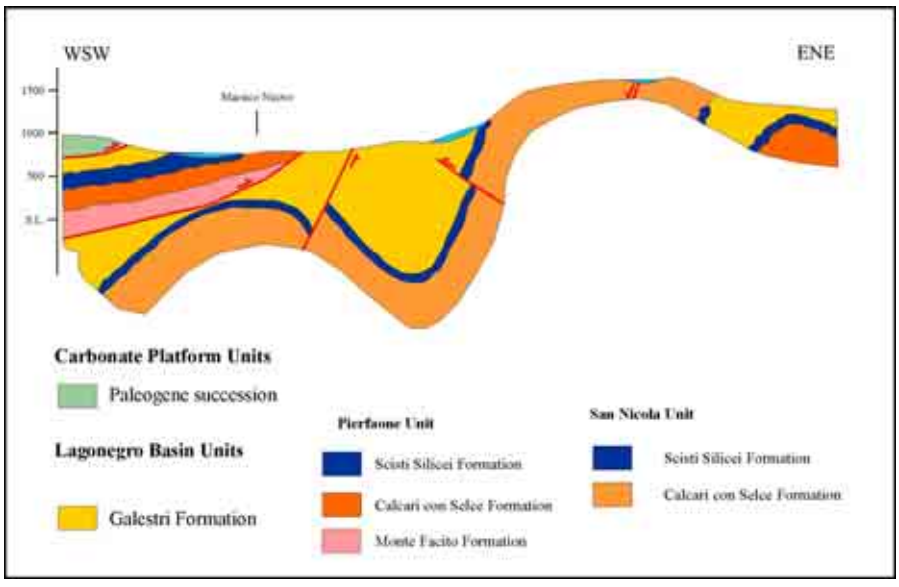

Fig. A5_3. Geological profile across the Torrente Molinara-M. Lama area (from Cello et al., 2003, redrawn).

From this stop the geometry of the fold can be clearly seen at Monte Lama along the flank of a lateral incision of the uppermost Agri river course (Fig. A5_4). Here, the western limb of the structure is back-thrust over the Galestri Fm Syncline (Fig. A5_4).

Fig. A5_4. Box fold at Monte Lama.

Notwithstanding the good understanding of the thrust structure achieved in recent work, the tilted depositional contact between Calcari con Selce and Scisti Silicei has been represented in several papers and maps as a W-dipping fault related to the Quaternary tectonics (Lentini et alii, 1991; Pescatore et alii, 1999). Benedetti et al., (1999) have claimed that the mountain slope represents a 250 m high Pleistocene fault-controlled escarpment, and evidence of active faulting is present at the foot of the slope.
Recent work documents at this mountain front only a Jurassic normal fault system (Serra di Calvello fault in Bucci et al., 2006), already invoked by Scandone (1967) to explain the significant thickness variation of the Scisti Silicei moving across the present-day anticline. This fault is parallel to the anticline (indicating its pre-anticline geometry) and is sealed by the Galestri, and thus had no activity in the active margin stage (Bucci et al., 2006).

Turning back toward the hill behind (M. Cugnone), we have a panoramic view of the contact between the steep sloping Calcari con Selce bedrock and the gentler sloping breccia deposits where the village of Marsico Nuovo is built. The contact is characterized by a high-angle left-trastensive fault (Monte Cugnone border fault in Ferranti et al., 2005; Fig. A5_5 and 6).

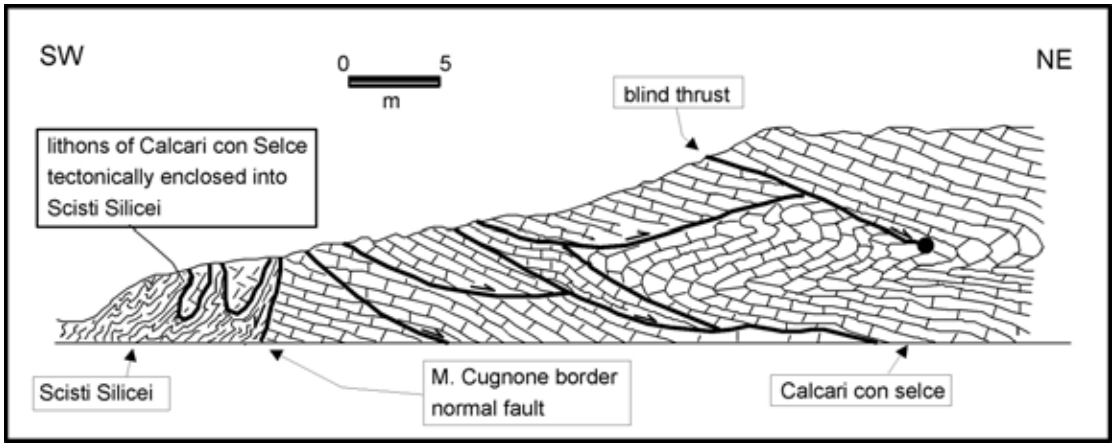

Fig. A5_5. Field drawing of a thrust-fold zone in the eastern limb of the Monte Cugnone anticline. Note the apparent extensional displacement on thrust faults is related to anticline folding and tilting of pre-existing, SW-dipping thrust surfaces. Also shown: a Quaternary normal fault (Monte Cugnone border fault). (Ferranti et al., 2005).

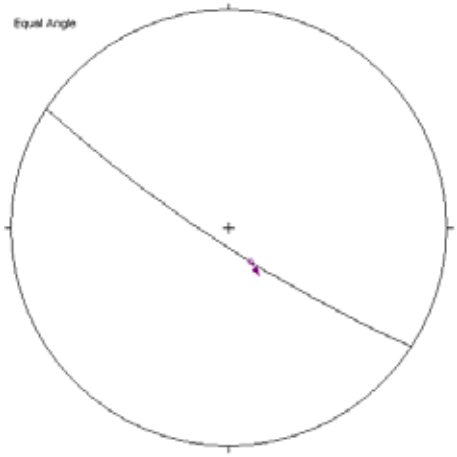

Fig. A5_6. Outcrop of the fault surface and fault slip analysis along the M. Cugnone border fault. The picture shows in the foreground the M. Cugnone fault and in the background the pentagonal facets of Serra Calvelluzzo.

We suggest that this and a sub-parallel fault downhill represents the western prosecution of the EAFS, which at this location turns from a NW-SE to a WNW-ESE trend (see Field trip map**).** Thus, whereas the thrust anticline at M. Volturino (the southern prosecution of the M. Lama-Calvelluzzo anticline) is in effect cut by Quaternary normal faults, the M. Lama-Calvelluzzo escaped down-faulting during recent extension.

A6 Stop: Camporeale

Location and aim
On the west flank of Serra Calvelluzzo, a light stroll will bring us at the base of the pentagonal facets presented in the previous stop. This will allow checking the nature of the pentagonal facets and discussing the debated evidence for active faulting.

Outcrop description
(with contribution of F. Bucci)

From the hamlet of Camporeale, east of Marsico Nuovo (see Field trip map) we have firstly a lateral view of the pentagonal facets (Fig. A6_1). The main slope is formed by steeply (~ 50 °-60 °) W-dipping limestones of the Calcari con Selce and the piedmont is floored by more erodible Scisti Silicei.
The facets are separated by perched, wine-glass canyons (Fig. A6_1), which have been regarded as evidence for active faulting and footwall uplift (Benedetti et al., 1999). The knick-point is located at a marked lithological change from more erodible argillites to well-bedded limestone. In addition, the facets do not cut the bedding but form a bed-parallel envelope with average ~35° dip (upper part of Fig. A6_1). At the base of the facet, the slope dips ~50-60° being developed on single beds. Thus, a flat-iron nature of the facets seems plausible, with the wine-glasses being controlled by lithology.

Fig. A6_1. Lateral view of the pentagonal facets at Serra Calvelluzzo. Note the perched “wine-glass” rills.

From the car stop, we walk north on gentle ground underlain by argillites of the Galestri. The Galestri are highly incised and thus no subsidence (as expected in the hanging-wall of a normal fault) is documented at this site. A first some ten meters-high step occurs downhill the mountain slope at the lithological transition between radiolarite and limestone of the Scisti Silicei and more erodible argillites of the Galestri.
Locally, asymmetric mesofolds related either to parasitic folding (Z-type) or to out-of-limb shearing expose gently basinward-dipping beds. These outcrop-scale structures form 1-2 m high scarplets which are laterally discontinuous and locally promote minor landslides (Fig. A6_2; foreground of Fig. A6_3).

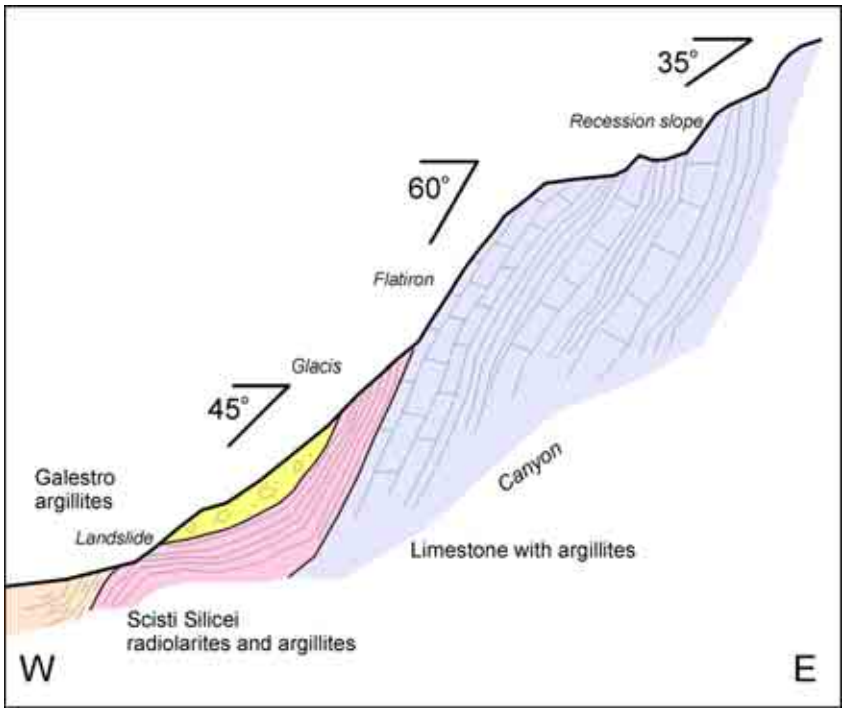

Fig. A6_2. Sketch of lithologic and morphologic relation at the lower slope of M.te Calvelluzzo (not to scale).

Further high, the Calcari con Selce are affcted by sub-horizontal or gently E-dipping fractures, which are thus almost orthogonal to bedding (Fig. A6_3).

Fig. A6_3. The pentagonal facets at Serra Calvelluzzo. Note the steep basin-ward dipping bedding and the gently mountain-ward-dipping fractures.

The angular relations between beds and fractures can be interpreted as a result of wholesale tilting of beds and fabrics that was formed when beds were horizontal, i.e. before Neogene folding (Bucci, 2004). Conversely, no evidence of basin-ward dipping fractures forming the damage zone of a recent normal fault (whose existence was claimed by Benedetti et al., (1999) can be seen.

We finally reach a gully at the base of the fourth facet (counting from S to N). Here, crudely bedded loose debris has been deposited at the mouth of the gully and is unconformable lying on a tilted argillitic limestone bed of the Scisti Silicei (Fig. A6_2 and A6_4). The fan deposit is itself incised for a height of 3-4 m. The bevelled upper surface of the fanglomerate continues into the bedrock until the thicker limestone of the facet is reached. The ~45° dipping surface is probably an erosional glacis formed during the last glaciation and subsequently incised (Fig. A6_2). No evidence of faulting of the deposit and of the glacis is found at this site.

Fig. A6_4a and b. Fanglomerate at the mouth of a lateral canyon.

In summary, the evidence rules out Quaternary large-displacement normal faults at this mountain front.

B1 Stop: View point from Camporotondo on the high Agri Valley and the Maddalena Mts.

Location and aim

Like the first stop of Day 1, this stop is aimed to give an overview of the geology, geomorphology and tectonics of the high Agri Valley (HAV), in particularly of the fault system cutting through the western basin shoulder. To reach the location of the stop we will follow the road that from Piazzolla, a small village near Paterno, goes to Camporotondo (one of the Quaternary basins perched on top of the Maddalena Mts.). After parking the cars we will follow a small track to reach the top of Serra Mare ridge. This stop offers a scenic view of the middle reach of the high Agry Valley and of its western shoulder, with the Magorno Plain at our right, Monte Aquila in front of us and the Pertusillo Lake and the Agri gorge in the far distance.

Outcrop description

The road stands on limestones of Cretaceous age that are locally pervasively shattered by thrust faults. At the base of the relief where the stop is located, the N-S valley of the Rio Cavolo, a right tributary of the Agri River, is floored by Miocene siliciclastic deposits. More to the south, the limestones outcrops again and form the relief around Tramutola (Fig. B1_1).

Figure B1_1. Panorama from the location of Stop B1. The center of the image views towards east.

The Rio Cavolo follows an L-shaped course, and its catchment appears to have increased by capture and expansion into neighbouring catchments (Fig. B1_2). Its valley is very close to drain also the Magorno plain that is the largest of the Quaternary basins perched on top of the Maddalena Mts., since only a small threshold separates it from the Agri drainage system. The Magorno plain during the wet season is in part occupied by an ephemeral lake, which is drained through karstic sink-hole(s). Robert Mallet coming from the Vallo di Diano crossed this lake (*Lago Maorno*) before going to Moliterno (not visible from this location).

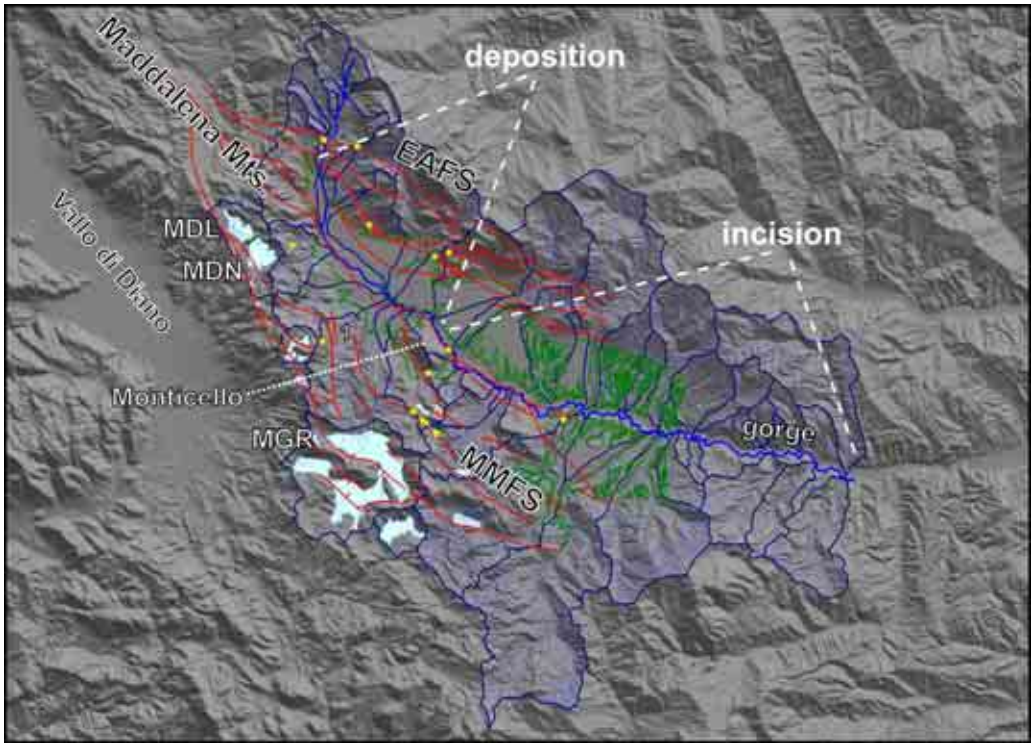

Figure B1_2. Map showing the High Agri valley catchments, plotted onto a 20-m DEM. Symbols: red, faults; green: outline of the Quaternary deposits of the valley; heavy dark blue, divides of catchments; dark blue, drainage; light blue: small Quaternary basin on top of the Maddalena Mts.. Basins: MDL, Mandranello; MDR, Mandrano; MGR, Magorno. The number 1 indicates the Rio Cavolo catchment. The yellow stars are the field trip Stop locations, shown for reference.

From this stop we can observe the southern termination of the Maddalena Mts., whose hat-like topography is spatially coincident with swarms of the NW–SE striking high-angle faults of the MMFS (refer to Fig. 16). The surface expression of individual faults is locally represented by splitting of the mountain crests and inversion of the topography. In same places they run along the main axes of the small basins perched at high elevation within the range. These basins commonly display L or T map-view shapes, with their long axes striking NW–SE. Oppositely, their minor axes strike ENE–WSW and are developed along subsidiary faults or fracture zones, which connect the main strands of the array.

The Agri River course in the section visible from this stop attains its higher asymmetry toward west, flowing very close to the eastern slope of the Monticello hill (profile E in Fig. A3_1). This is also the aggrading section of the Agri River (profile C in Fig. A3_1 and Fig. B1_2). Just downstream of the Monticello, the river starts incising its own deposits, and together with its right tributaries develops up to three orders of cut terraces. The Agri River eventually leaves the basin through a bedrock gorge (into Miocene flysch), coincident with a knickpoint.
At a regional scale the Agri Valley can be subdivided into three sectors bounded by major regional tectonic structures (Fig. B1_3; Bianca & Caputo, 2003). In each sector a distinct flight of river terraces developed during middle-upper Pleistocene-Holocene times. The lowermost sector, reach C in Fig. B1_3, is probably the only one where the incision of the river terraces was controlled by the eustatic sea level changes.

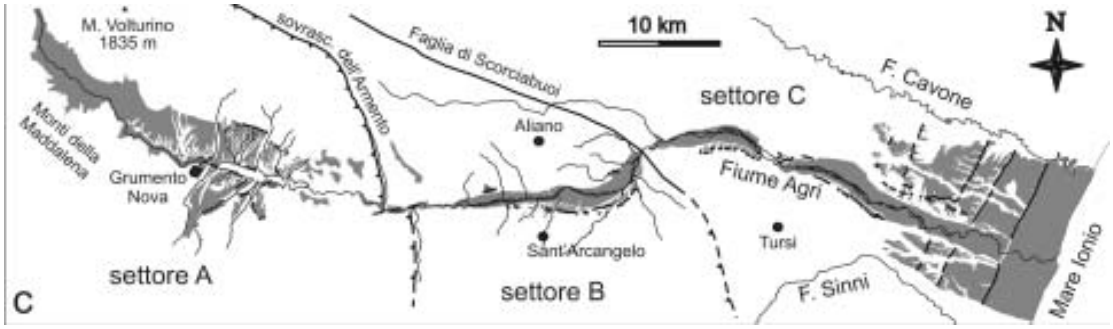

Figure B1_3. Morphotectonic sketch of the Agri Valley, showing fluvial and marine terraces (grey areas), and the main tectonic structures that define the three sectors of the valley (from Bianca & Caputo, 2003).

The High Agri Valley corresponds with the most upstream sector and is bounded to the east by the Armento thrust (Fig. B1_4). The knickpoint visible in the longitudinal profile of the Agri River (Fig. A3_1) indicates that this sector of the valley has been isolated from the eustatic oscillation, and the fluvial terraces can be ascribed to a probable climatic or local tectonic origin. Not existing dating control, the age of the terraces has been constrained by means of relative correlations (Di Niro et al., 1992). From older to younger the ages are (Bianca & Caputo, 2003): Middle Pleistocene – Terrace IV-a; Middle-Upper Pleistocene – Terrace III-a; Upper Pleistocene – Terrace II-a and Terrace I. However, tighter age constrain for the two younger terraces could arise from the recent revision of the stratigraphic sequence of the Complesso Val d'Agri into which the terraces II-a and I are cut (see Stop B8; Zembo, 2007).

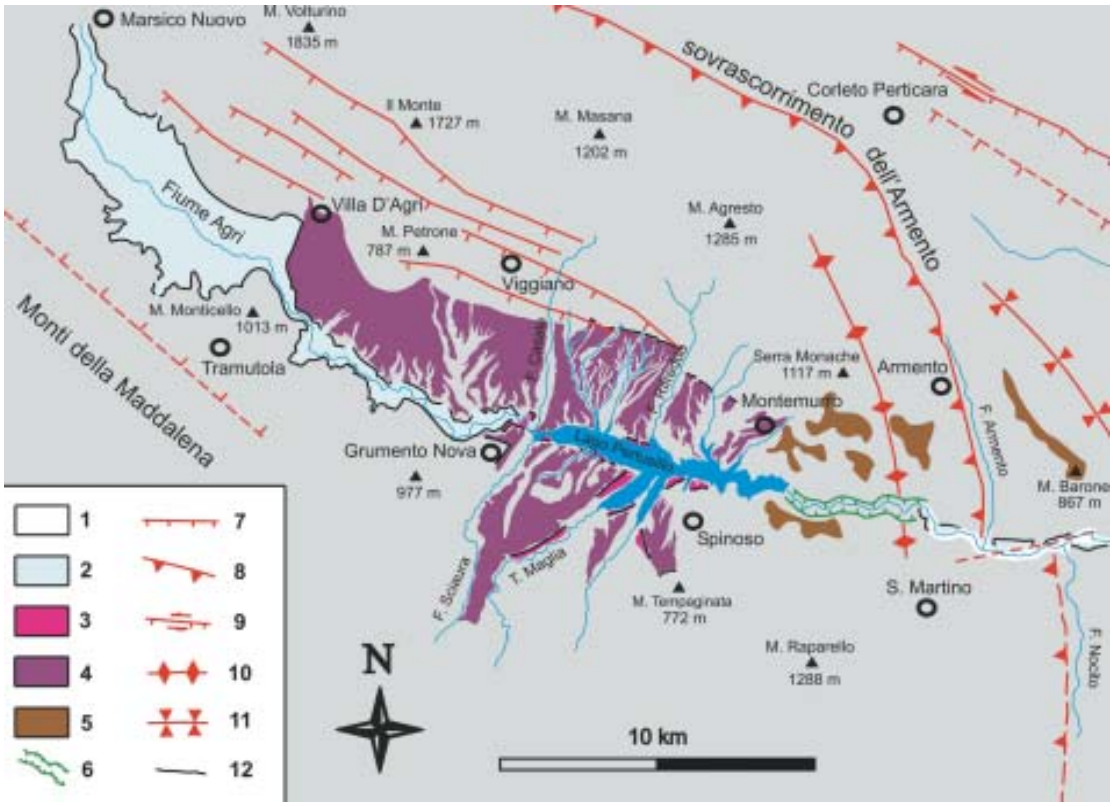

Figure B1_4. Morphotectonic map of the High Agri Valley, showing fluvial terraces, and the major faults. Colors: 1, pre-Quaternary bedrock; 2, terrace I; 3, terrace II-a; 4, terrace III-a; 5, terrace IV-a (from Bianca & Caputo, 2003).

B2 Stop: Monticello quarry

Location and aim
This stop is located precisely on the western border of the Agri basin, in a quarry on the NE side of the Monticello hill. We will inspect the fabrics related to the first outcropping of the NE-dipping faults, and the geomorphic response of the Agri River system to NE-directed displacement. Finally, we will discuss the very shallow (1 km) crustal expression of these faults imaged by high-resolution seismic tomography.

Outcrop description
At this stop, the NE-dipping Monticello fault cuts through open shelf Cretaceous limestone (Fig. B2_1).

Figure B2_1. Cataclastic limestone cut by the Monticello fault, NE to the right of picture.

Fault-kinematic analysis indicates that top down-northeast slip occurred in response to ENE-directed extension (Fig. B2_2).

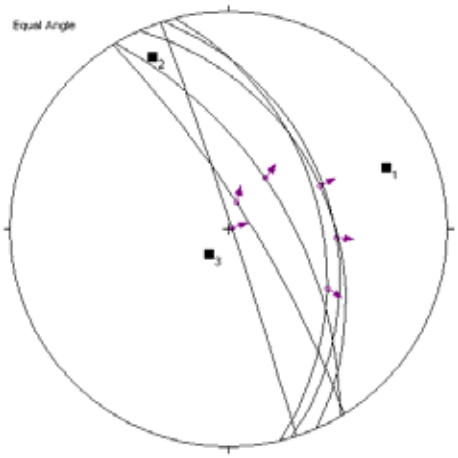

Figure B2_2. Fault-kinematic analysis along the Monticello fault at the quarry site.

The fabric related to the high-angle fault is superposed on low-angle NE-dipping cataclastic fabrics (Fig. B2_2). The origin of this older fabric is unknown, but few kinematic indicators suggest it is related to top-to-NE extensional motion (present-day attitude).

Figure B2_3. Moderately (~40°) NE-ward dipping cataclastic fabrics within lower Cretaceous limestone.

Geomorphologic features of the Agri river system

From this site we have a clear view of the asymmetry of the Agri River, which flows attached to the foot of Monticello hill on the western edge of the basin (Fig. B2_4).

Figure B2_4. The central part of the Agri river high valley from W (left) to E (right). Note the position of the Agri river very close ("shifted toward") the western border of the basin.

This shift, which can be followed for a long stretch of the river course in the Agri high valley (tract c-d in Fig. A3_1) has been explained by Maschio et al. (2005) as related to subsidence localized in the hanging-wall of the NE-dipping fault Monti della Maddalena Fault System.

In addition, this site lies in a stretch of the river valley where the topographic surface starts to be progressively incised (see the the increase in the differential profile in the same stretch c-d of Fig. A3_1); the differential profile is obtained by subtracting the elevation profile of the river bed from the elevation profile of the active alluvial plain (where present) or of the lowest terrace (where the river is nowadays incising). From this site, we can appraise the beginning of the inciding pattern documented by development of strath terraces (Fig. B2_5).

Figure B2_6. View of the top surface of the Middle-Upper Pleistocene alluvial plain in the central part of the basin. Note the beginning development of strath terraces to the south (right in picture).

Shallow crustal structure imaged by seismic tomography
(contribution of L. Valoroso & L. Improta)

The shallow crustal structure underlying this section of the valley has been imaged by high resolution controlled source tomography (Valoroso et al., 2007).
The P-velocity image show abrupt vertical and lateral changes. Lower-Middle Pleistocene slope breccias (2500 - 2700 m/s) fill the eastern part of the basin and are covered by more recent alluvial deposits (1500 - 2000 m/s) whose thickness progressively increase westward and are the largest in this side of the valley. The carbonate bedrock has an irregular shape with rapid depth variations which is partly inherited by the previous thrust displacements, but is largely controlled by Quaternary normal faulting.
Three major west-dipping fault zones are evident on the eastern side of the basin with cumulative vertical throw of 300 - 500 m. These faults cut the slope breccias and well delineate an ancient depocenter located on the eastern side of the basin. Furthermore, sharp lateral velocity changes suggest the presence of east-dipping normal faults in the central and western sectors of the basin with minor total throws (< 200 m).
Sharp lateral changes in the carbonates of il Monticello are related to the pervasive cataclastic fabrics developed during prior extensional tectonism (Fig. B2_3).

B5 Stop: Tramutola cemetery

Location and aim

The stop is located on the southern side of the Monticello hill on the western border of the Agri basin, and allows a panoramic view of the crustal structure of the area around Tramutola village that will be compared with results of high-resolution seismic tomography.

Outcrop description

From this point we look at the contact between white stromatolitic dolomitic limestone (Triassic-Liassic) and overlying Jurassic oolitic and oncoid limestone. Although in official maps the carbonate sequence of il Monticello is shown as a coherent section, in fact it is sliced in several structural imbricates showing younger-on-older relationships (Fig. B3_1). Similar relations are found between uppermost Cretaceous (Turonian-?Paleogene) floatstone and packestone and underlying upper Cretaceous rudistid limestone moving here from the previous stops (see previous section). Minor imbricates are also found within the Jurassic and lower Cretaceous section (Fig. B3_1).

The contacts are represented by medium-angle (30°-40°), NE-dipping shear zones marked by a pervasive cataclastic texture, indicative of displacement under low-confining pressure. Stratigraphical relations and structural observations point that the contacts are extensional.

High resolution seismic tomographic images in this part of the basin show unexpected lateral and vertical changes, which are likely related to the thick cataclastic zone at these contacts.

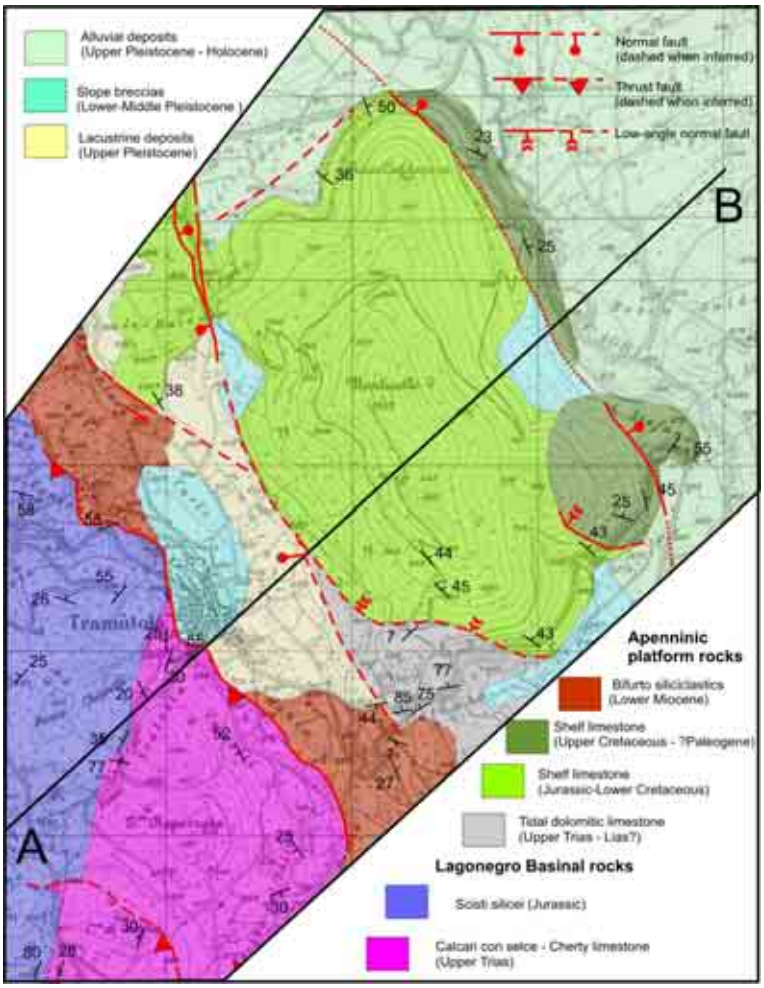

Figure B3_1. Geologic map of il Monticello

The western side of il Monticello hosts lacustrine Quaternary deposits overlying Miocene siliciclastics (Bifurto formation) which typically reside stratigraphically above the Mesozoic platform to slope rocks of the Maddalena unit.
The genesis of this small basin is not simply due to extensional tectonics. The western border of il Monticello is limited by a SW-dipping fault (Figs. B3_1 and B3_2) that does not have a significant expression in seismic tomographic images. Based on this, we infer that the displacement on this fault is minor (question mark in Fig. B3_2), and Miocene siliciclastic rocks are not dropped down from the top of il Monticello, but their present position is a result of articulated paleogeography and late Neogene thrusting.
Looking west, we have a clear view of the mountain escarpment limiting westward the village of Tramutola. Although resembling a normal-fault generated scarp, detailed mapping does not show a normal fault at this locale. Instead, map pattern are consistent with thrusting of Lagonegro rocks on top of Miocene Bifurto silicilastics (Fig. B3_2). This thrust is part of late .generation shortening episodes that invert the older thrust relationships, breaching across the previous regional thrust carrying the Maddalena limestone and its cover (Bifurto) on top of the Lagonegro rocks (western side of Fig. B3_2). Seismic tomography shows a wedge of low-velocity reflectors dipping beneath the Lagonegro rocks west of Tramutola, and precisely image the breaching thrust of the Lagonegro units.

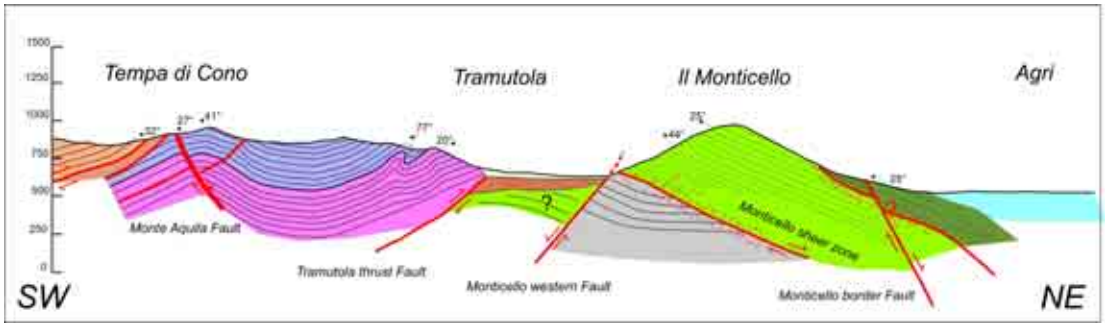

Figure B3_2. Geologic profile through Tramutola-il Monticello. Keys as in Fig. B3_1

B4 Stop: Cozzi Crocevie quarry

Location and aim
This stop at a quarry will allow inspecting bedrock outcrops of the M. Aquila fault and its relation with the pre-existing geological frame.

Outcrop description
The quarry exploits Jurassic shelf mudstone to grainstone, pervasively shattered largely in response to thrusting on a low-angle detachment bringing the Maddalena carbonates on top of the Lagonegro rocks, which is exposed on the southern side of the quarry (Fig. B3_1).

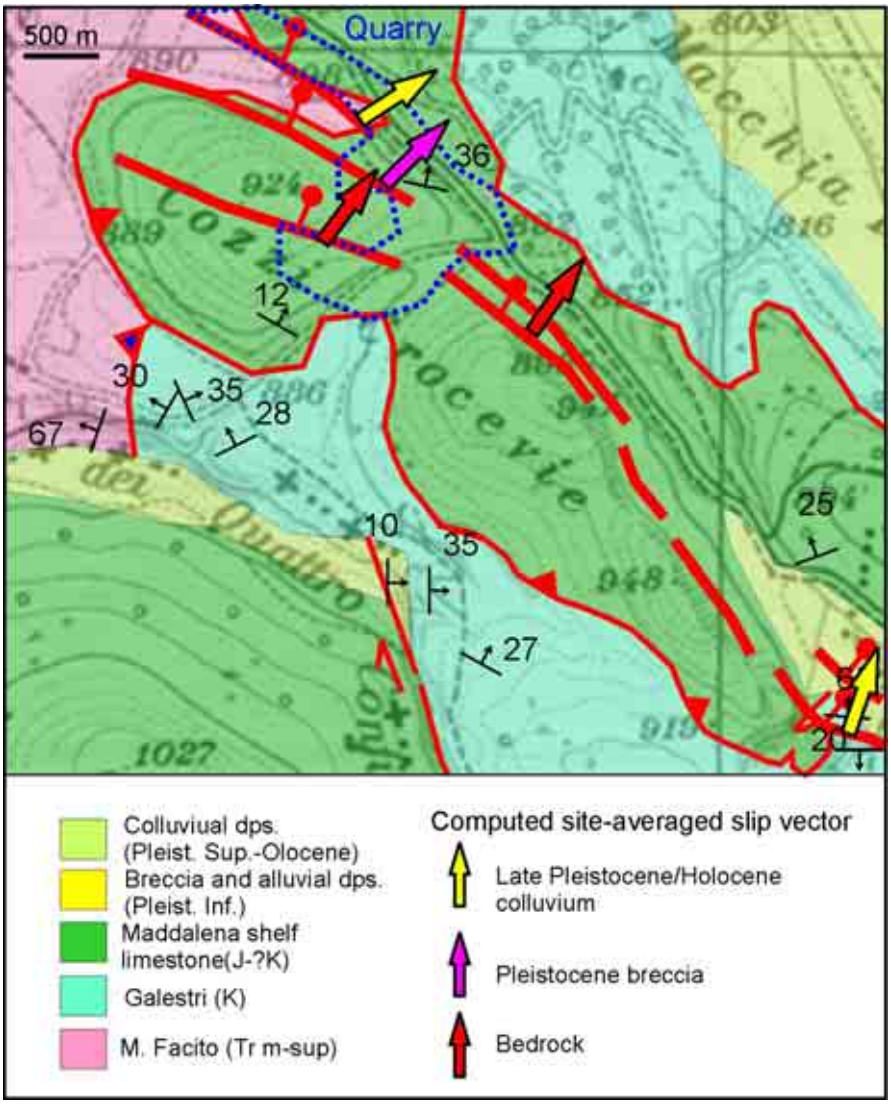

Figure B3_1 – Map of the M. Aquila fault at the Cozzi Crocevie quarry site.

The low-angle shear zone is cut by high-angle (70°-80°) brittle faults (Fig. B3_2) forming the northern part of the M. Aquila fault, which further south involves Holocene deposits exposed in paleoseismological trenches.

Figure B3_2 – Cataclastic shear zone at the contact between Maddalena shelf carbonate and Lagonegro basinal rock. The low-angle shear surfaces are cut by high-angle planes of the MAF showing dip-slip striations.

In detail, three closely spaced faults can be seen at this site (Fig. B3_1). The uppermost fault is in the Mesozoic bedrock (Fig. B3_2). The middle strand involves cemented breccia deposits probably correlative with the Middle Pleistocene Marsico breccia, and the lowermost and northernmost fault involves colluvium of probable Holocene age underlying the present-day soil (Fig. B3_3).

Figure B3_2. Northernmost strand of the M. Aquila fault cutting recent colluvium.

Kinematic indicators collected on bedrock faults suggest the possible existence of an older episode of left-transtensional slip (Fig. B3_4, left). However, the prevailing slips on these faults indicate normal faulting and NE-directed extension (Fig. B3_4, center and right; Fig. B3_1).

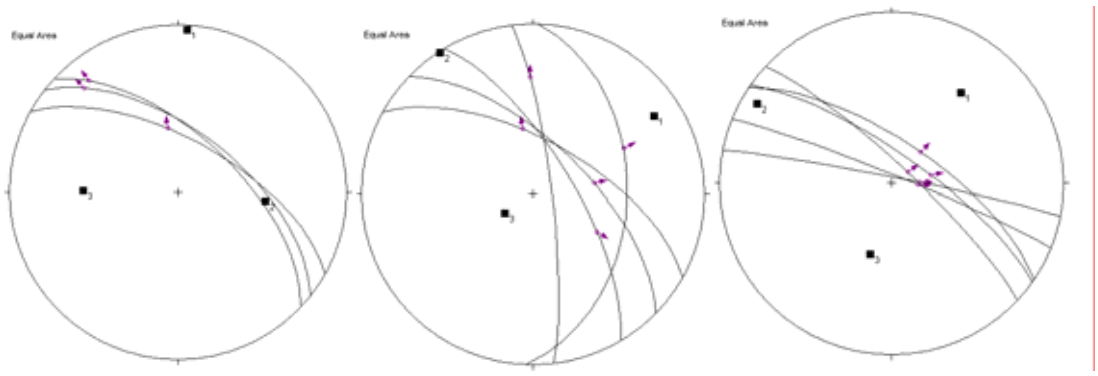

Fig. B3_4. Fault-kinematic analysis on mesofaults of the northern and central (left) and the southern (right) strands of the Monte Aquila fault at Cozzi Crocevia site.
We remark that the pre-existing structure is not significantly offset by these faults, although unquestionable pin-points for offset calculation are lacking.

B5 Stop: Trench 1 site
B6- Covoni site (trench 2)
B7- F.ce di Calce site

Location and aim
These stops are aimed at describing the results of the recent multidisciplinary researches conducted on the surface trace of the Monte Aquila Fault. We will present results from morphotectonic, structural, palaeoseismological, high-resolution stratigraphic and petrophysical correlation of bore holes cores, high-resolution seismic surveys and electrical resistivity tomography (ERT) surveys.

Outcrop description
We will make few stops along the southern part of the central segment of the Monte Aquila Fault (MAF), where detailed investigations have been carried on in the last few years. A detailed description of the studied sector of the MAF is given in the M. Aquila Fault chapter of the Introduction of this Guidebook.
The three stops are located in the structurally controlled Macchitelle basin (Fig. 21). This 1.5 km long basin is bounded to the north by the Monte Aquila peak (1096 m a.s.l.) with limestone outcrops, while the southern margin is less well defined by a rolling topography associated with the outcrop of argillites of the Galestri Formation. Locally, the Monti della Maddalena carbonates are thrust over the argillites of the Galestro fm. (Fig. 21). The basin is filled by a thin veneer of recent colluvial and alluvial deposits, with a maximum thickness of few tens of meters. The basin is drained by two fluvial systems flowing in the opposite directions (Fig. 22), which drainage basins are divided by a threshold locate in the middle of the depression. A karstic cave located close to the central divide drains part of the surficial waters.
The main creeks are originated from the southwestern slope, and consistently present small scale off-set when meet the surface trace of the MAF.
The MAF is associated with a well expressed scarp developed in recent soils. Detailed micro-topographic profiles across the main scarp (Fig. 23) show a cumulative morphologic throw of ~3.5 m.

Cave exploration
Just few ten meters NE of the Covoni trench site in the hanging-wall of the M. Aquila fault, the Grotta dell'Aquila is located within the carbonate rocks of Monte Aquila. It is a fairly sub-horizontal cave running N-S for slightly more than 100 m. (Fig. 1).

Figure B5_1. Location of the Grotta dell'Aquila in the M. Aquila block.

Although the cave developed along a ~N-S trending fracture network within the carbonates (likely related to thrusting or folding), structural analysis inside the cave has documented the control of extensional or transtensional faults (Fig. B5_2). These are minor antithetic and synthetic structures to the MAF.

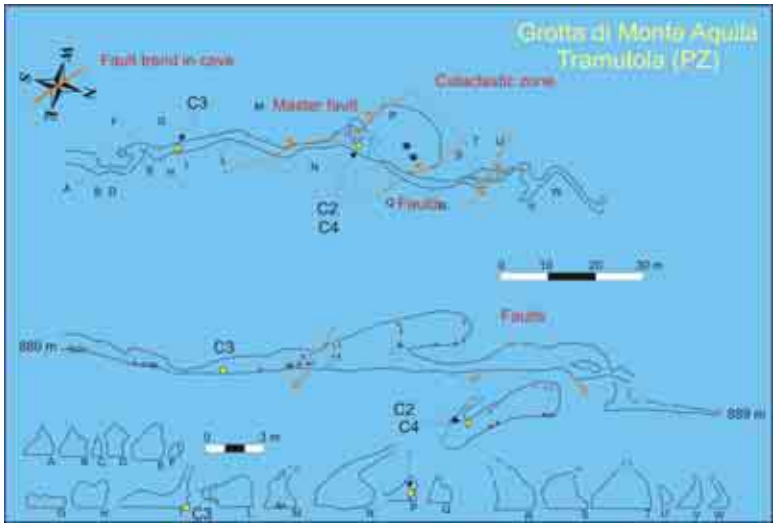

Figure B5_2. Structural map and section of the Grotta dell'Aquila.

One of these faults involves fluvial-hypogean clastic and clays and displacement is compatible with NE-SW extension (Fig. B5_3)

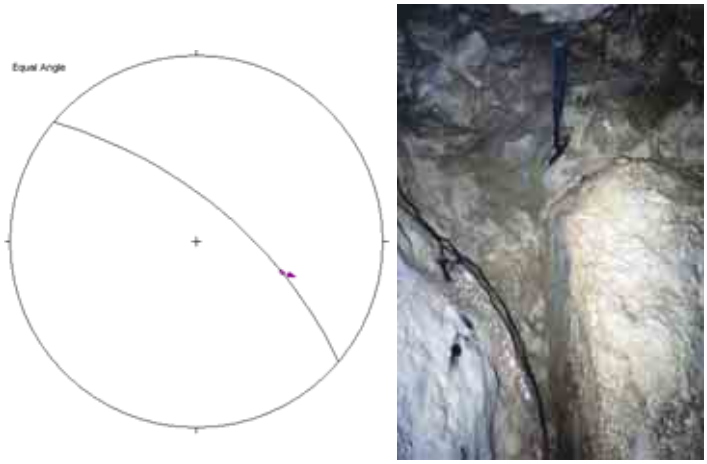

Figure B5_3. Fault and related slip kinematics involving recent hypogean deposits.
Another of the faults mapped in Fig. B5_2 has caused breakage of columnar concretions and has sheared and tilted thin stalactites (Fig. B5_4).

Figure B5_4. Tilting and shearing of a column (left) and offset of the growth axis of a stalactite (center). The rose diagram (right) shows the measured tilt direction of stalactites (n=5).

Measured horizontal offset of growth axes document displacements between 3 cm and up to 10-20 cm along a NNE-SSW (N15°-30°) direction (Fig. B5_4, right) in agreement with the displacement field of the MAF.
14C AMS ages from a tilted stalactite (Fig. B5_5) constrain an Early Holocene displacement event, which, based on the relatively narrow age gap we attribute to co-seismic faulting. Sample C2a (tilted stalactite) has an 11210-11350 2-σ calibrated age, whereas sample C2b (undeformed stalactite grown upon the tilted one) has a 9530-9680 2-σ calibrated age. Thus, a possible c-seismic displacement occurred between ~9.6-11.3 ka.

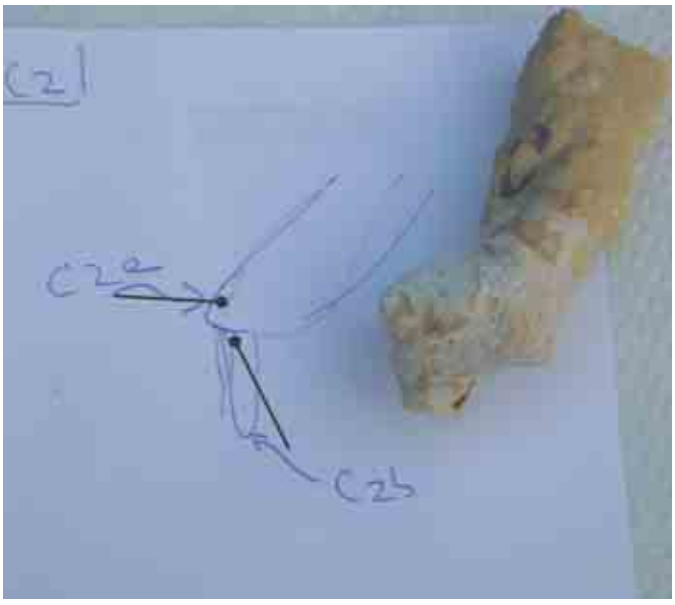

Figure B5_5. Dated stalactite. Sample is about 10 cm long.

Tommaso Maggi, Geologist of Villa d'Agri, is acknowledged for support in exploration of the cave.

Palaeoseismology
(contribution of Giuliana D'Addezio)
We present preliminary results coming from the analysis of the stratigraphy exposed on the walls of two palaeoseismological trenches dug across the MAF trace at Monte Aquila Trench1 and Covoni sites.

Monte Aquila Trench1 (Stop B5)
The 40-m long trench exposed a series of silt and clay deposits deformed in three main fault zones (Fig. B5_7). In the 10 m-long fault zone 1 the deformation produced a series of normal high-angle synthetic and anthythetic faults defining a graben-like structure. In fault zone 2 the units glided northwards along low-angle reverse fault planes. The deformation is less evident for the older units respect to the youngest one. Fault zone 3 is composed by a single high-angle normal fault.
Several units present diffused volcanic material and there are two well developed tephra layers, described by D'Addezio et al. (2006).
Based on a detailed stratigraphic and structural analysis we recognized at least three single events of deformation (earthquakes). Because of the lack of the same stratigraphic unit between the footwall of the main fault zone and the hanging-wall, it was not possible to estimate the total displacement produced by the fault activity.
Ev 1
Affect the sequence up to unit c. The top of this unit can be considered as the event horizon. We have direct evidence for this event only in the graben zone but at the time of the event this unit was probably continuous all along the trench and the deformation took place also in correspondence of the main fault zone. After the event an erosional phase removed the unit on the uplifted side.
Ev 2
Evidences for this event appear distributed along the whole section. In fault zone 1 removing the deformation produced by Ev 1 the sequence (see Fig. B5_7, second pannel) appears still deformed up to unit l in the graben zone. A complex deformation affects the units in correspondence of m 11 to 15 with reverse, normal anthithetic and low-angle fault and folding. In fault zone 2 the style of deformation is characterized by the low-angle reverse faults producing sliding and melting of the units between 25 and 27 m. Considering the thickening of the lower part of unit g the event could be occurred during its deposition. Based on that, the event horizon could be located somewhere in the lower part of unit g or at the top of unit l.
Ev 3
Evidence for this event is the 0.6 m of vertical separation of the thepra unit y (dated to 266 ± 6 ka by D'Addezio et al., 2006) along an anthythetic fault. Two synthetic faults at m 32 and 36 produced little deformation of unit p and q but could be also an effect of a previous event.
Older event
The single fault in fault zone 3 is sealed by unit l and h. This latter unit is probably involved on the sliding in fault zone 2 during Ev 2. So that the fault acted in a previous event (Ev 3) or could by an evidence of an older not yet well recognized event. The vertical separation evaluated along this fault is about 1.3 m.

Figure B5_6. View of the western wall of the Monte Aquila trench 1. The sharp contact between the argillitic bedrock (Liguride Unit) and the soils is evident.

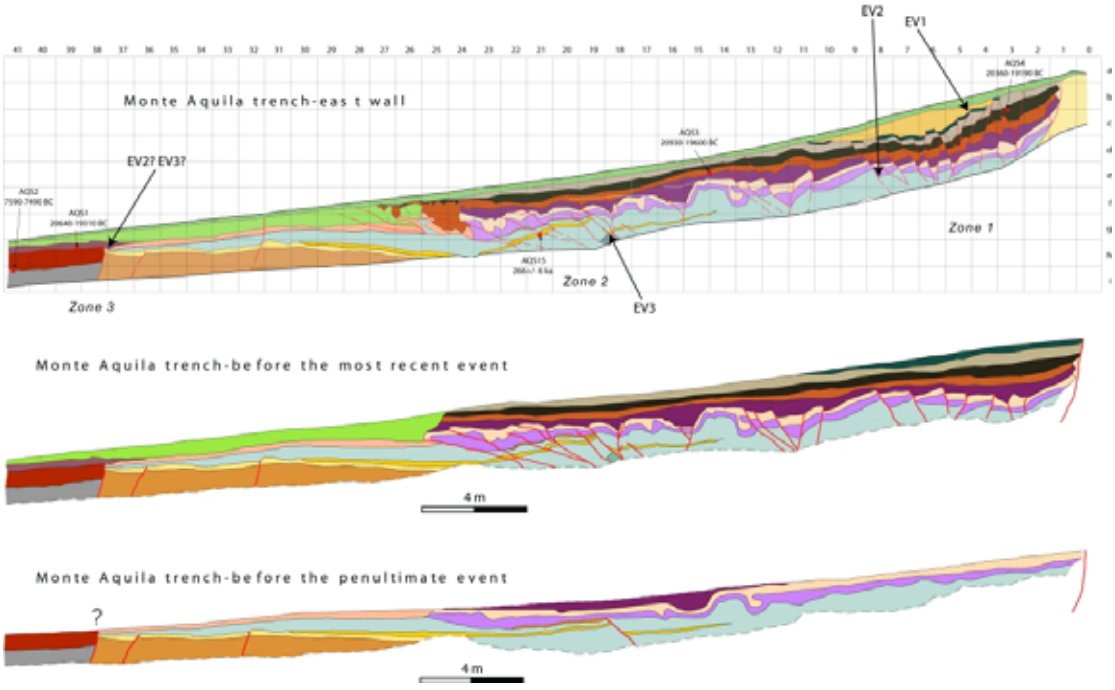

Figure B5_7. The upper pannel shows the log of the western wall of the Monte Aquila trench. North to the left, south to the right. The two lower panels show a reconstruction of the geometry of the strata previous than the most recent and the penultimate events.

In summary, this trench highlighted the occurrence of at least three earthquakes on the MAF, but unfortunately it did nit yield good age constraints on them.

Covoni trench (Stop B6)
The original 40 m long excavation showed a sequence of silty and silty clay alluvial, colluvial deposits and soils.

As a consequence of major wall collapse we were able to investigate only the initial part of the excavation close to the topographic scarp for a total of 12 m.
On this part of the trench wall we found evidence of a sharp contact between lithologically different units. Along and around the contact area carbonate encrustment are diffused (possibly because of preferential carbonatic rich water circulation) that partially hide the original contacts (Figs. B5_8 and B5_9).
Based on the stratigraphical and structural analysis we interpreted the contact as a fault produced by a sharp slip of the two sides. Unfortunately, there is not a clear correspondence between the units on the two sided of the fault; this prevents the evaluation of the amount of vertical slip and possibly the discrimination of multiple events. On the other hand, the mismatching of the units may also suggest possible horizontal component of the movement.
The deformation we observe was produced by a single event that affected the sequence up to unit d. This unit is present only on the footwall of the fault and its shape suggests a channel deposit. Unit c is a partially colluviated soil developed on unit d. This unit is not directly involved in the deformation but appears reworked as unit n on the hanging wall. Probably unit c was the surface horizon at the time of the event. Old root systems are possibly responsible of the blackish organic infiltrations of unit c on unit d. Unit b represents a post event deposit and is continuous along the studied part of the trench. On the downthrown part below unit b there is a chaotic mess of reworked and slid units overlapped. Units n and p are related to units c and d, respectively. The wedge shape of unit p and its abrupt laying on unit r suggest a rapid sliding of unit p during the event. Unit r appears muddled and irregular especially on the top and could be interpreted as a unit e disturbed by the event. Unit s predates the event. We may suggest 1 m of vertical slip based on the thickness of the colluvium on the downthrown side. To give chronological constrain to the sequence we collected several charcoal samples on the trench walls; some of those were selected and dated at the Poznan and Beta Analytic Radiocarbon Laboratories. Sample 7, collected on the upper part of unit b1 (post event deposit) provided an age of 1280-1400 AD whereas from sample 1 from unit c1 (pre event deposit) we obtained an age of 520-370 BC. From sample 13 (unit d, located just below the soil unit c) we obtain an age of 800-530 BC. Therefore, the event occurred between 520 BC e 1400 AD, with the older interval preferred considering the position of sample 1 very close to the event horizon.

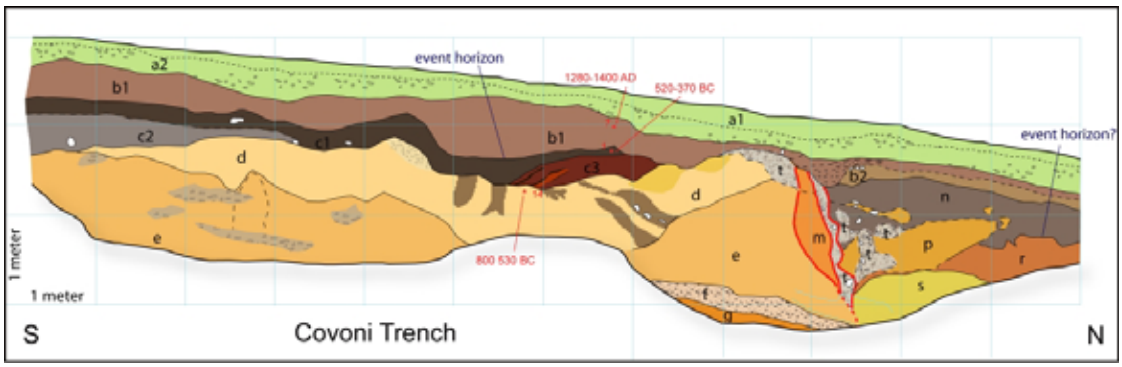

Figure B5_8. Log of the eastern wall of the Covoni trench.

Figure B5_9. Detail of the fault zone in the Covoni trench.

In summary, the stratigraphy exposed on the walls of this trench registered one event occurred about 1000 years earlier than the 1857 earthquake (a previous event of the same fault?).

High-resolution stratigraphic and petrophysical correlation of borehole cores
(contribution of Riccardo Civico, Marina Iorio; Daniela Pantosti and Paolo Marco De Martini)

During paleoseismological investigations at Fornace di Calce site eight cores were drilled down to maximum depth of 7 m using a vibracoring (gasoline power percussion hammer).
Three of them were sampled with pvc tubes in order to have almost undisturbed sediments to be analyzed in detail in the laboratory.
All the selected cores sampled with pvc tubes were taken in the IAMC Laboratory to perform accurate sedimentological description and to measure their physical properties using a non pervasive logging system.
Both the sedimentological and petrophysical observations were done at a centimetric scale.
We used the fully automated GEOTEK Multi-Sensor Core Logger (MSCL) (Fig. B5_10) available at the IAMC-CNR Petrophysical Laboratory.
The MSCL system includes a Bartington MS2E Point sensor, for measuring the low-field magnetic susceptibility, a Gamma Ray Attenuation Porosity Evaluator (GRAPE) sensor to determine the bulk density (GRP), a Minolta Spectrophotometer CM 2002 to measure the reflectance parameter (the percentage of reflected energy in 10 nm wavelength steps), and two Acoustic Rolling Contact (ARC) transducers, for evaluating the P-wave velocity.

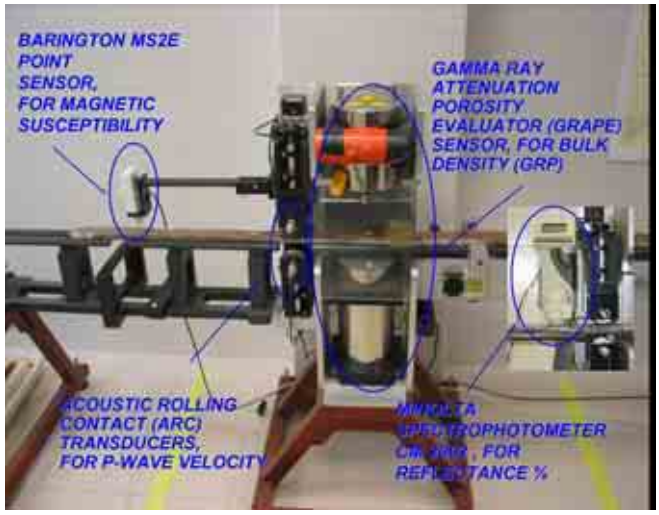

Figure B5_10. Photo of multisensor core logger (IAMC-CNR laboratories).

Most stratigraphic applications of MSCL logs rely on the relative values of logged parameters for detecting geological events, commonly applied on deep oceanic cores.
Our aim is to experimentally use the MSCL tool on continental deposits in order to relate measured physical properties to sediment characteristics. The final goal is to obtain a high resolution stratigraphic correlation able to highlight possible tectonic offsets.
At first, the sedimentological and petrophysical data from the three cores are of good quality and could be potentially correlated. In Figure B5_11 we present the stratigraphic log of borehole FC-06 and its petrophysical properties.

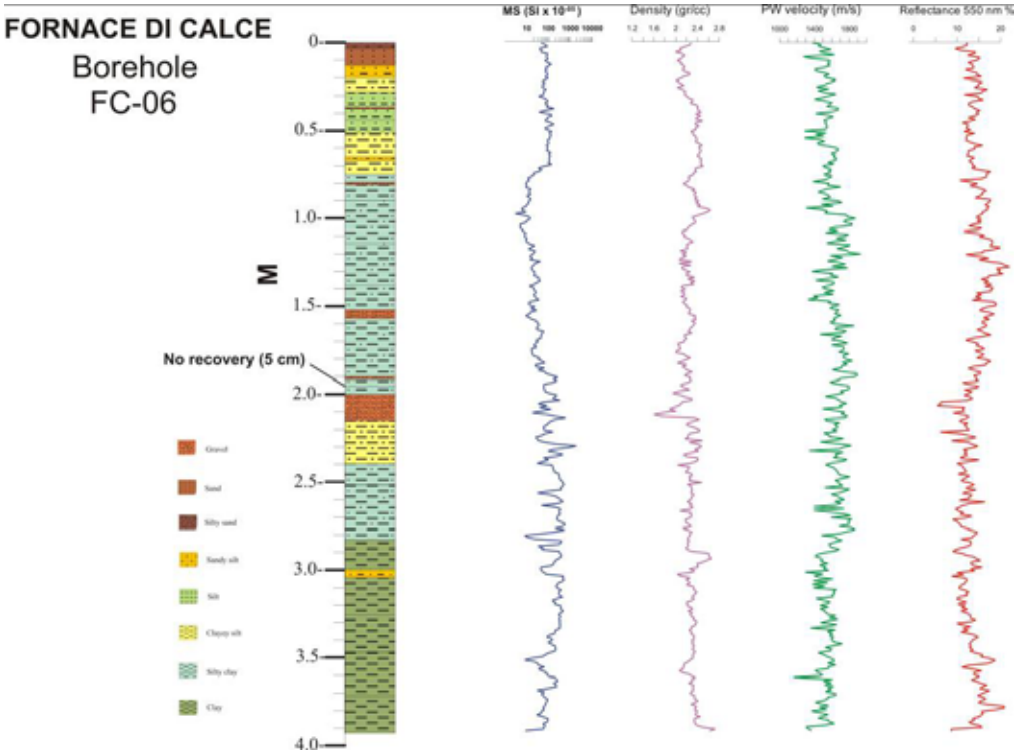

Figure B5_11. Example of a stratigraphic and petrophysical log.

Seismic tomography
(contribution of Luigi Improta)

High-resolution seismic tomography (HRST) is combined with reflection profiling to image the shallow structure of the Monte Aquila Fault in two sites. In site Trincea (stop B5) a 3-m-high scarp and the trench document recent faulting activity; in site Fornace (stop B7) the fault is only inferred from a subtle surface warping. Small cumulative displacements across the fault and soft soil conditions make fault imaging challenging. Smooth Vp and reflectivity images are jointly interpreted and compared to Electrical Resistivity Tomographies, trench excavations and shallow drillings.
We recorded both multifold wide-aperture and near-vertical reflection data along two profiles about 200 m long. We obtained from this combined data set P-velocity images by multiscale HRST and reflectivity images by CDP-processing of near-vertical/wide-angle reflection data.
In Monte Aquila Trench site (Fig. B5_12) seismic exploration has a very good performance. Seismic images allow pinpointing the fault location and provide details on the fault-zone internal structure. A sharp Vp lateral change reveals a major step in the bedrock caused by an NE-dipping normal fault. Repeated surface faulting episodes are suggested by a low-velocity colluvial package 12-15 m thick, which is imaged in the fault hanging-wall just behind the trench. A CDP stack section highlights that the fault zone is 15-20 m wide and includes 3 fault splays at least. Slip concentrates along the northernmost splay located beneath the central trench section. Both Vp and reflectivity images indicate a cumulative vertical slip of 35-40 m.

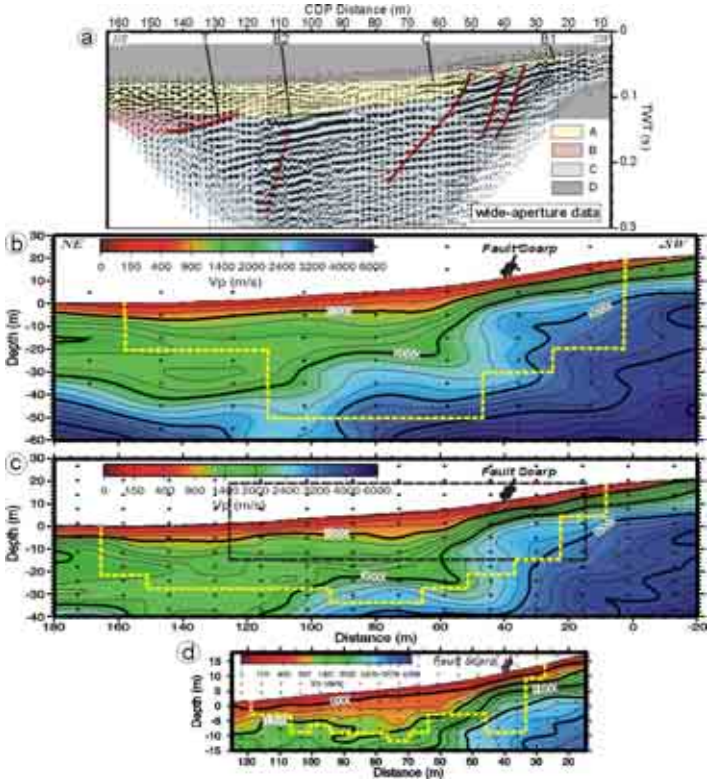

Figure B5_12. Site Trincea - (a) Wide-aperture CDP stack section; A. basin, B. limestones, C. argillite, D. exploration depth of the tomography. (b) Long-, (c) intermediate- and (d) short-wavelength Vp models. The yellow line defines the resolution depth; nodes are depicted by circles. The dashed box outlines extent of model (d).

Performance of HRST in Fornace site is lower likely due to a softer substratum. Here comparison with resistivity images and shallow drilling is crucial to support fault detection (Fig. B5_13). A rapid deepening of a high-velocity/high resistivity substratum is evident north of the surface warping. To the north, the bedrock is covered by an intermediate-velocity/low resistivity layer 15-20 m thick interpreted as a (saturated) alluvial infill. A low-velocity/low-resistivity colluvial wedge 6-9 m thick is imaged just behind the surface warping. Reflectivity images show events truncations in this zone consistently with a NE-dipping normal fault. Drillings confirm the abrupt deepening of the bedrock as well as the presence of thick colluvial soils in the fault hanging-wall.

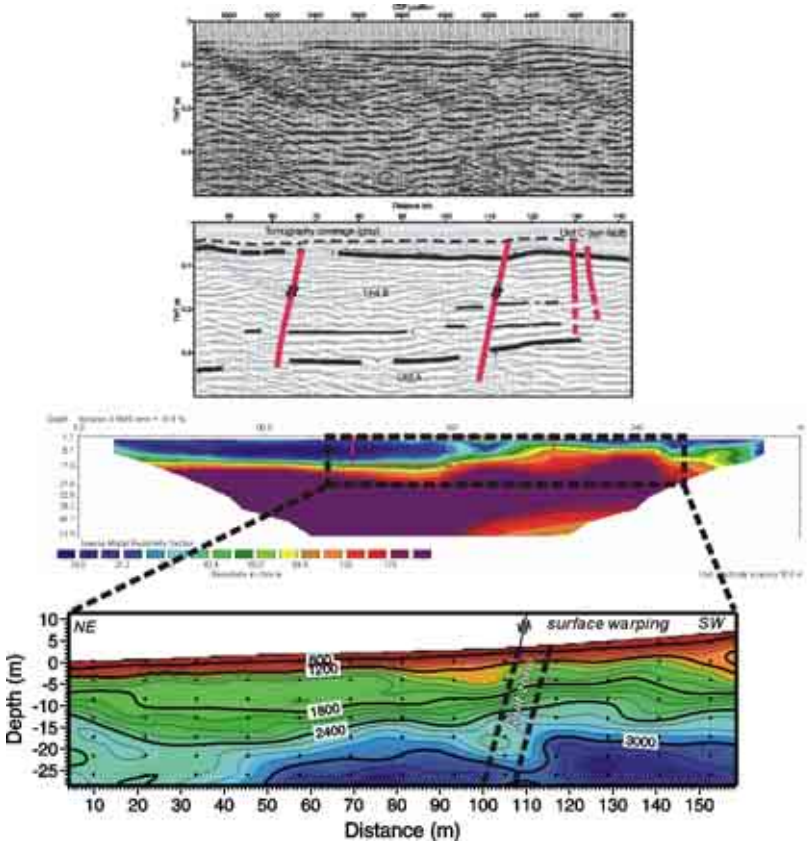

Figure B5_13. CDP stack section from near-vertical reflection data, electrical resistivity and P-wave velocity images obtained in site Fornace.

Electrical Resistivity Tomography (ERT)
(contribution of Alessandro Giocoli and Sabatino Piscitelli)

An Electrical Resistivity Tomography (ERT) survey was carried out to study the geometry of the Quaternary alluvial and colluvial bodies across the M. Aquila fault, at Covoni, Fornace and Trench Sites.
A georesistivimeter Syscal R2 (Iris Instruments) equipped with a multielectrode system was used to obtain high resolution ERT, using Dipole-Dipole and Wenner Schlumberger arrays with electrode spacing varying from 1 to 10 m and penetration depth from about 5 to 50 m. Apparent resistivity data were inverted using the RES2DINV software.

Trench ERT Profile
A high resolution ERT survey of 62 m of length was performed in the north part of Covoni site near the palaeoseismological Trench 1 (Fig. B5_14).

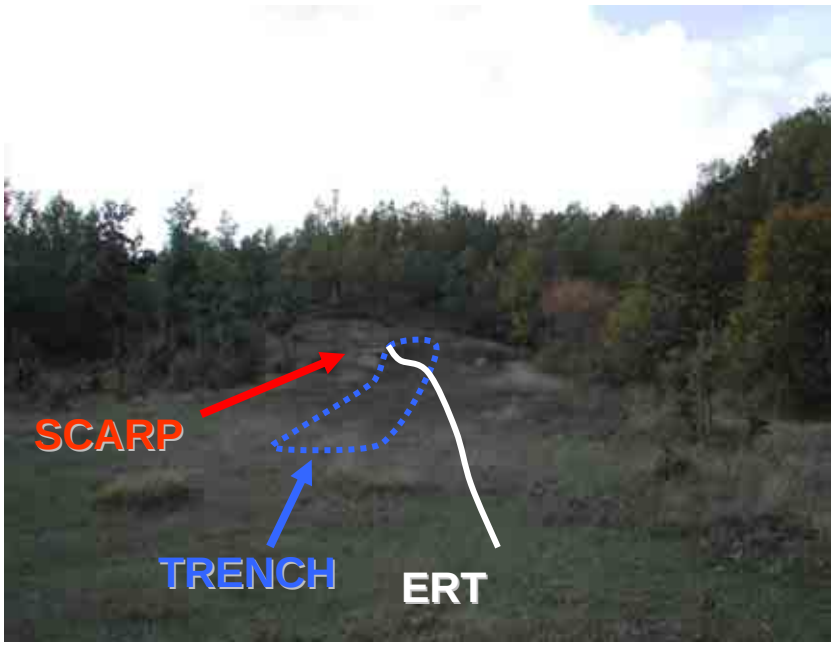

Figure B5_14. Photos showing the locations of the shallow ERT profile, trench and morphological scarp.

The electrical image was carried out using a 32-multielectrode system, with an electrode spacing of 2 m, obtaining a length of 62 m and an investigation depth of about 10 m (Fig. B5_15).

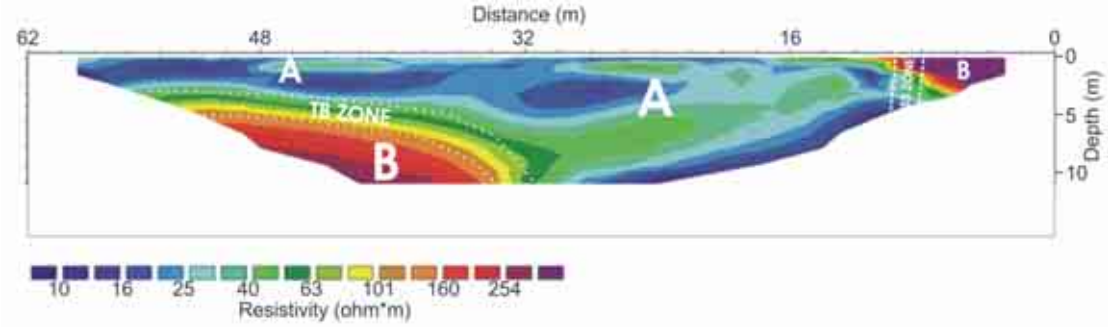

Figure B5_15. Electrical Resistivity Tomography performed near paleoseismological trench 1.

The electrical image shows resistivity values varying in the range 10–254 ohm*m. Relatively high resistivity values (rho>90 ohm*m) can be associated to the pre-Quaternary bedrock (B), while low resistivity values (rho<90 ohm*m) can be related to the shallow recent sediments (A). The moderate resistivity contrasts between the shallow recent deposits (A) and the bedrock (B) highlights the geometry of the top of the bedrock (TB zone). On the upper right hand of the tomography (SS zone), a relatively strong lateral variation of the resistivity values can be observed, due to the fault zone, as observed in the trench.

Covoni ERT Profile

Covoni ERT is a 155 m long profile crossing both outcropping bedrock and Quaternary deposits located in a small intramountain basin; the investigated depth is about 25 m. Fig. B5_16 shows the electrical image obtained at Covoni site.

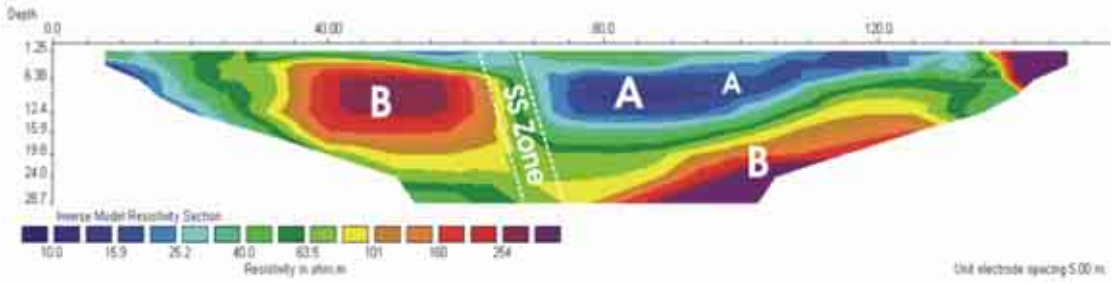

Figure B5_16. Electrical Resistivity Tomography performed in Covoni site. NE to right.

The electrical image shows electrical resistivity values varying from about 10 ohm*m (Quaternary sediment wedge; A) to more than 90 ohm*m (bedrock; B), with the presence of a remarkable vertical resistivity contrast (SS zone) associated to the tectonic lineament observed in the field.

Fornace ERT Profile

At Fornace site, two ERTs were carried out: a high resolution ERT with an electrode spacing of 10 m, obtaining a section 310 m long and an investigation depth of about 50 m, and a very high resolution ERT with an electrode spacing of 3 m, a length of 93 m and an investigation depth of about 15 m (B5_17).

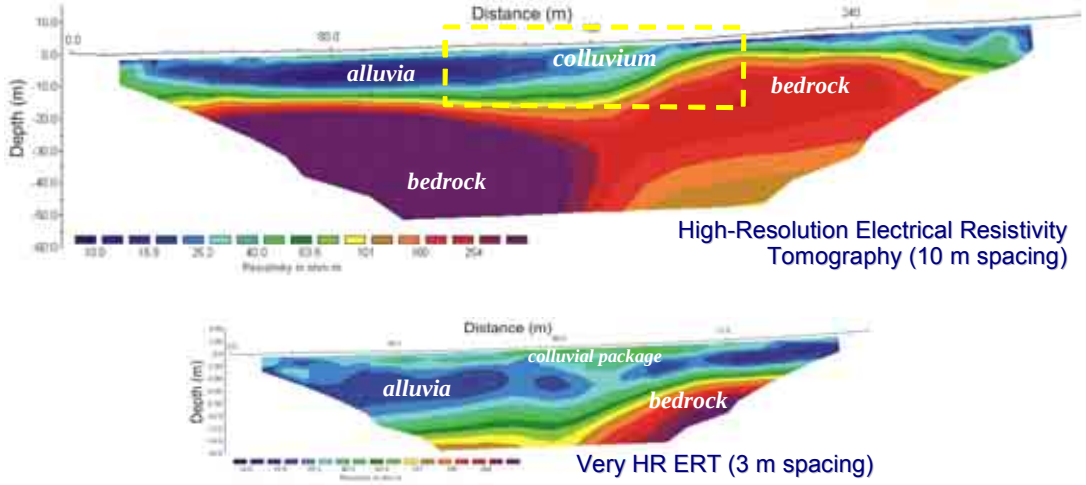

Figure B5_17. Electrical Resistivity Tomographies carried out at Fornace site. NE to left. The yellow box indicates the sector investigated by the very high resolution tomography (3m spacing).

Both the electrical images show a relatively low resistivity zone on the top (rho<90 Ohm*m), that can be associated to colluvium/alluvia sediments, having a thickness up to about 10 m. The underlying relatively high resistivity sector can be related to the bedrock (?). The gentle slope observed in the bedrock, in the range 160-200 m of the profile, can be due to a possible fault zone.

B8 Stop: Grumento Nova

Location and aim

This stop is aimed at the observation of the easternmost section of the High Agri Valley, from the panoramic terrace of Grumento Nova.

Outcrop description

Grumento Nova is perched on the flat top of a ridge of Cretaceous limestone on the southern valley side. The Quaternary alluvial, colluvial and lacustrine sediments of this section of the valley are deeply incised by the Agri River and its tributaries, thus exposing the older part of the whole Complesso Val'Agri (Fig. A1_1; Giano et al., 2000). The depositional top of this sedimentary sequence constitutes the bulk of the fluvial terrace III-a described by Bianca & Caputo (2003) (Fig. B1_4). The Agri River few km downstream Grumento Nova leaves the basin through a deep gorge cut into Miocene Gorgoglione Flysch. The fluvial terraces of the High Agri Valley are isolated from the middle and lower sections of the Agri River Valley by a knickpoint developed in coincidence with the Armento Thrust, as such they are not related to the eustatic sea level changes (Bianca & Caputo, 2003).

Stratigraphic architecture and sedimentary evolution of the Agri intermontane basin

(contribution of Irene Zembo)

The basin consists of three tectonically controlled and diachronous depocenters, bounded by WNW-ESE and NE-SW faults; outcrops occur in the southeastern one ("Pertusillo depocenter"; Fig. 12; Colella et al., 2004), which was deeply dissected by the drainage network during the Late Pleistocene-Holocene. In this area, close to the basin threshold, detailed mapping of lithofacies, architectural elements and their bounding surfaces and analysis of palaeocurrent directions have been selected as the primary criteria for stratigraphic subdivision and geological mapping.

Physical stratigraphy, facies analysis (Miall, 1996) and palaeopedological characterization (mainly micromorphological) are the key to decipher the sedimentary evolution of the basin and the contemporaneous palaeogeographic and climatic changes. These data, in combination with OSL, 14C, AFTA dating methods, provide insights into the tectono-sedimentary evolution of the area during the Pleistocene.

In this contribution a new stratigraphic framework is presented for the outcropping part of the Agri Basin fill, which has been subdivided into four allostratigraphic units, following the recognition and correlation of the major basin-wide unconformities. These units, accumulated in response to changes in intrabasinal subsidence, catchment relief, regional tectonics and climate, form the Agri Valley Allogroup, up to 100 m thick (Zembo, 2007). Their erosional boundaries can be associated with preserved weathering profiles and/or palaeosoils ("palaeosurfaces"; Widdowson, 1997). In the all studied area, these profiles correspond to deeply truncated palaeosoils, developed during geomorphological stability stages.

The unconformable boundary with the tectonic substratum crops out only at places, close to the basin margins (Fig. B8_1-A) and along the actual shore of Pietra del Pertusillo Lake, in the regions of minimum thickness of the clastic succession.

The early basin fill was associated with Spinoso Conglomerates Formation (Unit I, Early Pleistocene ?) that is formed by stratified and weathered conglomerates, locally up to 20±30 m thick, which are strongly deformed and disconnected to the original source area. The conglomerates are probably cut by transtensional faults and are uplifted at different elevations only along the southeastern basin flank. These deposits have been interpreted as the result of coarse-grained alluvial fans that were probably dominated by braided channels.

The lowermost Lago di Pietra del Pertusillo Alloformation (Unit II, Middle Pleistocene) is exposed in the axial sector of the all outcrop area and its total thickness is unknown at present; a minimum of 30-40 m can be figured out by the available exposures (Fig. B8_1-A). Unpublished subsurface data suggest that the maximum thickness of Unit II can reach 200 m along the northeastern basin flank. At its base, this unit rests unconformably over the bedrock along the surface S2. The contact with the pre-Pleistocene deposits or Spinoso Conglomerates Formation is covered. Unit II is composed of lacuo-palustrine silty-clay and silt with interbedded fan-delta lens-shaped gravel bodies, prograding into the lacustrine area. Sources were from both the western and the southern slopes of the basin. Upward-coarsening sequences are common in the fan fringe lacustrine deposits where carbonate layers (calcrete), root traces and vertebrate remains locally occur.

The erosional surface S3 between Unit II and III delineates the change from lacustrine to alluvial environment (Valle del Nasillo Alloformation; Unit III, Middle-Late Pleistocene; Fig. B8_1-A). The latter unit includes coarse-grained conglomerates and gravels with subordinate silts and fine sands deposited in coalescent alluvial fans. The fans prograded north-northeastwards, forming wedge-shaped bodies, that filled the lacustrine area. Valle del Nasillo Alloformation reaches 40 m in thickness adjacent to the southeastern basin margin and thins to the northwest. In the upper part of this unit, a laterally continuous, truncated (surface S4) fersiallitic palaeosol indicates decreasing aggradation rate during a fan-surface stability stage and provides a key-surface for correlation at the basin-scale (Fig. B8_1-A). This strongly weathered palaeosol appear to be related to long-cycle pedogenesis (i.e. some ten thousand years) rather than extreme palaeoclimatic conditions and suggests a rather humid climate with hot and dry seasons, alternating with semiarid ones.

Subsequently the fans retreated and were overlain by the deposits of an axial braided alluvial system (Vallone dell'Aspro Alloformation; Unit IV, Late Pleistocene) that drained towards the SE. This unit, up to 70 m thick, is made up of multistory gravel/sand bodies (channel fills and gravel-sand bars; Fig. B8_1-A). The poorly drained environment of the alluvial plain is documented by hydromorphic palaeosoils and vertisoils (Fig. B8_1-A). Transverse alluvial fan bodies interfinger with the axial unit from the southern and northern basin margins. A centimeter thick ash-fall deposit is locally preserved in the intermediate portion of this unit. Chemical composition and mineral assemblage of the volcanic fraction suggest to correlate this layer with the Tufo Verde Epomeo of Ischia and the pyroclastic fall deposit Y-7 recognised in the Ionian Sea cores, dated as 56±4 ka (40Ar/39Ar on sanidine; Allen et al., 1999; Kraml, 1997). This volcanic level is expected to offer a good geochronological marker as a result of the dating of the pyroclastic apatites currently in progress.

The boundary between Vallone dell'Aspro Alloformation and the overlying Torrente Casale Alloformation (Unit V, Late Pleistocene-Holocene?) is an erosional surface (surface S5), locally underlined by the remains of a reddish brown palaeosol (Fig. B8_1-B). Torrente Casale Alloformation crops out close to the marginal slopes of the basin and is represented by prograding-aggrading coarse alluvial fan deposits developing from both the northern and the southern borders of the basin, above the underlying axial braid plain (Unit UIV; Fig. B8_1).

In order to produce a detailed chronostratigraphy and sedimentary evolution, optically stimulated luminescence (OSL) datings were applied. Samples were collected from a variety of environments (sandy bars, crevasse splays and sheetflood deposits); quartz extracted was analyzed using the coarse-grained, single-aliquot regenerative-dose (SAR; Murray & Wintle, 2000 and 2003) technique. The estimated optical ages range from 50 to 5 ka, consistent with the available independent (radiocarbon, tephrocronology) and relative age constraints, provide the first contribution to the chronology of the sedimentary evolution of the upper part of the Agri Basin fill.

The data presented for the younger phase of sediment deposition suggest a Late Pleistocene age for the upper part of Vallone dell'Aspro Alloformation (Unit IV) and a

Late Pleistocene-Holocene? age for Torrente Casale Alloformation (Unit V). As a consequence, the Middle-Late Pleistocene age of Valle del Nasillo Alloformation (Unit III) at present can be only inferred.
Asymmetric subsidence in the Middle (?)–Late Pleistocene Agri Basin is indicated by the accumulation of a very thick pile of aggrading deposits, restricted to the northeastern faulted margin of the basin (Unit II and IV; unpublished subsurface data; Fig. B8_1-B). The alluvial depocenter gradually moved towards the southwestern border of the Agri Basin during the latest Pleistocene, testifying to the shift of maximum subsidence towards the opposite (southern) basin margin. This is interpreted by Morandi & Ceragioli (2002) and Maschio et al. (2005) as reflecting a recent fault control at the southwestern side of the valley.
Finally, during latest Pleistocene-Holocene time the Agri Valley Allogroup succession was incised and terraced by the modern Agri River and its lateral streams.

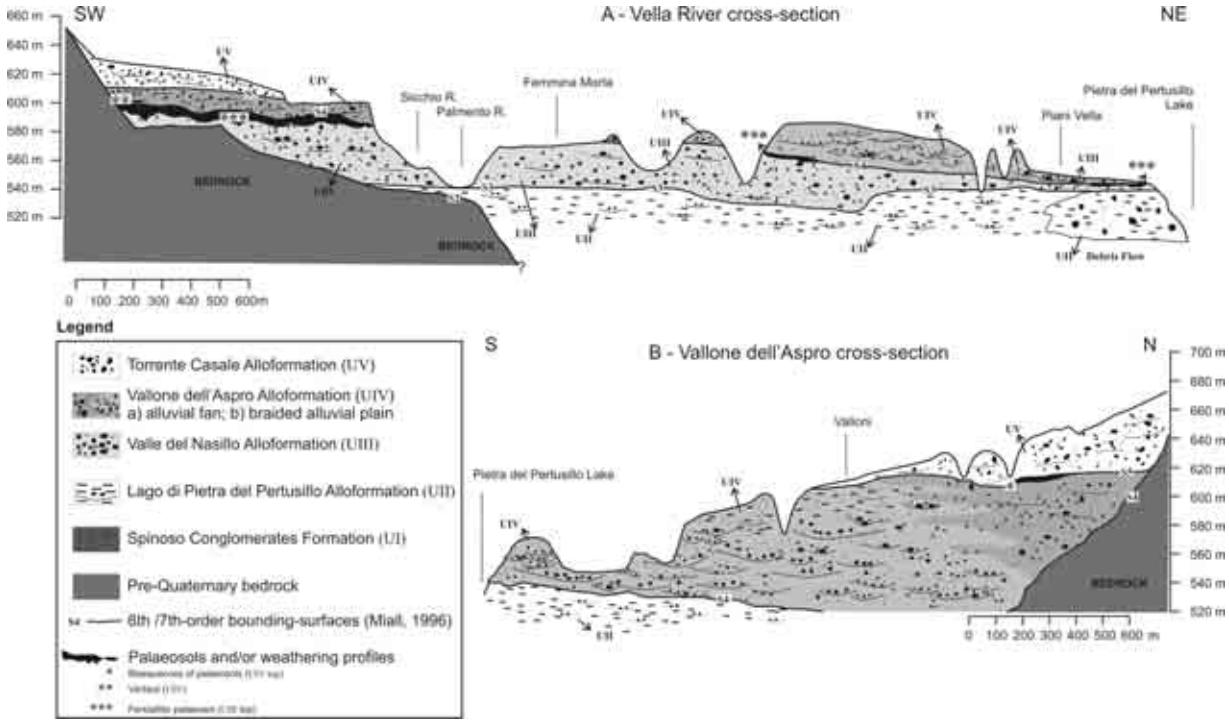

Figure B8_1. Representative stratigraphic cross-sections of the southeastern part of the Agri Basin ("Pertusillo depocenter"): (A) stratigraphic cross-section of the Vella River; (B) stratigraphic cross-section of the Vallone dell'Aspro.

Quoted references and other relevant papers

Alessio G., Esposito E., Gorini A. and Porfido S. (1995) - Detailed study of the Potentino seismic zone in the Southern Apennines, Italy. Tectonophysics, 250, 113–134.

Amato A. and Montone P. (1997) - Present-day stress field and active tectonics in southern peninsular Italy. Geophys. J. Int., 130, 519–534.

Amato A., Montone P. and Cesaro M. (1995) - State of stress in Southern Italy from borehole breakout and focal mechanism data. Geophys. Res. Lett., 22(23), 3119–3122.

Ascione A., Cinque A., Santangelo N. and Tozzi M. (1992/1) - Il bacino del Vallo di Diano e la Tettonica trascorrente plio-quaternaria: nuovi vincoli cronologici e cinematica. Studi Geologici Camerti, 201–208.

Baratta M. (1901) – I terremoti d'Italia. Arnoldo Forni Editore.

Barchi M., Amato A., Cippitelli G., Merlini S. and Montone P. (2007) - Extensional tectonics and seismicity in the axial zone of the Southern Apennines. Boll.Soc.Geol.It. (Ital.J.Geosci.), Spec. Issue 7, 47-56. CROP-04 (ed. by A. Mazzotti, E. Patacca and P. Scandone).

Basili R., Valensise G., Vannoli P., Burrato P., Fracassi U., Mariano S. and Tiberti M.M. (2007) - The Database of Individual Seismogenic Sources (DISS), version 3: summarizing 20 years of research on Italy's earthquake geology. 2nd Version, submitted to Tectonophysics.

Bavusi M., Chianese D., Giano S. I. and Mucciarelli M. (2004) - Multidisciplinary investigations on the Roman aqueduct of Grumentum (Basilicata, Southern Italy) Ann. Geophys., 47, 6, 1-12.

Benedetti, L. (1999). Sismotectonique de l'Italie et des régions adjacentes: fragmentation du promontoire adriatique. Unpublished Ph.D. Thesis, Université Paris 7, 358 pp.

Benedetti, L., Tapponier, P., King, G.C.P. and Piccardi, L. (1998) - Surface rupture of the 1857 southern Italian earthquake. TerraNova, 10(4), 206–210.

Bianca, M., and R. Caputo (2003). Analisi morfotettonica ed evoluzione quaternaria della Val d'Agri, Appennino meridionale, Il Quaternario, 16, 2, 158-170.

Boenzi F., Capolongo D., Cecaro G., D'andrea E., Giano S.I., Lazzari M. and Schiattarella M. (2004) - Evoluzione geomorfologica polifasica e tassi di sollevamento del bordo sud-occidentale dell'alta Val d'Agri (Appennino meridionale). Boll. Soc. Geol. It., 123 (2004), 357-372.

Bordoni P. and Valensise G. (1998) - Deformation of the 125 ka marine terraces in Italy: tectonic implications. In: Coastal Tectonics, I. Stewart, C. Vita-Finzi, eds., London: Geological Society of London Special Publication, 146, 71-110.

Borraccinni, F., De Donatis M., Di Bucci D. and Mazzoli S. (2002) - 3D Model of the active extensional fault system of the high Agri River valley, Southern Apennines, Italy, Journal of the Virtual Explorer 6, 1-6.

Boschi E., Guidoboni E., Ferrari G., Mariotti D., Valensise G. and Gasperini P. (2000) - Catalogue of Strong Italian Earthquakes. Ann. Geofis., 2000; 43(4), 340–868 with CD-Rom, 259 pp.

Branno A., Esposito E.G.I., Maturano A., Porfido S. and Rinaldis V. (1983) - Studio, su base macrosismica, del terremoto della Basilicata del 16 dicembre 1857. Bollettino della Società dei Naturalisti di Napoli, 1985; 92, 249–338.

Burrato P. (1995) - Tettonica attiva, sismogenesi e caratteri evolutivi del reticolo idrografico: tre esempi dall'Italia meridionale. Unpublished MS thesis, 69 pp and 26 images.

Burrato P. and Valensise G. (2007) - Rise and fall of a hypothesized seismic gap: source complexity in the 16 December 1857, Southern Italy earthquake (Mw 7.0). Bull. Seism. Soc. Am., accepted manuscript.

Camassi, R., and M. Stucchi (1997). NT4.1, un catalogo parametrico di terremoti di area italiana al di sopra della soglia del danno (published by GNDT, Milano), pp. 95 (also available at: http://emidius.mi.ingv.it/ NT/home.html).

Capolongo D., Cecaro G., D'Andrea E., Giano S.I., Lazzari M. and Schiattarella M. - Evoluzione geomorfologia polifasica e tassi di sollevamento del bordo sud-occidentale dell'alta Val d'Agri. In: 3◦ Forum Italiano di Scienze della Terra, Geoitalia, 2001, 338–340, Media Print Editrice, Livorno, Italy.

Carbone S., Catalano S., Lazzari S., Lentini F. and Monaco C. (1991) - Presentazione della carta geologica del Bacino del Fiume Agri (Basilicata). Mem. Soc. Geol. It., 47, 129-143.

Catalano S., Monaco C., Tortorici L., Paltrinieri W. and Steel N. (2004) - Neogene-Quaternary tectonic evolution of the Southern Apennines. Tectonics, 23, TC2003, doi: 10.1292003TC001512.

Cello G., Coccia B., Mancinelli A., Mattioni L., Mazzoli S. & Shiner P. 2002. Architettura pre-orogenica della piattaforma carbonatica appenninica nell'alta Val d'Agri (Lucania, Italia meridionale). Studi Geologici Camerti, Nuova Serie Vol. 2/2002, 45-52.

Cello G., Gambini R., Mattioni L., Mazzoli S., Read, A., Tondi, E., Zucconi, V. (2000) – Geological analysis of the High Agri Valley (Lucania Apennines, Southern Italy). Mem. Soc. Geol. It., 55, 149-155.

Cello G., Gambini R., Mazzoli S., Read, A., Tondi, E., Zucconi, V. (2000) – Fault zone characteristics and scaling properties of the Val d'Agri Fault System (Southern Apennines, Italy). J. Geodyn., 29, 293-307.

Cello G., Mazzoli S., Tondi, E., L. Mattioni, DAY 2: Alta Val d'Agri, in Patacca and Scandone, GIGS – Gruppo Italiano Di Geologia Strutturale, Field Trip 2003 – Southern Apennines.

Cello, G., Tondi E., Micarelli L., and Mattioni L. (2003). Active tectonics and earthquake sources in the epicentral area of the 1857 Basilicata earthquake (southern Italy), J. Geodyn., 36, 37–50, doi: 10.1016/S0264-3707(03)00037-1.

Chiarabba, C., P. De Gori, L. Chiaraluce, P. Bordoni, M. Cattaneo, M. De Martin, A. Frepoli, A. Michelini, A. Monachesi, M. Moretti, G. P. Augliera, E. D'Alema, M. Frapiccini, A. Gassi, S. Marzorati, P. Di Bartolomeo, S. Gentile, A. Govoni, L. Lovisa, M. Romanelli, G. Ferretti, M. Pasta, D. Spallarossa, and E. Zunino (2005). Mainshocks and aftershocks of the 2002 Molise seismic sequence, southern Italy, J. Seism. 9, 487–494, doi: 10.1007/s10950-005-0633-9.

Cinque A., Patacca E., Scandone P. and Tozzi M. (1993) - Quaternary kinematic evolution of the southern Apennines. Relationship between surface geological features and deep lithosferic structures. Annali di Geofisica, 36 (2), 249– 260

Cinti, F.R., M. Moro, D. Pantosti, L. Cucci and G. D'Addezio (2002). New constraints on the seismic history of the Castrovillari fault in the Pollino gap (Calabria, southern Italy), J. Seismol., 6, 199-217.

Colella A., Lapenna V., Rizzo E. (2004) - High-resolution imaging of the High Agri Valley Basin (Southern Italy) with electrical resistivity tomography Tectonophysics 386, 29–40.

Corrado S., Aldega L., Di Leo P., Giampaolo C., Invernizzi C., Mazzoli S. and Zattin M. (2005) Thermal maturity of the axial zone of the southern Apennines fold-and-thrust belt (Italy) from multiple organic and inorganic indicators. Terra Nova, 17, 56–65, 2005.

CPTI Working Group (2004). Catalogo Parametrico dei Terremoti Italiani, version 2004 (CPTI04). INGV, Milan, available from http://emidius.mi.ingv.it/CPTI/

Cucci L., Pondrelli S., Frepoli A., Mariucci M.T. and Moro M. (2004) - Local pattern of stress field and seismogenic sources in the Pergola-Melandro basin and the Agri valley (Southern Italy), Geophys. J. Int. 156, 575–583

D'Addezio G., Karner D.B., Burrato P., Insinga D., Maschio L., Ferranti L. and Renne P.R. (2006) - Faulted Middle Pleistocene tephra layer in the Val d'Agri area (Southern Italy), Ann. Geophys. 49 (4-5), 1,029-1,040

D'Argenio B., Pescatore T. and Scandone P. (1975) - Structural pattern of the Campania-Lucania Apennines. Le Scienze, Quaderni de La Ricerca Scientifica, 90, 313–327

Di Luccio, F., A. Piscini, N.A. Pino and G. Ventura (2005). Reactivation of deep faults beneath Southern Apennines: evidence from the 1990–1991 Potenza seismic sequences, Terra Nova, 10.1111/j.1365-3121.2005.00653.x.

Di Niro A. and Giano S.I., (1995) - Evoluzione geomorfologica del bordo orientale dell'alta val d'Agri (Basilicata). Studi Geologici Camerti, 1995/2, 207–218

Di Niro A., Giano S.I. and Santangelo N. (1992) - Primi dati sull'evoluzione geomorfologica e sedimentaria del bacino dell'alta Val d'Agri (Basilicata). Studi Geologici Camerti, 1992/1, 257–263

DISS Working Group (2007). Database of Individual Seismogenic Sources (DISS), Version 3.0.4: A compilation of potential sources for earthquakes larger than M 5.5 in Italy and surrounding areas, http://www.ingv.it/DISS/, © INGV 2005, 2007

Doglioni C., Harabaglia P., Martinelli F., Monelli F. and Zito G. (1996)- A geodynamic model of the Southern accretionary prism. TerraNova, 8, 540–547

Doglioni C., Mongelli F. and Pieri P. (1994) - The Puglia uplift (SE Italy): An anomaly in the foreland of the Apenninic subduction due to buckling of a thick continental lithosphere. Tectonics, 13:1309-1321

Ekström G. (1994) - Teleseismic analysis of the 1990 and 1991 earthquakes near Potenza, Ann. Geofis. 37, 1591-1599

Fedi M., Ferranti L., Florio G., Giori I. and Italiano F. (2005) - Understanding the structural setting in the Southern Apennines (Italy): insight from Gravity Gradient Tensor. Tectonophysics 397, 21– 36

Ferranti L. and Oldow J.S. (2005) - Rates of late neogene deformation along the southwestern margin of Adria, Southern Apennines orogen, Italy, in The Adria Microplate: GPS Geodesy, Tectonics, and Hazards, eds Pinter

Ferranti L. and Oldow J.S. (1999) - History and tectonic implications of lowangle detachment faults and orogen parallel extension, Picentini Mountains, Southern Apennines fold and thrust belt, Italy. Tectonics, 1999; 18(3), 498–526

Ferranti L., Gialanella P.R., Heller F. and Incoronato A. (2005) - Structural and magnetic record of superposed non-coaxial deformation in the Lagonegro thrust nappe, Southern Apennines of Italy. Boll. Soc. Geol. It., 124, 345-365

Ferranti L., Oldow J.S. and Sacchi M. (1996) - Pre-Quaternary orogen-parallel extension in the Southern Apennine belt, Italy. Tectonophysics, 260, 325–347

Ferranti L., Oldow J.S., D'argenio B., Catalano R., Lewis D., Marsella E., Maschio L., Pappone G., Pepe F. and Sulli A. (2007) - Active deformation in Southern Italy, Sicily and southern Sardinia from GPS velocities of the Peri-Tyrrhenian Geodetic Array (PTGA). Boll. Soc. Geol. It., accepted manuscript.

Fracassi, U., and G. Valensise (2007). Unveiling the sources of the catastrophic 1456 multiple earthquake: hints to an unexplored tectonic mechanism in southern Italy, Bull. Seism. Soc. Am. 97 (3), 725–748, doi: 10.1785/0120050250.

Frepoli A. and Amato A. (2000)- Fault plane solutions of crustal earthquakes in Southern Italy (1988-1995): seismotectonic implications. Ann. Geofis., 43(3), 437–468.

Galadini F., Meletti C. and Rebez A. (2000) - Le ricerche del GNDT nel campo della pericolosità sismica (1996-1999), CNR-Gruppo Nazionale per la Difesa dai Terremoti, Roma

Galadini F., Meletti C. and Vittori E. (2001) - Major active faults in Italy: available surficial data. Netherlands J. Geosci. 80, 273-296.

Galli P., Bosi V., Piscitelli S., Giocoli A. and Scionti V. (2006) - Late Holocene earthquakes in southern Apennines: paleoseismology of the Caggiano fault, Int. J. Earth Sci. (Geol. Rundsch.). doi:10.1007/s00531-005-0066-2.

Gallipoli M.R., Mucciarelli M., Albarello D., Lapenna V., Schiattarella M. and Calvano G. (2003) - Hints about site amplification effects comparing macroseismic hazard estimate with microtremor measurements: the Agri Valley (Italy) example. J. Earthq. Eng. 7 (1), 51-72, doi:10.1142/S1363246903000948.

Gallipoli, M., D. Albarello, G. Calvano, V. Lapenna and M. Mucciarelli 1998) - Stime di pericolosità sismica e misure di amplificazione locale relative ai centri urbani dell'alta Val d'Agri. Ingegneria Sismica, 15, 3.

Gambini S. (2003) - Structural evolution of the Val d'Agri fault system, Southern Apennines, Italy". PhD Thesis. University of Leeds, UK.

Gasparini C., Iannaccone G. and Scarpa R. (1985) - Fault-plane solutions and seismicity of the Italian peninsula. Tectonophysics, 117, 59–78.

Gasperini P., Bernardini F., Valensise G. and Boschi E. (1999) - Defining seismogenic sources from historical earthquake felt reports. Bull. Seism. Soc. Am. 89, 94-110.

Giano, S.I., Lapenna, V., Piscitelli, S., Schiattarella, M., 1997. Nuovi dati geologici e geofisici sull'assetto strutturale dei depositi continentali quaternari dell'alta Val d'Agri (Basilicata). Il Quaternario 10, 591–596.

Giano S.I. and Martino C. (2003) - Assetto morfotettonico e morfostratigrafico di alcuni depositi continentali pleistocenici del bacino del Pergola-Melandro (Appenino Lucano). Il Quaternario 16 (2), 289–297.

Giano S.I., Lapenna V., Piscitelli S. and Schiattarella M. (1997) - Nuovi dati geologici e geofisici sull'assetto strutturale dei depositi continentali quaternari dell'alta Val d'Agri (Basilicata). Il Quaternario 10, 591–596.

Giano, S. I., V. Lapenna, S. Piscitelli and M. Schiattarella (2000) - Electrical imaging and self-potential surveys to study the geological setting of the Quaternary slope deposits in the Agri high valley (Southern Italy). Ann. Geofis., 43, 409-419.

Giano S.I., Maschio L., Alessio M., Ferranti L., Improta S. and Schiattarella M. (2000) - Radiocarbon dating of active faulting in the Agri high valley. Southern Italy. J. Geodyn., 2000; 29, 371–386.

Guidoboni, E., and G. Ferrrari (1987). Robert Mallet, first modern seismologist, in E. Guidoboni and G. Ferrari (Editors), "Mallet's macroseismic survey on the Neapolitan earthquake of 16th december 1857", anastatic reprint of the original volume, ING, Bologna 1987, 17-48.

Harvard CMT Catalogue http://www.seismology.harvard.edu/CMTsearch.html

Hippolyte J.C., Angelier J. and Roure F. (1994) - A major geodynamic change revealed by Quaternary stress patterns in the Southern Apennines (Italy). Tectonophysics, 230, 199–210.

Improta, L. & Bruno P.P. (2007) - Combining seismic reflection with multifold wide-aperture profiling: an effective strategy for high-resolution shallow imaging of active faults. Gephys. Res. Lett., 34, L20310, doi:10.1029/2007GL031893, 2007.

Lazzari S. & Lentini F. (1991). Carta geologica del Bacino del Fiume Agri. Scala 1:50.000. S.E.L.C.A. In: Carbone S., Catalano S., Lazzari S., Lentini F. & Monaco C. (1991) – Presentazione della Carta geologica del Bacino del Fiume Agri (Basilicata). Memorie della Società Geologica Italiana, 47, 129-143.

Lucente F.P., Piana Agostinetti N., Moro M., Selvaggi G. and Di Bona M. (2005) - Possible fault plane in a seismic gap area of the Southern Apennines (Italy) revealed by receiver function analysis. J. Geophys. Res., 110 (B04307), doi: 10.1029/2004JB003187

Malinverno A. and Ryan W.B.F. (1986) - Extension in the Tyrrhenian Sea and shortening in the Apennines as a result of arc migration driven by sinking of the lithosphere. Tectonics, 5:227-245.

Mallet R. (1848) - Dynamics of earthquakes. Trans. R. Irish Acad. 21, 50-106.

Mallet R. (1862) - The great Neapolitan earthquake of 1857. The first principles of observational seismology. Chapman and Hill (Publ.), London.

Martino C. (2007) - Stima dei tassi di scorrimento delle faglie ed evoluzione tettonica quaternaria della valle del Melandro (Appennino campano-lucano). Boll. Soc. Geol. It. (Ital. J. Geosci.), 126, 1, pp. 37-53.

Maschio L., Ferranti L. and Burrato P. (2005) - Active extension in Val d'Agri area, Southern Apennines, Italy: implications for the geometry of the seismogenic belt. Geophys. J. Int. 162 (2), 591–609, doi:10.1111/j.1365-246X.2005.02597.x.

Mazzoli S., Barkham S., Cello G., Gambini R., Mattioni L., Shiner P. and Tondi E. (2001) - Reconstruction of continental margin architecture deformed by the contraction of the Lagonegro Basin, Southern Apennines, Italy. J. Geol. Soc. London, 158, 309-319.

Mazzoli S., Corrado S., De Donatis M., Scrocca D., Butler R.W.H., Di Bucci D., Naso G., Nicolai C. and Zucconi V. (2000) - Time and space variability of "thin-skinned" and "thick-skinned" thrust tectonics in the Italian Apennines. Rend. Fis. Acc. Lincei s. 9,11, 5–39.

Mazzoli S. & Di Bucci D. 2003. Critical displacement for normal fault nucleation from en-échelon vein arrays in limestones: a case study from the southern Apennines (Italy). Journal of Structural Geology, 25(7), 1011-1020.

Mazzotti A., Stucchi E., Fradelizio G.L., Zanzi L. and Scandone P. (2000) - Seismic exploration in complex terrains: a processing experience in the Southern Apennines. Geophysics, 65(5), 1402–1417.

Melville C. and Muir Wood R. (1987) - Robert Mallet, first modern seismologist. in E. Guidoboni and G. Ferrari (Editors), "Mallet's macroseismic survey on the Neapolitan earthquake of 16th december 1857", anastatic reprint of the original volume, ING, Bologna 1987, 17-48.

Menardi Noguera A. and Rea G. (2000) - Deep structure of the Campanian-Lucanian Arc (southern Appennine, Italy). Tectonophysics 324 (4), 239–265.

Miall, A. (1996). The geology of fluvial deposits: sedimentary facies, basin analysis and petroleum geology, Springer, Toronto, 582 pp.

Monaco C., Tortorici L. and Paltrineri W. (1998) - Structural evolution of the Lucanian apennines, southern Italy. J. Struct. Geol., 20(5), 617–638

Montone P., Mariucci M.T., Pondrelli S. and Amato A. (2004) - An improved stress map for Italy and surrounding regions (Central Mediterranean). J. Geophys. Res. 109, B10410, doi:10.1029/2003JB002703

Montone, P., M. T. Mariucci, S. Pondrelli, and A. Amato (2004). An improved stress map for Italy and surrounding regions (Central Mediterranean), J. Geophys. Res. 109, B10410, doi:10.1029/2003JB002703.

Morandi S. and Ceragioli E. (2002)- Integrated interpretation of seismic and resistivity images across the 'Val d'Agri' graben (Italy). Annals of Geophysics, 45(2), 259–271

Moro M., Amicucci L., Cinti F.R., Doumaz F., Montone P., Pierdominici S., Saroli M., Stramondo S. and Di Fiore B. (2007) - Surface evidence of active tectonics along the Pergola-Melandro fault: a critical issue for the seismogenic potential of the southern Apennines, Italy. J. Geodyn. 44, 19–32, doi:10.1016/j.jog.2006.12.003

Mucciarelli, M., Valensise G., Gallipoli M.R. and Caputo R. (1999) - Reappraisal of a XVI century earthquake combining historical, geological and instrumental information. In: Castelli, V. (Editor), Proc. of the First Workshop of thr WG "Historical Seismology" of the European Seismological Commission (Macerata, Italy, 1-5 September 1999), 64-67

Murray, A.S. and A.G. Wintle (2000). Luminescence dating of quartz using an improved single-aliquot regenerative-dose protocol, Radiation Measurements, 32: 57-73.

Murray, A.S. and A.G. Wintle (2003). The single aliquot regenerative dose protocol: potential for improvements in reliability, Radiation Measurements, 37: 377-381.

Pantosti D. and Valensise G. (1988) - La faglia sud-appenninica: identificazione oggettiva di un lineamento sismogenetico nell'Appennino meridionale. Proc. VII Meeting G.N.G.T.S., Rome 1988, 205-220

Pantosti D. and Valensise G. (1990) - Faulting mechanism and complexity of the November 23, 1980 Campania-Lucania earthquake, inferred from surface observations. J. geophys. Res., 95(15), 15319–15341

Papanikolau D. I. and Roberts G. P. (2007) - Geometry, kinematics and deformation rates along the active normal fault system in the southern Apennines: Implications for fault growth. J. Struct. Geol., 29, (2007), 166-188.

Patacca, E., Sartori, R. and Scandone, P. (1990) - Tyrrhenian Basin and Apenninic arcs: kinematic relations since late Tortonian times. Memorie della Società Geologica Italiana, 45:425-451

QRCMT http://mednet.ingv.it/events/QRCMT/ Welcome.html).

Racioppi G. (1858) - Memoria sui tremuoti di Basilicata nel Dicembre 1857. Giornale l'Iride, anno II n. 41.

Rizzo, E., A. Colella, V. Lapenna and S. Piscitelli (2004) - High-resolution images of the fault-controlled High Agri Valley basin (Southern Italy) with deep and shallow electrical resistivity tomographies. Phys. Chem. Earth, 29, 321-327.

Santangelo N. (1991) - Evoluzione stratigrafica, geomorfologica e neotettonica di alcuni bacini lacustri del confine campano lucano (Italia meridionale), Ph.D. thesis, Università degli Studi di Napoli Federico II, Napoli

Scandone P. (1967) - Studi sulla geologia lucana: le serie calcareo-silicomarnosa e i suoi rapporti con l'Appennino Calcareo. Bollettino della Società dei Naturalisti in Napoli, 76, 1–175

Scandone P. (1972) - Studi di geologia Lucana: Carta dei terreni della serie calcareo-silico-marnosa e note illustrative. Boll. Soc. Natur., Napoli, 81, 225-300

Schiattarella M., Di Leo P., Beneduce P. and Giano S.I. (2003) - Quaternary uplift vs. tectonic loading: a case study from the Lucanian Apennine, southern Italy. Quatern. Int., 101–102, 239–251

Schiattarella M., Ferranti L., Giano S.I. and Maschio L. (1998) - Evoluzione tettonica quaternaria dell'alta val d'Agri. In: Atti del 79◦ Congresso Nazionale Società Geologica Italiana, ed. Lo Cicero, G., Vol. B, pp. 726–727 Offset Studio, Palermo, Italy

Shiner P., Beccacini A., Mazzoli S. (2004) - Thin-skinned versus thick-skinned structural models for Apulian carbonate reservoirs: constraints from the Val d'Agri Fields, S Apennines, Italy. Marine and Petroleum Geology 21, 805–827

Turco E. and Malito M. (1988) - Formazione di bacini e rotazione di blocchi lungo faglie trascorrenti nell'Appennino meridionale. Riassunti 74° Congr. Soc. Geol. It., Sorrento, 1988.

Turco, E., Maresca, R., & Cappadona, P. (1990). La tettonica pliopleistocenica del confine calbro-lucano: modello cinematico. Mem. Soc. Geol. It., 45, 519–529.

Valensise G. and Pantosti D. (2001a) - The investigation of potential earthquake sources in peninsular Italy: a review, J. Seismol. 5, 287–306

Valensise G. and Pantosti D. (Editors) (2001b) - Database of Potential Sources for Earthquakes Larger than M 5.5 in Italy (DISS version 2.0), Ann. Geofis. 44/4, Suppl. 1, 797–964, with CD-ROM

Vannucci G. and Gasperini P. (2004) - The new release of the database of Earthquake Mechanisms of the Mediterranean Area (EMMA Version 2). Ann. Geophys. 47(1), Suppl. 1, 307-334.

Verstappen, H. T. (1983) - Geomorphology of the Agri Valley, southern Italy. ITC Journal 1983-4, 291-301.

Wells D.L. and Coppersmith K.J. (1994) - New Empirical Relationships among Magnitude, Rupture Length, Rupture Width, Rupture Area, and Surface Displacement. Bull. Seism. Soc. Am. 84, 974-1002

Widdowson, M. (1997). The geomorphological and geological importance of paleosurfaces, In: Palaeosurfaces: Recognition, Reconstruction and Palaeoenvironmental Interpretation (Ed A.J. Fleet), Special Publication n. 120, pp. 1-12. The Geological Society, London.

Zembo, I. (2007). Evoluzione Quaternaria del Bacino Intermontano Alta Val d'Agri. Dipartimento di Scienze della Terra "Ardito Desio". Milano, Università degli studi di Milano. Unpublished Ph.D. Thesis, pp. 191.

List of partecipants

Giuseppe Avellone	UniPa	giuavellone@unipa.it
Paolo Giannandrea	UniBa	giannandre@geo.uniba.it
Francesco Bucci	UniSi	bucci14@unisi.it
Annamaria Blumetti	APAT	annamaria.blumetti@apat.it
Pio Di Manna	APAT	pio.dimanna@apat.it
Marcello Bianca	UniBas	bianca@unibas.it
Luigi Salviulo	UniBas	luigi.salviulo@unibas.it
Luigi Vignola	Geo Archeo Research S.N.C.	luigivignola@hotmail.com
Mauro Gimigliano	libero professionista	
Romeo Mariano Toccaceli	libero professionista, collab. esterno UniNa	rmtoccaceli@tiscali.it
Antonio Priore	libero professionista, collab. esterno UniNa	geol.priore@tiscali.it
Giovanni Lavecchia	libero professionista	giolavecchia2004@libero.it
Alessandro Giocoli	CNR-IMAA	giocoli@imaa.cnr.it
Sabatino Piscitelli	CNR-IMAA	piscitelli@imaa.cnr.it
Enzo Rizzo	CNR-IMAA	rizzo@imaa.cnr.it
Luigi Improta	INGV-RM1	improta@ingv.it
Fabio Villani	INGV-RM1	villani@ingv.it
Luisa Valoroso	INGV-RM1	valoroso@ingv.it
Francesca Balestra	INGV-RM1	fbalestra@gmail.com
Pierfrancesco Burrato	INGV-RM1	burrato@ingv.it
Riccardo Civico	UniRomaTre	riccardo.civico@gmail.com
Luigi Ferranti	UniNA	lferrant@unina.it
Laura Maschio	UniNA	lmale@freemail.it
Enrico Santoro	UniNA	enrico.santoro@hotmail.it
Maria Enrica Mazzella	UniNA	ikeira82@hotmail.com
Elisabetta Napolitano	UniNA	takles@libero.it
Fernando Casillo	UniNa	
Marina Iorio	IAMC-CNR	marina.iorio@iamc.cnr.it
Irene Zembo	UniMi	irene.zembo@unimi.it
Michele Saroli		
Stefano Gori	INGV-RM1	gori@ingv.it
Elena Cubellis	OV-INGV	cubellis@ov.ingv.it
Aldo Marturano	OV-INGV	marturano@ov.ingv.it
Giuliana Alessio	OV-INGV	alessio@ov.ingv.it
Rosa Nappi	OV-INGV	nappi@ov.ingv.it
Paolo Boncio	UniCh	pboncio@unich.it
Eugenio Auciello	UniCh	
Debora Finocchio	UniCh	